Preparation of Porous Scaffolds with Controlled Pore Structures for Tissue Engineering

Qin Zhang

Doctoral Program in Materials Science and Engineering

Submitted to the Graduate School of
Pure and Applied Sciences
in Partial Fulfillment of the Requirements
for the Degree of Doctor of Philosophy in
Engineering

at the
University of Tsukuba

Content

List of abbreviations

3D	Three-dimensional
Acan	Aggrecan
ALP	Alkaline phosphatase
ANOVA	Analysis of variance
BSA	Bovine serum albumin
cDNA	Complementary DNA
Col	Collagen
Col2a1	Type II collagen
DAB	Diaminobenzidine
DMEM	Dulbecco's modified Eagle medium
DNA	Deoxyribonucleic acid
ECM	Extracellular matrix
EDTA	Ethylenediaminetetraacetic acid
EGF	Epidermal growth factor
EOG	Ethylene oxide gas
FBS	Fetal bovine serum
GAG	Glycosaminoglycan
GAPDH	Glyceraldehyde-3-phosphate dehydrogenase
HE staining	Hematoxylin and eosin staining
HPRT 1	Hypoxanthine guanine phosphoribosyl transferase 1
IBSP	Integrin binding sialoprotein
IGF-1	Insulin-like growth factor-1
iPSc	Induced pluripotent stem cell
mRNA	Messenger ribonucleic acid
hMSCs	Human mesenchymal stem cells
nCS	Wollastonite nanowires
PBS	Phosphate buffer saline
PFA	Perfluoroalkoxy
PLGA	Poly(DL-lactic-co-glycolic acid)
RGD	Argine-glycine-aspartic acid
RNA	Ribonucleic acid
RT-PCR	Real-time polymerase chain reaction
RUNX2	Runt-related transcription factor 2
SD	Standard deviation
SEM	Scanning electron microscope
SPP1	Secreted phosphoprotein 1, new name of Osteopontin (OPN)
VEGF	Vascular endothelial growth factor

Chapter 1

General introduction

1.1 Tissue engineering

Millions of people are suffering from tissue or organ failure and waiting from some kind of tissue or organ transplantation. Traditionally, tissue loss resulting from traumatic or nontraumatic destruction has been treated by methods such as autografting and allografting.[1] Although autologous tissue transplantation is clinically considered as a gold standard, it has the limitation of donor site shortage. On the other hand, allogenic transplantation is more prone to immunogenicity as well as inducing other transmissible diseases. Because of these clinical limitations, the concept of tissue engineering is introduced nearly two decades ago, considerably saving numerous lives and improving the quality of life of patients.[2,3]

1.1.1 Principles of tissue engineering

The term “tissue engineering” was firstly introduced in medicine in 1987 during a meeting of the National Science Foundation. The definition that was agreed on as: “Tissue Engineering is the application of the principles and methods of engineering and life sciences toward the fundamental understanding of structure-function relationships in normal and pathologic mammalian tissue and the development of biological substitutes to restore, maintain, or improve tissue function.” In 1993, Robert Langer and Joseph Vacanti further described that tissue engineering is an emerging multidisciplinary field that applies the principles of biology and engineering to the development of viable substitutes that restore, maintain or improve the function of human tissues.[4] Since then, tissue engineering has drawn world-wide concern. The general principle of tissue engineering involves combining living cells with a natural/synthetic support or scaffold to build a three dimensional living construct that is functionally, structurally and mechanically equal to or better than the tissue that is to be replaced. In this approach, new functional tissue is reconstructed by seeding functional cells from a patient in a biodegradable three-dimensional porous scaffold, followed by *in vitro* culture and *in vivo* implantation to the desired sites (Figure 1.1). The potential impact of tissue engineering from both a therapeutic and an economic standpoint is enormous. Using the patients’ own cells avoids many of the problems associated with immune rejection of foreign tissue. After proliferation, small amount cells can be expanded to a sufficient cell mass to replace the organ function. Meanwhile, the shape of the regenerated tissue can be designed to accommodate the desired repair sites.

The progressive tissue engineering accelerates the development of tissue engineering products into market during 21st century, such as Organogenesis' Apligraf® and Genzyme's Carticel®.[5] Until mid 2011, commercial sales of tissue engineering products are almost 3-fold higher than the past 4 years. In addition, the number of companies selling products or offering services has increased over 2-fold to 106, and they are generating a remarkable $3.5 billion in sales.[6] Tissue engineering has emerged as a rapidly expanding approach to address the problems of traditional therapies and is a major component of regenerative medicine.[7,8]

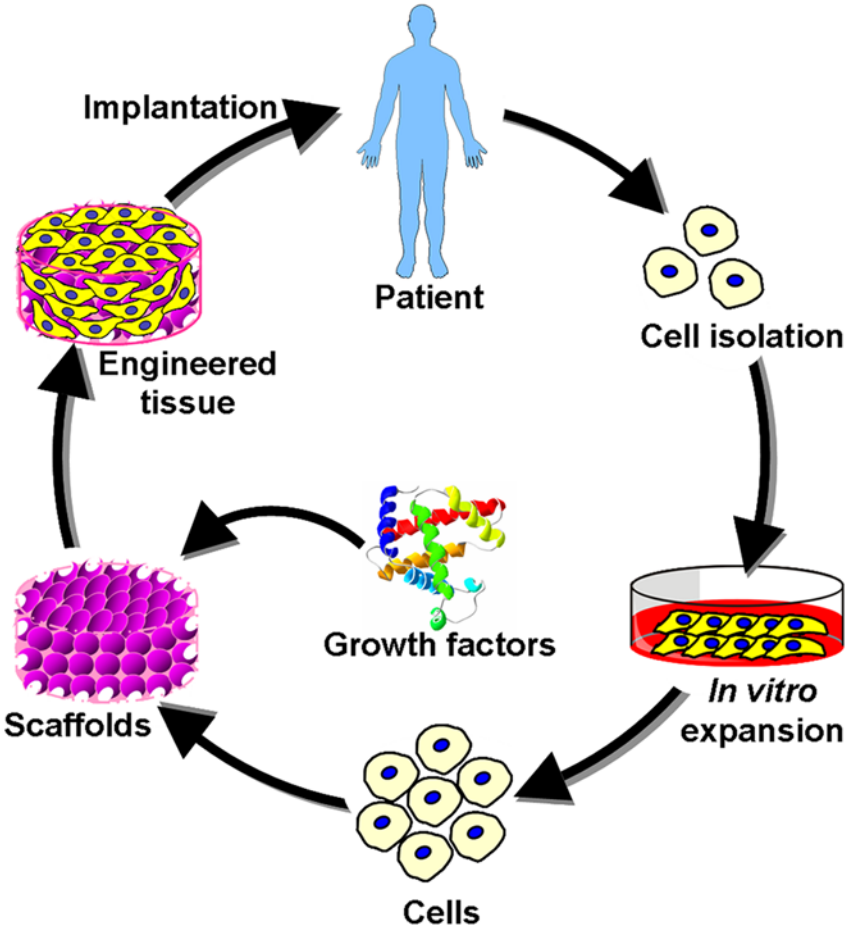

Figure1.1 Concept of tissue engineering. In general, tissue engineering involves the expansion of cells from a small biopsy, followed by culturing of the cells in temporary three-dimensional scaffolds to form the new organ or tissue.

1.1.2 Key factors of tissue engineering

Tissue engineering can be considered as a multidisciplinary technology to restore the function of diseased or damaged tissues through the combination of cells, scaffolds and growth factors using biology and engineering principles as shown in Figure 1.1. The three key components including cells, scaffolds and growth factors require a careful selection to build a three-dimensional construct that is functionally, structurally and mechanically equal to or better than the tissue that is to be replaced.[9]

1.1.2.1 Cells

To achieve the goal of tissue engineering, cells must satisfy a number of criteria in order to achieve effective, long-lasting repair of damaged tissues. (1) An adequate number of cells must be produced to fill the defect. (2) Cells must be able to differentiate into desired phenotypes. (3) Cells must adopt appropriate three-dimensional structural support/scaffold and produce ECM. (4) Produced cells must be structurally and mechanically compliant with the native cell. (5) Cells must successfully be able to integrate with native cells and overcome the risk of immunological rejection. (6) There should be minimal biological risks.

Cell sources utilized in tissue engineering can be autologous (from the patient), allogenic (from a human donor but not immunologically identical), or xenogenic (from a different species donor). Autologous cells represent an excellent source for use in tissue engineering because of the low association with immune complications and ethical issues. Most current strategies for tissue engineering depend upon a sample of autologous cells from the diseased organ of the host. However, for many patients with extensive end-stage organ failure, a tissue biopsy may not yield enough somatic cells for expansion and transplantation. In other instances, primary autologous human cells can not be expanded from a particular organ, such as the pancreas. In these situations, stem cells are envisioned as a viable source of cells because they can serve as an alternative source of cells from which the desired tissue can be derived.[10,11]

According to the origin of generation, stem cells can be classified into two main types, embryonic stem cells (ESCs) and adult stem cells. ESCs are derived from the inner cell mass of the pre-implantation blastocyst.[12] They are undifferentiated, immature cells that are capable of unlimited self-renewal with the ability to differentiate.[13] Adult stem cells are resident stem cells found in specific niches or tissue compartments and are important in maintaining the integrity of tissues like skin, bone and blood.[14] They are undifferentiated cells that can be programmed to differentiate into specific tissue types. For example, mesenchymal stem cells (MSCs), derived from bone marrow, umbilical cord, dental pulp and adipose tissues, are one of prospective adult stem cells. MSCs are relatively easy to obtain from a small aspirate of patients' donor sites and have multipotent capacity to differentiate into different cell lineage such as osteoblasts, chondrocytes, adipose cells, ligament cells and neural cell (Figure 1.2).[15]

According to the potential of differentiation, stem cells can be classified into three types, totipotent stem cells, pluripotent stem cells and unipotent stem cells. Totipotent stem cells, such as ESCs, have the potential to divide and produce all the differentiated cells in an organism including extraembryonic tissues, whereas unipotent stem cells only can differentiate into one cell type. Pluripotent stem cells have the potential to differentiate into any of the three germ layers: endoderm (interior stomach lining, gastrointestinal tract, lungs), mesoderm (muscle, bone, blood, urogenital), or ectoderm (epidermal tissues and nervous system). Pluripotent stem cells can give rise to any fetal or adult cell type.[16] However, they cannot develop into a fetal or adult organism because they lack the potential to contribute to extraembryonic tissue, such as the placenta. Recently, 2012 Nobel Prize in Physiology or Medicine was awarded to Shinya Yamanaka for the discovery that mature cells can be reprogrammed to become pluripotent, named as induced pluripotent stem cells (iPS). In his research, four specific transcription factors were identified to induce pluripotency, including Octamer-binding transcription factor-3/4 (Oct3/4), Sry-related HMG-box gene 2 (Sox2), Kruppel-like factor 4 (KLF4), MYC protooncogene (c-Myc).[17,18] The iPS cells technology will provide unprecedented opportunities in biomedical research and regenerative medicine.[19]

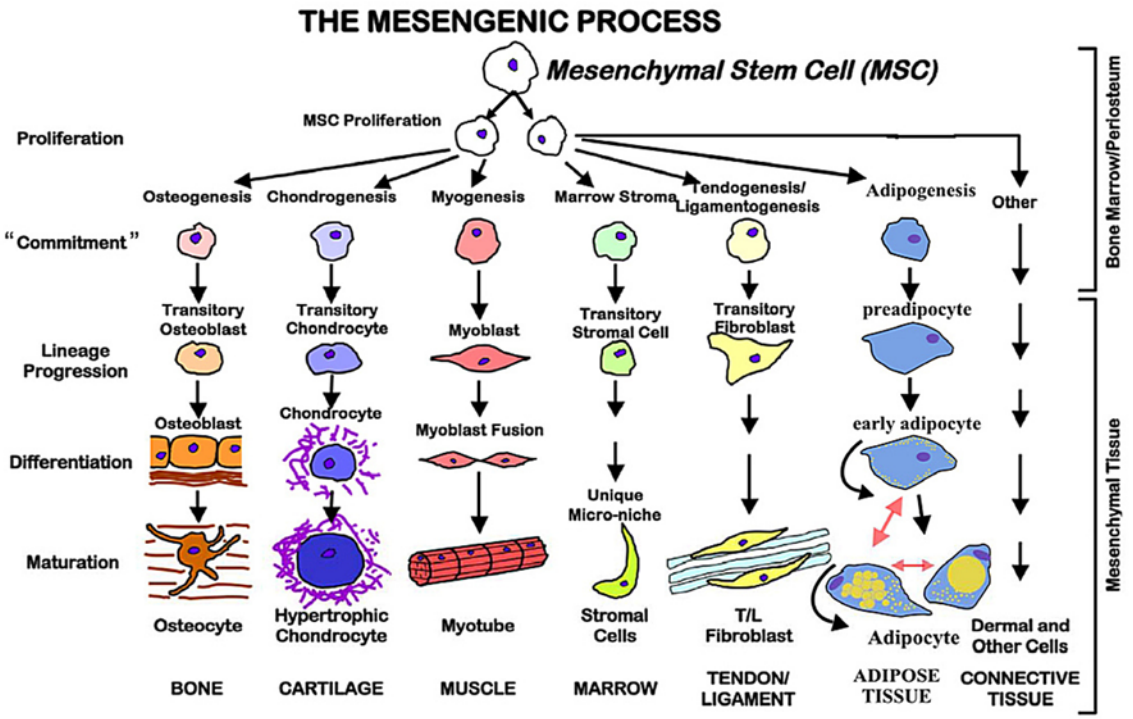

Figure 1.2 Differentiation scheme of MSCs. MSCs can be cultured *in vitro* to generate a variety of differentiated cells and demonstrate their multipotent capacity and differentiation plasticity. The end-stage cell type is dependent on the culture conditions, media and supplements.[20]

1.1.2.2 Scaffolds

It is well know that the extracellular matrix (ECM) produced by cells is not only a physical support of cells, but also an important influence on cell proliferation and differentiation, which contributes to tissue regeneration. It is impossible that a large-sized defect of tissue will be naturally regenerated only by supplying cells to the defects. Thus, three dimensional scaffolds are highly demanded for induction of tissue regeneration, acting as an artificial ECM.[21] In this approach, scaffolds serve as a temporary template to provide biological and physical cues to support cell adhesion, to promote proliferation and to induce differentiation of stem cells or progenitor cells into specific lineage, and finally the newly regenerated tissue is formed while the scaffold is degraded.[22,23] The microenvironment of scaffolds can be adjusted according to the specificities of different tissues, such as bone, cartilage, ligament, skin, vascular tissues, neural tissues, skeletal muscle and etc (Figure 1.3). Since scaffolds play a critical role in regulation of cell function and tissue formation, various technologies come together to construct porous scaffolds to regenerate the tissues/organs and also for controlled and targeted release of bioactive agents in tissue engineering applications.[24] An ideal tissue engineering scaffold would not only replicate the structure of ECM, but would also replicate the many functions that the ECM performs.[25,26]

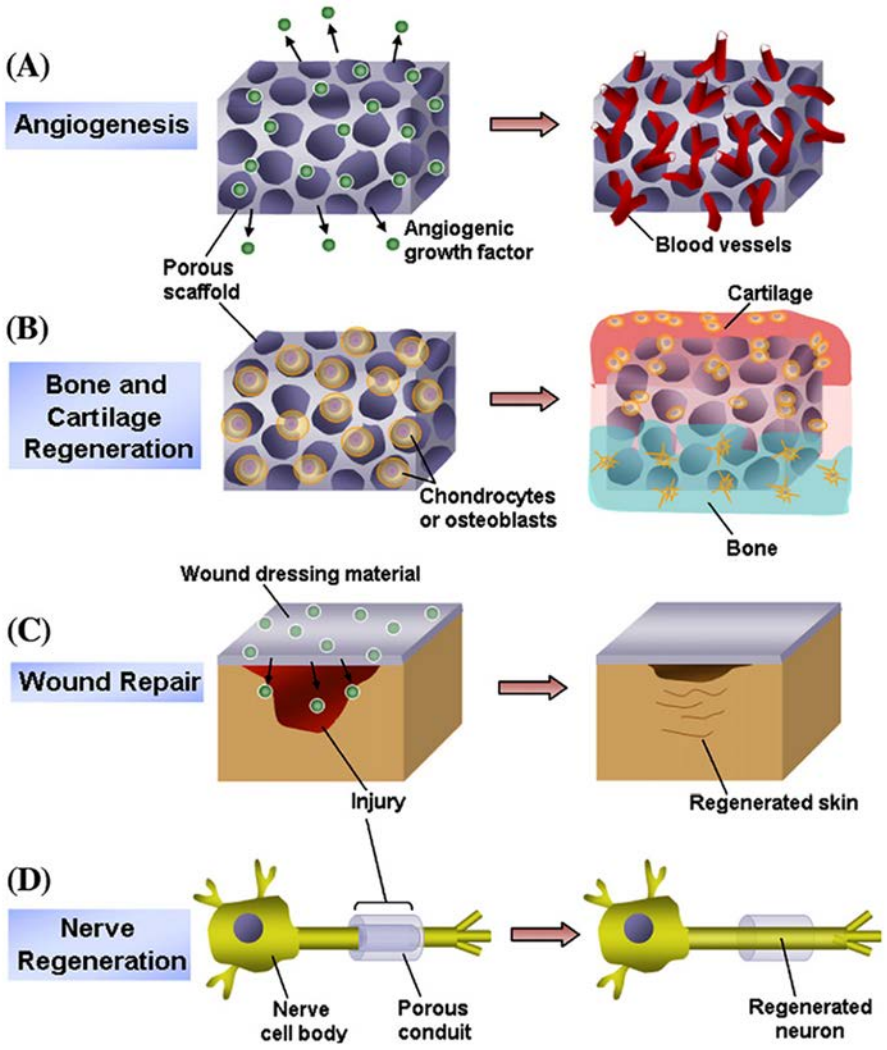

Figure 1.3 Multi-functional scaffolds for regeneration of various tissues. Examples include (A) scaffolds delivering angiogenic growth factor to induce blood vessel formation, (B) scaffolds seeded with osteoblasts/chondrocytes for bone and cartilage regeneration, (C) growth factor releasing film as wound dressing material, and (D) porous conduits for nerve regeneration.[27]

1.1.2.3 Growth factors

To fulfill functional tissue regeneration, growth factors are a necessary component to stimulate cell growth, proliferation and differentiation, acting as signaling molecules among cells.[28-30] Growth factors are soluble secretion signaling proteins or polypeptides capable of regulating the cellular processes. The common growth factors include vascular endothelial cell growth factor (VEGF: stimulates the growth of new blood vessels), fibroblast growth factor (FGF: protein is associated with the ECM and promotes proliferation of many cells), epithelial cell growth factor (EGF: promotes proliferation of mesenchymal, glial and epithelial cells), transforming growth factor beta (TGF-beta: suppresses cytokine production, promotes wound healing, inhibits macrophage and lymphocyte proliferation), keratinoctye growth factor (KGF), hepatocyte growth factor (HGF), platelet derived growth factor (PDGF: promotes proliferation of connective tissue, glial and smooth muscle cells) and bone morphogenetic protein (BMP) and so on. Two strategies are widely used to release growth factors to desired sites, including chemical immobilization of the growth

factor into or onto the scaffolds and physical encapsulation of growth factors in the delivery system. In the physical encapsulation, synthetic and nature polymers have been used as growth factor carrier materials, such as polylactide, poly(ortho esters), poly(anhydrides), poly(amino acids), silk, keratin, collagen, gelatin, fibrinogen, elastin, chitosan, hyaluronic acid, starch, carrageenan, cellulose, alginate and so on.[31-33] A number of fabrication techniques of carriers are developed, but the denaturation or deactivation, release efficiency and target control of growth factors still need to be considered.[34-36]

1.2 Scaffolds for in tissue engineering

1.2.1 Scaffold requirements

Significant attention has been paid to scaffolds for tissue engineering since they provide a biomimetic environment for cell growth and tissue regeneration. With the approach of tissue engineering, porous three-dimensional temporary scaffolds essentially act as a template to manipulate cell function and guide new organ formation. Isolated and expanded cells adhere to the temporary scaffold in all three dimensions, proliferate, and secrete their own extracellular matrices (ECM), replacing the biodegrading scaffold. Significant challenges to this approach include the design and fabrication of the scaffolds. Ideally, scaffolds for tissue engineering should meet several design criteria as follows (Figure 1.4).[37-42]

(1) Biochemical property: the surface should permit cell adhesion, promote cell growth and allow the retention of differentiated cell functions.

(2) Biocompatibility: the scaffolds should be biocompatible, neither the polymer nor its degradation by-products should provoke inflammation or toxicity *in vivo*.[43]

(3) Biodegradability: the scaffold should be biodegradable and eventually eliminated.

(4) Pore structure: the pore structure should allow even spatial cell distribution throughout the scaffold to facilitate homogeneous tissue formation. An interconnected pore structure is required to ensure cellular penetration and adequate diffusion of nutrients to cells and extracellular matrix (ECM) formed by these cells and diffusion of waste products out of the scaffold. The porosity should be high enough to provide sufficient space for cell adhesion, extracellular matrix regeneration and minimal diffusional constraints during culture. An appropriate pore size is necessary for cell attachment, cellular movement, spreading and intracellular communication.

(5) Mechanical property: the scaffold should have appropriate mechanical property to resist the contractile force exerted by cells. The deformation of scaffold may result in a failed regenerated tissue. Meanwhile, the mechanical property of scaffold needs to be consistent with the implanted site. From a practical perspective, it must be strong enough to allow surgical handling during implantation.

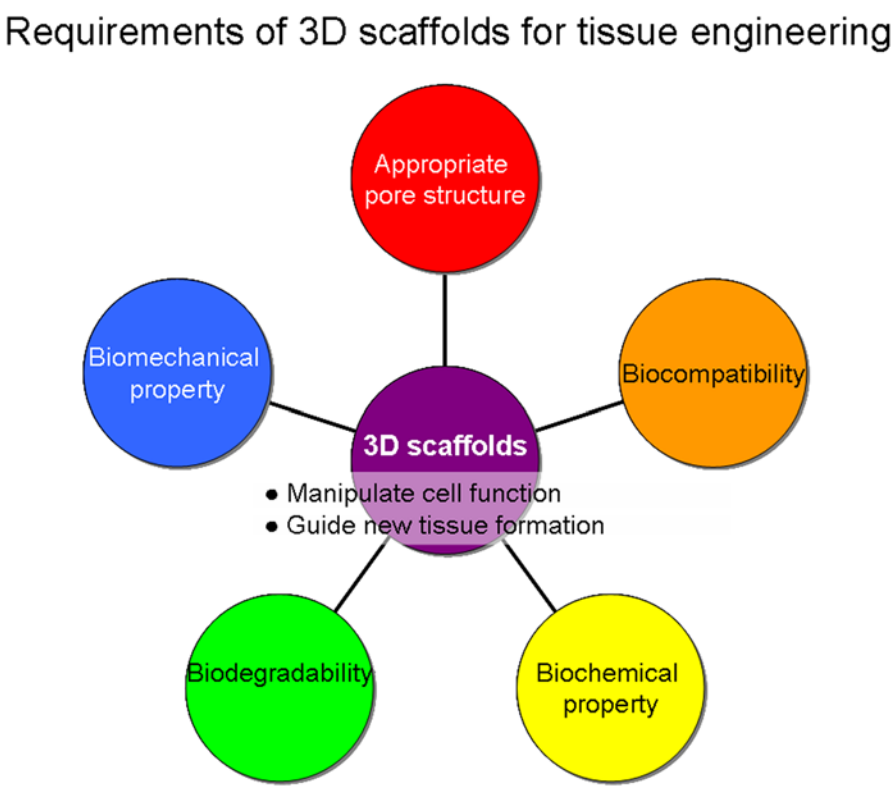

Figure 1.4 Requirements of an ideal scaffold for tissue engineering.

1.2.2 Scaffold materials

The choice of biomaterials as scaffolds is critical to the success of tissue engineering.[44] Large numbers of scaffolds from different biomaterials are available for clinical uses which are listed in Table 1.1. Typically, three individuals groups of biomaterials, synthetic polymers, natural polymers and ceramics, are used in the fabrication of scaffolds for tissue engineering. Each of these biomaterials plays central roles in modern strategies in tissue engineering as designable biophysical and biochemical milieus that direct cellular behavior and function.[45] The guidance provided by biomaterials may facilitate restoration of structure and function of damaged or dysfunctional tissue.

1.2.2.1 Synthetic polymers

Langer and Vacanti postulated that if synthetic polymer could act as cell anchorage sites, they could potentially serve as three-dimensional scaffoldings for the delivery and support of transplanted cells. Synthetic polymers can allow the precise engineering of matrix configuration to permit optimal cell survival, proliferation and subsequent tissue formation.[4] The physical properties of synthetic matrices can be altered in order to obtain desired characteristics of the engineered tissue. For example, the configuration of the synthetic matrix could be manipulated to vary the surface area available for cell attachment as well as to optimize the exposure of the attached cells to nutrients. Similarly, the chemical properties of synthetic matrices also can be modified by incorporating growth factors, hormones or adding multiple side chains to the polymer structure to promote cell growth and differentiation.[46-48] Commonly, biodegradable synthetic polymers such as poly(glycolic acid) (PGA), poly(lactic acid) (PLA), and their copolymer of

poly(lactic-co-glycolic acid) (PLGA) are widely used for tissue engineering.[49] They have gained the approval of the US Food and Drug Administration for certain human clinical use, such as surgical sutures and some implantable devices. PLA undergoes hydrolytic scission to its monomeric form, lactic acid, which is eliminated from the body by incorporation into the tricarboxylic acid cycle. The principal elimination path for lactic acid is respiration and it is primarily excreted by lungs as CO_2. PGA can be broken down by hydrolysis, nonspecific esterases and carboxypeptidases. The glycolic acid monomer is either excreted in the urine or enters the tricarboxylic acid cycle. Other advantages for these materials are that they can be fabricated with a tailored architecture and their degradation characteristics can be controlled by varying the polymer itself or the composition of the individual polymer.

Although the applications of biodegradable synthetic polymers have got great successes in both research and clinical applications, there are some limitations. One of the major limitations of the non-informational synthetic polymers (e.g., PLGA, PLA, PGA) is that they can't provide an extracellular matrix (ECM) and informational signals (such as the Arg-Gly-Asp sequence), which facilitate cell attachment and proliferation.[50] Another major problem is the *in vivo* degradation. *In vivo*, massive release of acidic degradation and resorption by-products results in inflammatory reactions, as reported in the bioresorbable device literature.[51-54] If the capacity of the surrounding tissue to eliminate the by-products is low, due to the poor vascularization or low metabolic activity, the chemical composition of the by-products may lead to local temporary disturbances. Potential problems of biocompatibility in tissue engineering bone and cartilage, by applying biodegradable polymer scaffolds, may also be related to biodegradability and bioresorbability. Therefore, it is important that the 3D scaffold/cell construct is exposed at all times to sufficient quantities of neutral culture media, especially during the period where the mass loss of the polymer matrix occurs.[24]

1.2.2.2 Nature polymers

Unlike synthetic polymer-based scaffolds, natural polymers are biologically active and typically promote excellent cell adhesion and growth. Furthermore, they are also biodegradable and so allow host cells, over time, to produce their own extracellular matrix and replace the degraded scaffold. The natural polymers include proteins of natural extracellular matrices, such as collagen, glycosaminoglycan, alginic acid, alginate, chitosan, hyaluronic acid, polypeptides and etc. Collagen is the prevalent structural biomolecule in the tissues including skin, blood vessels, tendon, cartilage and bone, making it a logical choice for deriving a tissue-engineering scaffold.[55] The collagen molecule, also known as the "tropocollagen", is part of larger collagen aggregates such as fibrils. The whole molecule is approximately 300 nm long and 1.5 nm in diameter (Figure 1.5). Collagen has been known to exhibit minimal inflammatory and antigenic responses, and contains cell adhesion domain sequences which show specific cellular interactions.[56,57] In comparison to other synthetic polymer scaffolds, collagen scaffolds show favorable results with regard to chondrocyte adherence and their ability to maintain a differentiated chondroccyte phenotype.[58] Yannas et al. conducted pioneering studies on collagen-glycosaminoglycan scaffolds to induce the regeneration of dermis of skin, sciatic nerve and knee meniscus.[59] Chemical crosslinking by glutaraldehyde has been proposed to control the stability and degradation rate of these matrices, whereas porosity has been changed by both chemical and physical techniques. Alginic acid,[60] a polysaccharide from seaweed, is a family of natural copolymers of β-D-mannuronic acid (M) and α-L-guluronic acid (G). They have been processed in gel beads encapsulating living cells as a means of immunoprotection.[61,62] Alginates crosslinked with calcium sulfate have been recently used as cell delivery vehicles for tissue engineering, however gelation kinetics by the use of calcium

sulfate is difficult to control and the resulting structure is not uniform. Chitosan is a natural polysaccharide, whose structural characteristic is similar to glycosaminoglycans. It has been used in a variety of biomedical applications, such as hemodialysis membranes, drug delivery systems, orthopaedic and dental coating materials and artificial skin.[63-65] Hyaluronic acid (HA) is a hydrophilic and natural glycosaminoglycan that is found in human skin, cartilage, intra-articular joint fluid and vitreous humor. It is one of the base connective materials in extracellular matrix. HA plays an important role in the lubrication of soft tissues, cushion cells, water absorbance, cell differentiation, migration and cell growth. HA-based scaffolds have been widely used in the tissue engineering of skin, cartilage tissue, bone and soft tissue filler.[66-69] The other natural polymers are silk fibroin,[70] gelatin[71], alginate[64] and etc.[66,72,73] Polypeptides with some amino acid sequences can be favorable to cell adhesion and function and thus they may have potential for cell attachment and transplantation. However, fabricating scaffolds from biological materials with homogeneous and reproducible structures presents a challenge. In addition, the scaffolds generally have poor mechanical properties, which limit their use in, for example, load-bearing orthopedic applications.

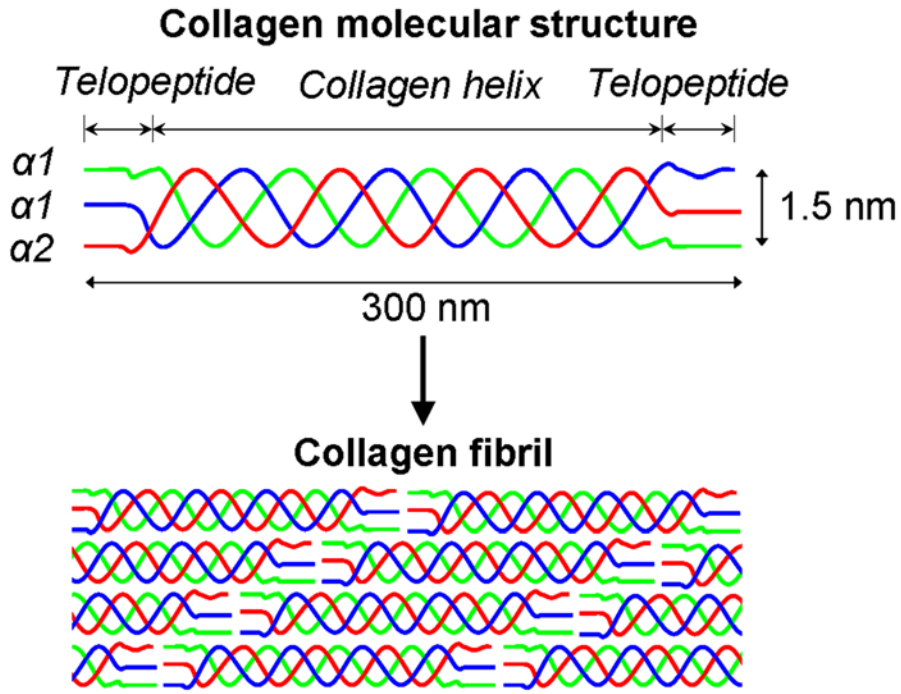

Figure 1.5 Collagen structure from tropocollagen molecule to fibril level. The collagen molecules consist of three polypeptide chains (α-chains) each of which is coiled into a left-handed helix and the three chains are twisted around each other into a right-handed super-helix forming a rod-like molecule.

Table 1.1 List of some common commercial polymeric scaffold products[74-80]

Polymer	Property	Biomedical application	Trade name
PGA	Regenerate biological tissue Good mechanical properties	First biodegradable synthetic suture in 1969 Bone internal fixation devices	DEXON Biofix
PLLA	Good tensile strength Improved suture Fiber-based devices	Orthopaedic fixation devices High-strength fibers (FDA approved at 1971) Blood vessel conduits	Bio-Anchor DEXON
PLGA	High degradation Form of meshes	Multifilament suture Skin graft Drug delivery vehicle	Vicryl Vicryl Mesh
PLGA-collagen	Matrix	Tissue regeneration membrane	CYTOPLAST
Collagen	Scaffolds for cardiovascular, musculoskeletal & nervous tissue engineering	Bioengineered skin equivalents	TransCyte
HA	Promote angiogenesis Sponge as a carrier vehicle for osteoinductive protein	Wound dressing application Synthetic bone graft	HYAFF OSSIGEL
Viscous HA	Synovial fluid substitute	To relieve pain and improve join mobility in osteoarthritis patients	SYNVISC ORTHOVISC

1.2.2.3 Ceramics

Ceramic biomaterials such as hydroxyapatite (HA) and beta-tricalcium phosphate (TCP) have been widely used to prepare bone tissue engineering scaffolds because of their similarity to the inorganic component in bone and excellent mechanical stiffness. The interaction of osteogenic cells with ceramics is important for bone regeneration as ceramics are known to enhance osteoblast differentiation and proliferation.[81,82] Hydroxyapatite is a naturally occurring mineral form of calcium apatite with the formula $Ca_5(PO_4)_3(OH)$, but is usually written $Ca_{10}(PO_4)_6(OH)_2$ to denote that the crystal unit comprises two entities. Hydroxyapatite can be found in teeth and bones within the human body. Thus, it is commonly used as a filler to replace amputated bone or as a coating to promote bone ingrowth into prosthetic implants.[83] Tricalcium phosphate is a compound with formula $Ca_3(PO_4)_2$. It is also known as calcium orthophosphate, tertiary calcium phosphate, tribasic calcium phosphate, or “bone ash” (calcium phosphate being one of the main combustion products of bone). It can be used as a tissue replacement for repairing bony defects when autogenous bone graft is not feasible or possible. It may be used alone or in combination with a biodegradable, resorbable polymer such as polyglycolic acid.[84] It may also be combined with autologous materials for a bone graft. From a bone perspective, they exhibit excellent biocompatibility due to their chemical and structural similarity to the mineral phase of native bone. Wollastonite, a naturally occurring calcium silicate, has attracted much attention for its excellent bioactivity and biocompatibility in bone tissue engineering.[85] The Si and Ca ions released from wollastonite have been reported to stimulate proliferation and osteogenic differentiation of osteoprogenitor cells. Recently angiogenesis effect of calcium silicates has been reported.[86-91]

1.3 Role of scaffold pore structure in tissue regeneration

1.3.1 Pore structure effect on tissue regeneration

The pore architecture of scaffolds has been shown to have a significant effect on both physical properties and cellular activity.[39,92-97] Appropriate pore structure, such as interconnected pore structure, optimal pore size and high porosity, is highly demanded for tissue engineering and regenerative medicine.[98-102] The pore structure affects spatial cell distribution throughout the scaffold which will finally affect homogeneous tissue formation.[92,95,98,103] The interconnectivity of pore structure affects cellular penetration, nutrient supply and waste removal throughout the whole scaffold.[104-106] The porosity affects cell adhesion, extracellular matrix regeneration and diffusional constraints during culture.[107,108] The pore size affects cell attachment, cellular movement, spreading and intracellular communication. Cells primarily interact with scaffolds via chemical groups (ligands) on the material surface. Scaffolds synthesized from natural extracellular materials (e.g. collagen) possess these ligands in the form of Arg-Gly-Asp (RGD) binding sequences, whereas scaffolds made from synthetic materials may require deliberate incorporation of these ligands through, for example, protein adsorption. The ligand density is influenced by the specific surface area, i.e. the available surface within a pore to which cells can adhere. This depends on the mean pore size in the scaffold.[109] The pores thus need to be large enough to allow cells to migrate into the structure where they eventually become bound to the ligands within the scaffold, but small enough to establish a sufficiently high specific surface, leading to a minimal ligand density to allow efficient binding of a critical number of cells to the scaffold. Therefore, for any scaffold, a critical range of pore sizes exists, which may vary depending on the cell type used and tissue being engineered.[25,110-115]

1.3.2 Fabrication techniques of scaffolds with suitable pore structures and current challenges

To achieve the goal of tissue engineering, the scaffold with controlled pore structure to facilitate spatial cell distribution and homogeneous tissue formation is highly demanded. Until now, many fabrication techniques have been developed to obtain porous scaffolds with appropriate pore structure, including porogen leaching, freezing-drying, gas foaming and rapid prototyping. All of these techniques have their own advantages, but none of them are without drawbacks. Preparation of scaffolds with controlled pore structure is still an urgent topic for tissue regeneration.

1.3.2.1 Porogen leaching

Porogen-leaching method offers many advantages for the easy manipulation and control of pore size and porosity. In porogen leaching, the polymer solution is introduced into the gaps among the microporogens to form a polymer-porogen composite (Figure 1.6). After the porogens are dissolved and removed, the remaining polymeric structure takes the form of a porous matrix as a reverse replica of the microporogen assembly. Various porogens, such as salt,[116,117] gelatin,[118] paraffin[119] and sugar,[120] have been utilized. Although the porogen materials can leave replica pores after leaching, they cannot initiate the formation of surrounding pores. As a result, isolated pores are formed in the scaffolds, a situation which is not desirable for tissue engineering scaffolds. To improve pore interconnectivity, the porogen materials are bonded before mixing them with polymer matrix. However, the bonded porogen materials require organic

solvents for leaching of the porogen materials, and the residual solvents are toxic to cells. Penetration of the polymer solution into the bonded porogen material becomes difficult if the polymer solution has a high viscosity.

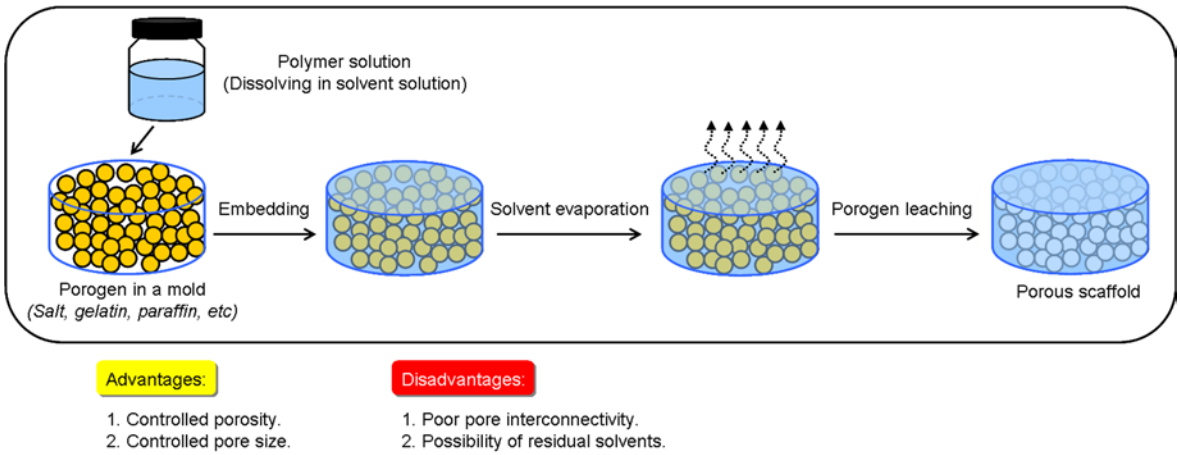

Figure 1.6 Schematic diagram of porogen leaching technique for tissue engineering applications.

1.3.2.2 Freeze-drying

Freeze-drying is a simple process whereby solutions are frozen and then the frozen solvents are removed via sublimation under high vacuum, leading to formation of porous structures. The pore structure of scaffolds, such as pore size, pore volume and pore morphology, can be controlled by altering freeze temperature, solution concentration, nature of solvent and the control of the freeze direction.[121-124] After freeze-drying, the pore structure of the scaffolds is a replica of the ice crystal morphology after freezing (Figure 1.7). By this method, the scaffolds show highly interconnected pore structure and high porosity. Another advantage of this technique is that it ensures complete evaporation of the organic solvent from the scaffold and that it eliminates a porogen-leaching step which could have compromised the purity of the scaffold by the trace amount of organic solvent remaining in the scaffold.

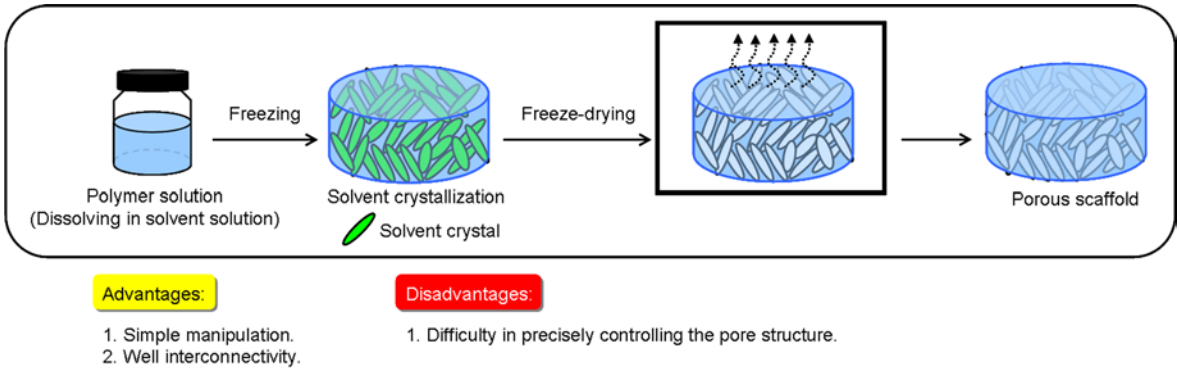

Figure 1.7 Schematic diagram of freeze-drying technique for tissue engineering applications.

1.3.2.3 Gas foaming

The gas foaming method uses high pressure carbon dioxide gas for the fabrication of highly porous scaffolds.[125-127] The process involves saturating a polymer solution with carbon dioxide at a high pressure

which results in the phase separation of clustered carbon dioxide molecules and the creation of pore nucleation, a process called “foaming” (Figure 1.8). Upon the completion of the foaming process, the polymeric scaffold turns into a three dimensional porous scaffold with expanded polymeric volume and a decrease in polymeric density. The amount of carbon dioxide dissolved in the polymer solution determines the porosity and porous structures of the scaffolds. However, the scaffolds fabricated by this method often lack the suitable pore interconnectivity.

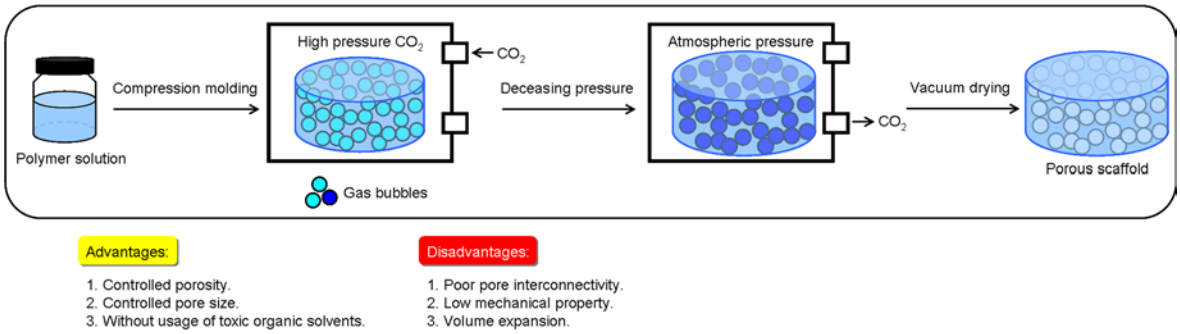

Figure1.8 Schematic diagram of gas foaming technique for tissue engineering applications.

1.3.2.4 Rapid prototying

Rapid prototyping (RP), also referred to as solid freeform fabrications (SFF), is comprised of a group of mechanical processes technologies that fabricate a 3D object in a layer by layer fashion.[128,129] The PR applies computer-aided design (CAD) and computer-aided manufacturing (CAM) program to build highly complex structure by layering a series of thin 2D slices with defined properties (Figure 1.9).[130,131] The cross sections are designed by CAD programs, and corresponding to each cross section, the RP machine fabricates layers of materials which are laid down one at a time, moving from the bottom to the top to build the scaffold with predefined properties, such as porosity, interconnectivity and pore size. Based on high fabrication accuracy and repeatability by a computer-aided design (CAD) system, these methods have been widely applied to prepare scaffolds for the regeneration of various tissues, such as bone, skin, cartilage, etc. However, although the methods possess huge potential for scaffold fabrication, there are several limitations, such as low-resolution struts, limited material selection, long processing times and smooth-surfaced struts, which deteriorate initial cell attachment and proliferation.

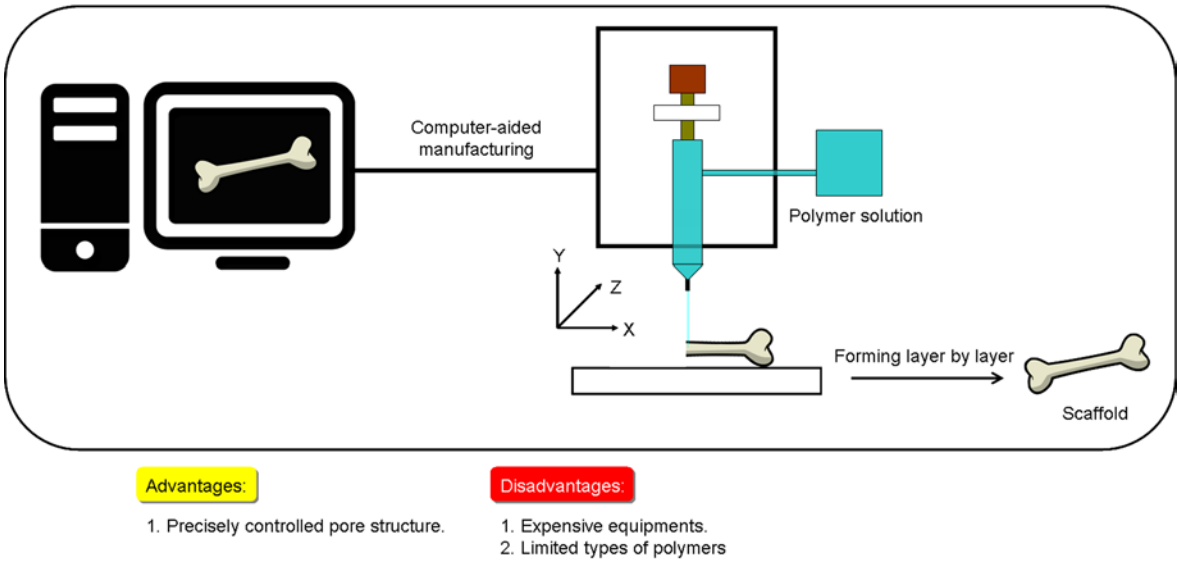

Figure 1.9 Schematic diagram of rapid prototyping technique for tissue engineering applications.

1.4 Motivation and objectives

Appropriate pore structures are required for the scaffolds that are used for tissue engineering and regenerative medicine. Although a number of three-dimensional porous scaffolds have been developed from various types of biodegradable polymers, it has been difficult to ensure homogenous tissue formation in the scaffolds because of uncontrolled pore structure and poor interconnectivity (Figure 1.10). In general, cells are easily allocated and distributed in the peripheral areas, resulting in partial tissue regeneration in the outermost peripheral layers of the scaffolds. The regeneration of functional tissues requires smooth cell delivery and distribution throughout the scaffolds.

To improve spatial cell distribution and promote homogeneous regeneration, some preparation methods have been developed for controlling various aspects of the pore structures, such as pore size, porosity and interconnectivity of the scaffolds. Among these methods, porogen-leaching method offers many advantages for the easy manipulation and control of pore size and porosity. Although the porogen materials can leave replica pores after leaching, they cannot initiate the formation of surrounding pores. As a result, isolated pores are formed in the scaffolds, a situation which is not desirable for tissue engineering scaffolds. To improve pore interconnectivity, the porogen materials are bonded before mixing them with polymer matrix. However, the bonded porogen materials require organic solvents for leaching of the porogen materials, and the residual solvents are toxic to cells. Penetration of the polymer solution into the bonded porogen material becomes difficult if the polymer solution has a high viscosity. Therefore, development of easy and effective methods for preparation of porous scaffolds with well controlled pore structures is strongly desirable.

The purpose of this study is to develope a method by using pre-prepared ice particulates as porogen materials to precisely control the pore structures of collagen-based porous scaffolds. At first, the detailed preparation conditions, such as mixing temperature, ice particulates/collagen solution ratio and collagen aqueous solution concentration, will be investigated. Subsequently, the method will be used to prepare a collagen scaffold with a gradiently changed pore size to investigate the effect of pore size on cartilage tissue

regeneration. Furthermore, individual collagen porous scaffolds with different pore sizes will be prepared to compare the pore size effect on proliferation and cartilaginous gene expression of chondrocytes. Finally, the method will be used to prepared hybrid scaffolds of collagen and wollastonite nanowires with precisely controlled pore structures for bone tissue engineering.

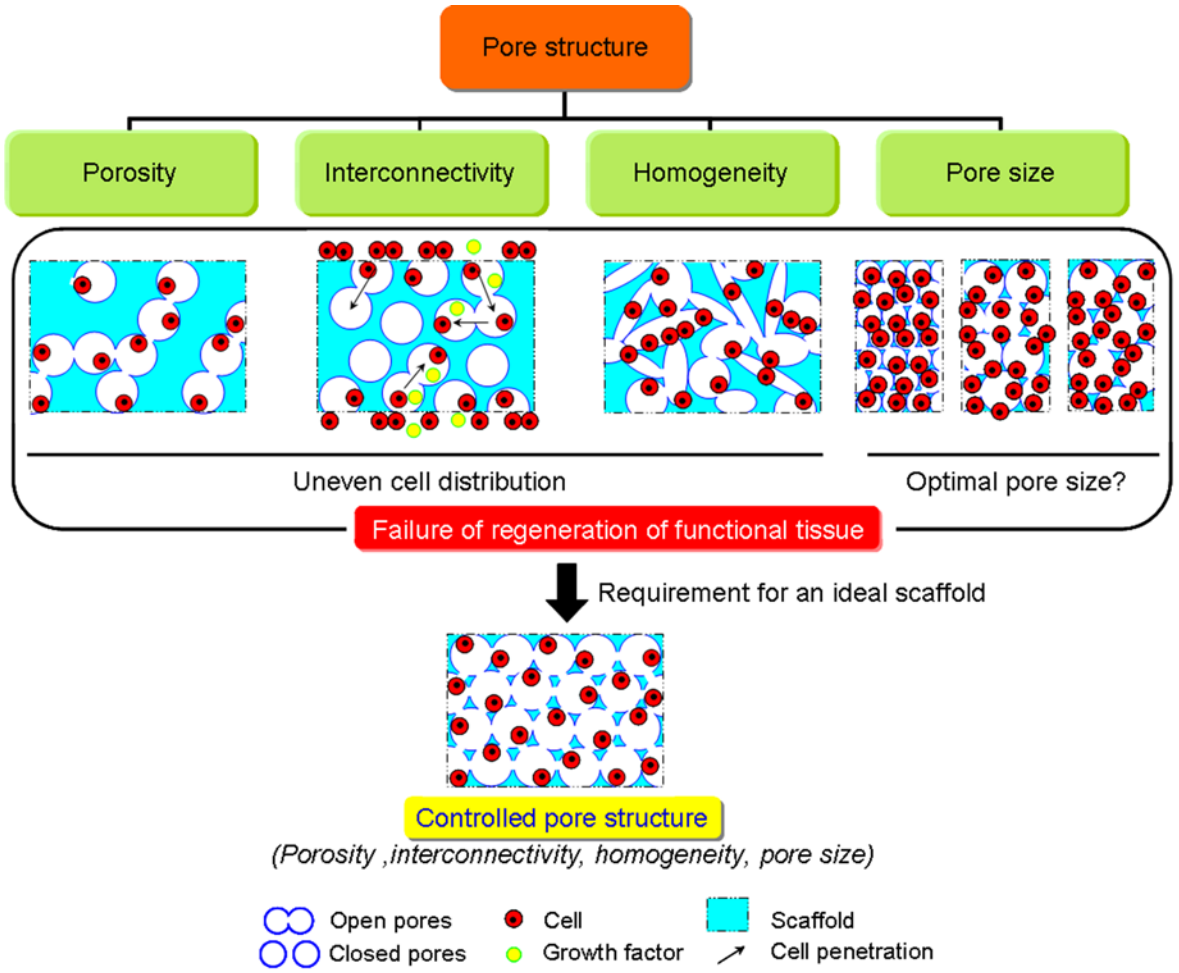

Figure 1.10 Illustration of the importance of controlled pore structure for successful tissue regeneration. The controlled pore structure should have high porosity, interconnectivity, homogeneity and appropriate pore size, which can improve spatial even cell distribution and promote homogeneous regeneration.

1.5 References

1. Vacanti, J.P.,Langer, R. Tissue engineering: the design and fabrication of living replacement devices for surgical reconstruction and transplantation. *Lancet* **354**, Si32-Si34 (1999).
2. Shum-Tim, D., Stock, U., Hrkach, J., Shinoka, T., Lien, J., Moses, M.A., Stamp, A., Taylor, G., Moran, A.M., Landis, W., Langer, R., Vacanti, J.P.,Mayer, J.E. Tissue engineering of autologous aorta using a new biodegradable polymer. *Ann Thorac Surg* **68**, 2298-2304 (1999).
3. Vacanti, J.P. Tissue engineering and the road to whole organs. *Brit J Surg* **99**, 451-453 (2012).
4. Langer, R.,Vacanti, J.P. Tissue Engineering. *Science* **260**, 920-926 (1993).

5. Lysaght, M.J., Nguy, N.A.P.,Sullivan, K. An economic survey of the emerging tissue engineering industry. *Tissue Eng* **4**, 231-238 (1998).
6. Jaklenec, A., Stamp, A., Deweerd, E., Sherwin, A.,Langer, R. Progress in the Tissue Engineering and Stem Cell Industry "Are we there yet?". *Tissue Eng Part B-Re* **18**, 155-166 (2012).
7. Temenoff, J.S.,Mikos, A.G. Review: tissue engineering for regeneration of articular cartilage. *Biomaterials* **21**, 431-440 (2000).
8. Khademhosseini, A., Vacanti, J.P.,Langer, R. Progress in Tissue Engineering. *Sci Am* **300**, 64-+ (2009).
9. Reddi, A.H. Morphogenesis and tissue engineering of bone and cartilage: inductive signals, stem cells, and biomimetic biomaterials. *Tissue Eng* **6**, 351-359 (2000).
10. Malaitsev, V.V., Bogdanova, I.M.,Sukhikh, G.T. [Current views on the biology of the stem cell]. *Arkh Patol* **64**, 7-11 (2002).
11. Bianco, P.,Robey, P.G. Stem cells in tissue engineering. *Nature* **414**, 118-121 (2001).
12. Smith, A.G. Embryo-derived stem cells: of mice and men. *Annu Rev Cell Dev Biol* **17**, 435-462 (2001).
13. Thomson, J.A. Embryonic stem cell lines derived from human blastocysts (vol 282, pg 1147, 1998). *Science* **282**, 1827-1827 (1998).
14. Pittenger, M.F., Mackay, A.M., Beck, S.C., Jaiswal, R.K., Douglas, R., Mosca, J.D., Moorman, M.A., Simonetti, D.W., Craig, S.,Marshak, D.R. Multilineage potential of adult human mesenchymal stem cells. *Science* **284**, 143-147 (1999).
15. Oreffo, R.O.C., Cooper, C., Mason, C.,Clements, M. Mesenchymal stem cells - Lineage, plasticity, and skeletal therapeutic potential. *Stem Cell Rev* **1**, 169-178 (2005).
16. Ulloa-Montoya, F., Verfaillie, C.M.,Hu, W.S. Culture systems for pluripotent stem cells. *J Biosci Bioeng* **100**, 12-27 (2005).
17. Takahashi, K.,Yamanaka, S. Induction of pluripotent stem cells from mouse embryonic and adult fibroblast cultures by defined factors. *Cell* **126**, 663-676 (2006).
18. Takahashi, K., Tanabe, K., Ohnuki, M., Narita, M., Ichisaka, T., Tomoda, K.,Yamanaka, S. Induction of pluripotent stem cells from adult human fibroblasts by defined factors. *Cell* **131**, 861-872 (2007).
19. Nishikawa, S., Goldstein, R.A.,Nierras, C.R. The promise of human induced pluripotent stem cells for research and therapy. *Nat Rev Mol Cell Bio* **9**, 725-729 (2008).
20. Bonfield, T.L.,Caplan, A.I. Adult Mesenchymal Stem Cells: An Innovative Therapeutic for Lung Diseases. *Discov Med* **47**, 337-345 (2010).
21. Ali, O.A., Huebsch, N., Cao, L., Dranoff, G.,Mooney, D.J. Infection-mimicking materials to program dendritic cells in situ. *Nature Materials* **8**, 151-158 (2009).
22. Thomson, R.C., Wake, M.C., Yaszemski, M.J.,Mikos, A.G. Biodegradable polymer scaffolds to regenerate organs. *Adv Polym Sci* **122**, 245-274 (1995).
23. Lee, S.H.,Shin, H. Matrices and scaffolds for delivery of bioactive molecules in bone and cartilage tissue engineering. *Adv Drug Deliver Rev* **59**, 339-359 (2007).
24. Hutmacher, D.W. Scaffolds in tissue engineering bone and cartilage. *Biomaterials* **21**, 2529-2543 (2000).
25. O'Brien, F.J. Biomaterials & scaffolds for tissue engineering. *Mater Today* **14**, 88-95 (2011).
26. Ma, P.X. Biomimetic materials for tissue engineering. *Adv Drug Deliver Rev* **60**, 184-198 (2008).

27. Chung, H.J.,Park, T.G. Surface engineered and drug releasing pre-fabricated scaffolds for tissue engineering. *Adv Drug Deliver Rev* **59**, 249-262 (2007).
28. Lee, K., Silva, E.A.,Mooney, D.J. Growth factor delivery-based tissue engineering: general approaches and a review of recent developments. *J R Soc Interface* **8**, 153-170 (2011).
29. Cao, L.,Mooney, D.J. Spatiotemporal control over growth factor signaling for therapeutic neovascularization. *Adv Drug Deliver Rev* **59**, 1340-1350 (2007).
30. Discher, D.E., Mooney, D.J.,Zandstra, P.W. Growth Factors, Matrices, and Forces Combine and Control Stem Cells. *Science* **324**, 1673-1677 (2009).
31. Mitragotri, S.,Lahann, J. Physical approaches to biomaterial design. *Nature Materials* **8**, 15-23 (2009).
32. Richardson, T.P., Peters, M.C., Ennett, A.B.,Mooney, D.J. Polymeric system for dual growth factor delivery. *Nat Biotechnol* **19**, 1029-1034 (2001).
33. Chen, R.R., Silva, E.A., Yuen, W.W., Brock, A.A., Fischbach, C., Lin, A.S., Guldberg, R.E.,Mooney, D.J. Integrated approach to designing growth factor delivery systems. *Faseb J* **21**, 3896-3903 (2007).
34. Krishnamurthy, R.,Manning, M.C. The stability factor: importance in formulation development. *Curr Pharm Biotechnol* **3**, 361-371 (2002).
35. Eppler, S.M., Combs, D.L., Henry, T.D., Lopez, J.J., Ellis, S.G., Yi, J.H., Annex, B.H., McCluskey, E.R.,Zioncheck, T.F. A target-mediated model to describe the pharmacokinetics and hemodynamic effects of recombinant human vascular endothelial growth factor in humans. *Clin Pharmacol Ther* **72**, 20-32 (2002).
36. Kim, H.K., Chung, H.J.,Park, T.G. Biodegradable polymeric microspheres with "open/closed" pores for sustained release of human growth hormone. *J Control Release* **112**, 167-174 (2006).
37. Chen, G.P., Ushida, T.,Tateishi, T. Scaffold design for tissue engineering. *Macromol Biosci* **2**, 67-77 (2002).
38. Schmidt, C.E.,Leach, J.B. Neural tissue engineering: Strategies for repair and regeneration. *Annu Rev Biomed Eng* **5**, 293-347 (2003).
39. Hollister, S.J. Porous scaffold design for tissue engineering. *Nature Materials* **4**, 518-524 (2005).
40. Butler, D.L., Goldstein, S.A.,Guilak, F. Functional tissue engineering: the role of biomechanics. *J Biomech Eng* **122**, 570-575 (2000).
41. Rezwan, K., Chen, Q.Z., Blaker, J.J.,Boccaccini, A.R. Biodegradable and bioactive porous polymer/inorganic composite scaffolds for bone tissue engineering. *Biomaterials* **27**, 3413-3431 (2006).
42. Higuchi, A., Ling, Q.D., Chang, Y., Hsu, S.T.,Umezawa, A. Physical Cues of Biomaterials Guide Stem Cell Differentiation Fate. *Chem Rev* (2013).
43. Mooney, D.J., Kaufmann, P.M., Sano, K., Mcnamara, K.M., Vacanti, J.P.,Langer, R. Transplantation of Hepatocytes Using Porous, Biodegradable Sponges. *Transplant P* **26**, 3425-3426 (1994).
44. Freed, L.E., Vunjaknovakovic, G., Biron, R.J., Eagles, D.B., Lesnoy, D.C., Barlow, S.K.,Langer, R. Biodegradable Polymer Scaffolds for Tissue Engineering. *Bio-Technol* **12**, 689-693 (1994).
45. Dawson, E., Mapili, G., Erickson, K., Taqvi, S.,Roy, K. Biomaterials for stem cell differentiation. *Adv Drug Deliv Rev* **60**, 215-228 (2008).
46. Lutolf, M.P.,Hubbell, J.A. Synthetic biomaterials as instructive extracellular microenvironments for morphogenesis in tissue engineering. *Nat Biotechnol* **23**, 47-55 (2005).

47. Silva, E.A.,Mooney, D.J. Synthetic extracellular matrices for tissue engineering and regeneration. *Curr Top Dev Biol* **64**, 181-205 (2004).
48. Lutolf, M.P.,Hubbell, J.A. Synthetic biomaterials as instructive extracellular microenvironments for morphogenesis in tissue engineering. *Nature Biotechnology* **23**, 47-55 (2005).
49. Lee, N.K., Oh, H.J., Hong, C.M., Suh, H.,Hong, S.H. Comparison of the synthetic biodegradable polymers, polylactide (PLA), and polylactic-co-glycolic acid (PLGA) as scaffolds for artificial cartilage. *Biotechnol Bioproc E* **14**, 180-186 (2009).
50. Yang, Q., Peng, J., Guo, Q.Y., Huang, J.X., Zhang, L., Yao, J., Yang, F., Wang, S.G., Xu, W.J., Wang, A.Y.,Lu, S.B. A cartilage ECM-derived 3-D porous acellular matrix scaffold for in vivo cartilage tissue engineering with PKH26-labeled chondrogenic bone marrow-derived mesenchymal stem cells. *Biomaterials* **29**, 2378-2387 (2008).
51. Fu, K., Pack, D.W., Klibanov, A.M.,Langer, R. Visual evidence of acidic environment within degrading poly(lactic-co-glycolic acid) (PLGA) microspheres. *Pharmaceut Res* **17**, 100-106 (2000).
52. Ignatius, A.A.,Claes, L.E. In vitro biocompatibility of bioresorbable polymers: Poly(L,DL-lactide) and poly(L-lactide-co-glycolide). *Biomaterials* **17**, 831-839 (1996).
53. Ignatius, A.A., Betz, O., Augat, P.,Claes, L.E. In vivo investigations on composites made of resorbable ceramics and poly(lactide) used as bone graft substitutes. *J Biomed Mater Res* **58**, 701-709 (2001).
54. Bergsma, J.E., Debruijn, W.C., Rozema, F.R., Bos, R.R.M.,Boering, G. Late Degradation Tissue-Response to Poly(L-Lactide) Bone Plates and Screws. *Biomaterials* **16**, 25-31 (1995).
55. Eyre, D.R. Collagen - Molecular Diversity in the Bodys Protein Scaffold. *Science* **207**, 1315-1322 (1980).
56. Riesle, J., Hollander, A.P., Langer, R., Freed, L.E.,Vunjak-Novakovic, G. Collagen in tissue-engineered cartilage: Types, structure, and crosslinks. *J Cell Biochem* **71**, 313-327 (1998).
57. Song, E., Kim, S.Y., Chun, T., Byun, H.J.,Lee, Y.M. Collagen scaffolds derived from a marine source and their biocompatibility. *Biomaterials* **27**, 2951-2961 (2006).
58. Glowacki, J.,Mizuno, S. Collagen scaffolds for tissue engineering. *Biopolymers* **89**, 338-344 (2008).
59. Yannas, I.V., Lee, E., Orgill, D.P., Skrabut, E.M.,Murphy, G.F. Synthesis and Characterization of a Model Extracellular-Matrix That Induces Partial Regeneration of Adult Mammalian Skin. *P Natl Acad Sci USA* **86**, 933-937 (1989).
60. Diduch, D.R., Jordan, L.C.M., Mierisch, C.M.,Balian, G. Marrow stromal cells embedded in alginate for repair of osteochondral defects. *Arthroscopy* **16**, 571-577 (2000).
61. Mallett, A.G.,Korbutt, G.S. Alginate Modification Improves Long-Term Survival and Function of Transplanted Encapsulated Islets. *Tissue Eng Pt A* **15**, 1301-1309 (2009).
62. Zhang, X.L., He, H.Y., Yen, C., Ho, W.,Lee, L.J. A biodegradable, immunoprotective, dual nanoporous capsule for cell-based therapies. *Biomaterials* **29**, 4253-4259 (2008).
63. Nettles, D.L., Elder, S.H.,Gilbert, J.A. Potential use of chitosan as a cell scaffold material for cartilage tissue engineering. *Tissue Eng* **8**, 1009-1016 (2002).
64. Li, Z., Ramay, H.R., Hauch, K.D., Xiao, D.,Zhang, M. Chitosan-alginate hybrid scaffolds for bone tissue engineering. *Biomaterials* **26**, 3919-3928 (2005).
65. Howling, G.I., Dettmar, P.W., Goddard, P.A., Hampson, F.C., Dornish, M.,Wood, E.J. The effect of chitin and chitosan on the proliferation of human skin fibroblasts and keratinocytes in vitro. *Biomaterials* **22**, 2959-2966 (2001).

66. Yoo, H.S., Lee, E.A., Yoon, J.J.,Park, T.G. Hyaluronic acid modified biodegradable scaffolds for cartilage tissue engineering. *Biomaterials* **26**, 1925-1933 (2005).
67. Unterman, S.A., Gibson, M., Lee, J.H., Crist, J., Chansakul, T., Yang, E.C.,Elisseeff, J.H. Hyaluronic Acid-Binding Scaffold for Articular Cartilage Repair. *Tissue Eng Pt A* **18**, 2497-2506 (2012).
68. Manferdini, C., Guarino, V., Zini, N., Raucci, M.G., Ferrari, A., Grassi, F., Gabusi, E., Squarzoni, S., Facchini, A., Ambrosio, L.,Lisignoli, G. Mineralization behavior with mesenchymal stromal cells in a biomimetic hyaluronic acid-based scaffold. *Biomaterials* **31**, 3986-3996 (2010).
69. Davidenko, N., Campbell, J.J., Thian, E.S., Watson, C.J.,Cameron, R.E. Collagen-hyaluronic acid scaffolds for adipose tissue engineering. *Acta Biomater* **6**, 3957-3968 (2010).
70. Wang, Y.Z., Blasioli, D.J., Kim, H.J., Kim, H.S.,Kaplan, D.L. Cartilage tissue engineering with silk scaffolds and human articular chondrocytes. *Biomaterials* **27**, 4434-4442 (2006).
71. Huang, Y., Onyeri, S., Siewe, M., Moshfeghian, A.,Madihally, S.V. In vitro characterization of chitosan-gelatin scaffolds for tissue engineering. *Biomaterials* **26**, 7616-7627 (2005).
72. Perets, A., Baruch, Y., Weisbuch, F., Shoshany, G., Neufeld, G.,Cohen, S. Enhancing the vascularization of three-dimensional porous alginate scaffolds by incorporating controlled release basic fibroblast growth factor microspheres. *J Biomed Mater Res A* **65A**, 489-497 (2003).
73. Awad, H.A., Wickham, M.Q., Leddy, H.A., Gimble, J.M.,Guilak, F. Chondrogenic differentiation of adipose-derived adult stem cells in agarose, alginate, and gelatin scaffolds. *Biomaterials* **25**, 3211-3222 (2004).
74. Dhandayuthapani, B., Yoshida, Y., Maekawa, T.,Kumar, D.S. Polymeric Scaffolds in Tissue Engineering Application: A Review. *Int J Polym Sci* (2011).
75. Terasaka, S., Iwasaki, Y., Shinya, N.,Uchida, T. Fibrin glue and polyglycolic acid nonwoven fabric as a biocompatible dural substitute. *Neurosurgery* **58**, 134-138 (2006).
76. Lu, H.H., Cooper, J.A., Manuel, S., Freeman, J.W., Attawia, M.A., Ko, F.K.,Laurencin, C.T. Anterior cruciate ligament regeneration using braided biodegradable scaffolds: in vitro optimization studies. *Biomaterials* **26**, 4805-4816 (2005).
77. Cooper, J.A., Lu, H.H., Ko, F.K., Freeman, J.W.,Laurencin, C.T. Fiber-based tissue-engineered scaffold for ligament replacement: design considerations and in vitro evaluation. *Biomaterials* **26**, 1523-1532 (2005).
78. Sai, P.,Babu, M. Collagen based dressings - a review. *Burns* **26**, 54-62 (2000).
79. Hunt, D.R., Jovanovic, S.A., Wikesjo, U.M., Wozney, J.M.,Bernard, G.W. Hyaluronan supports recombinant human bone morphogenetic protein-2 induced bone reconstruction of advanced alveolar ridge defects in dogs. A pilot study. *J Periodontol* **72**, 651-658 (2001).
80. Kato, Y., Nakamura, S.,Nishimura, M. Beneficial actions of hyaluronan (HA) on arthritic joints: Effects of molecular weight of HA on elasticity of cartilage matrix. *Biorheology* **43**, 347-354 (2006).
81. Caplan, A.I. Adult mesenchymal stem cells for tissue engineering versus regenerative medicine. *J Cell Physiol* **213**, 341-347 (2007).
82. Habraken, W.J.E.M., Wolke, J.G.C.,Jansen, J.A. Ceramic composites as matrices and scaffolds for drug delivery in tissue engineering. *Adv Drug Deliver Rev* **59**, 234-248 (2007).
83. Wei, G.B.,Ma, P.X. Structure and properties of nano-hydroxyapatite/polymer composite scaffolds for bone tissue engineering. *Biomaterials* **25**, 4749-4757 (2004).

84. Erisken, C., Kalyon, D.M.,Wang, H.J. Functionally graded electrospun polycaprolactone and beta-tricalcium phosphate nanocomposites for tissue engineering applications. *Biomaterials* **29**, 4065-4073 (2008).
85. Padmanabhan, S.K., Gervaso, F., Carrozzo, M., Scalera, F., Sannino, A.,Licciulli, A. Wollastonite/hydroxyapatite scaffolds with improved mechanical, bioactive and biodegradable properties for bone tissue engineering. *Ceram Int* **39**, 619-627 (2013).
86. Li, H.,Chang, J. Bioactive silicate materials stimulate angiogenesis in fibroblast and endothelial cell co-culture system through paracrine effect. *Acta Biomater* (2013).
87. Li, H.Y.,Chang, J. Stimulation of proangiogenesis by calcium silicate bioactive ceramic. *Acta Biomater* **9**, 5379-5389 (2013).
88. Li, H.Y., Zhai, W.Y.,Chang, J. Effects of Wollastonite on Proliferation and Differentiation of Human Bone Marrow-derived Stromal Cells in PHBV/Wollastonite Composite Scaffolds. *J Biomater Appl* **24**, 231-246 (2009).
89. Zhu, H.L., Shen, J.Y., Feng, X.X., Zhang, H.P., Guo, Y.H.,Chen, J.Y. Fabrication and characterization of bioactive silk fibroin/wollastonite composite scaffolds. *Mat Sci Eng C-Mater* **30**, 132-140 (2010).
90. Zhao, L.,Chang, J. Preparation and characterization of macroporous chitosan/wollastonite composite scaffolds for tissue engineering. *J Mater Sci-Mater M* **15**, 625-629 (2004).
91. Zhang, N.L., Molenda, J.A., Fournelle, J.H., Murphy, W.L.,Sahai, N. Effects of pseudowollastonite (CaSiO3) bioceramic on in vitro activity of human mesenchymal stem cells. *Biomaterials* **31**, 7653-7665 (2010).
92. Indolfi, L., Baker, A.B.,Edelman, E.R. The role of scaffold microarchitecture in engineering endothelial cell immunomodulation. *Biomaterials* **33**, 7019-7027 (2012).
93. Lu, H.X., Kawazoe, N., Kitajima, T., Myoken, Y., Tomita, M., Umezawa, A., Chen, G.P.,Ito, Y. Spatial immobilization of bone morphogenetic protein-4 in a collagen-PLGA hybrid scaffold for enhanced osteoinductivity. *Biomaterials* **33**, 6140-6146 (2012).
94. Bhardwaj, N.,Kundu, S.C. Chondrogenic differentiation of rat MSCs on porous scaffolds of silk fibroin/chitosan blends. *Biomaterials* **33**, 2848-2857 (2012).
95. Moutos, F.T., Freed, L.E.,Guilak, F. A biomimetic three-dimensional woven composite scaffold for functional tissue engineering of cartilage. *Nature Materials* **6**, 162-167 (2007).
96. Liu, Y., Bharadwaj, S., Lee, S.J., Atala, A.,Zhang, Y. Optimization of a natural collagen scaffold to aid cell-matrix penetration for urologic tissue engineering. *Biomaterials* **30**, 3865-3873 (2009).
97. Dai, W.D., Kawazoe, N., Lin, X.T., Dong, J.,Chen, G.P. The influence of structural design of PLGA/collagen hybrid scaffolds in cartilage tissue engineering. *Biomaterials* **31**, 2141-2152 (2010).
98. Choi, S.W., Xie, J.W.,Xia, Y.N. Chitosan-Based Inverse Opals: Three-Dimensional Scaffolds with Uniform Pore Structures for Cell Culture. *Adv Mater* **21**, 2997-+ (2009).
99. Engelmayr, G.C., Cheng, M.Y., Bettinger, C.J., Borenstein, J.T., Langer, R.,Freed, L.E. Accordion-like honeycombs for tissue engineering of cardiac anisotropy. *Nature Materials* **7**, 1003-1010 (2008).
100. Caliari, S.R.,Harley, B.A.C. The effect of anisotropic collagen-GAG scaffolds and growth factor supplementation on tendon cell recruitment, alignment, and metabolic activity. *Biomaterials* **32**, 5330-5340 (2011).

101. Engelmayr, G.C., Jr., Cheng, M., Bettinger, C.J., Borenstein, J.T., Langer, R.,Freed, L.E. Accordion-like honeycombs for tissue engineering of cardiac anisotropy. *Nat Mater* **7**, 1003-1010 (2008).
102. Hollister, S.J., Maddox, R.D.,Taboas, J.M. Optimal design and fabrication of scaffolds to mimic tissue properties and satisfy biological constraints. *Biomaterials* **23**, 4095-4103 (2002).
103. Tanaka, Y., Yamaoka, H., Nishizawa, S., Nagata, S., Ogasawara, T., Asawa, Y., Fujihara, Y., Takato, T.,Hoshi, K. The optimization of porous polymeric scaffolds for chondrocyte/atelocollagen based tissue-engineered cartilage. *Biomaterials* **31**, 4506-4516 (2010).
104. Ko, Y.G., Grice, S., Kawazoe, N., Tateishi, T.,Chen, G.P. Preparation of Collagen-Glycosaminoglycan Sponges with Open Surface Porous Structures Using Ice Particulate Template Method. *Macromol Biosci* **10**, 860-871 (2010).
105. Chen, V.J.,Ma, P.X. Nano-fibrous poly(L-lactic acid) scaffolds with interconnected spherical macropores. *Biomaterials* **25**, 2065-2073 (2004).
106. Silva, M.M.C.G., Cyster, L.A., Barry, J.J.A., Yang, X.B., Oreffo, R.O.C., Grant, D.M., Scotchford, C.A., Howdle, S.M., Shakesheff, K.M.,Rose, F.R.A.J. The effect of anisotropic architecture on cell and tissue infiltration into tissue engineering scaffolds. *Biomaterials* **27**, 5909-5917 (2006).
107. Karageorgiou, V.,Kaplan, D. Porosity of 3D biomaterial scaffolds and osteogenesis. *Biomaterials* **26**, 5474-5491 (2005).
108. Woodard, J.R., Hilldore, A.J., Lan, S.K., Park, C.J., Morgan, A.W., Eurell, J.A.C., Clark, S.G., Wheeler, M.B., Jamison, R.D.,Johnson, A.J.W. The mechanical properties and osteoconductivity of hydroxyapatite bone scaffolds with multi-scale porosity. *Biomaterials* **28**, 45-54 (2007).
109. Lien, S.M., Ko, L.Y.,Huang, T.J. Effect of pore size on ECM secretion and cell growth in gelatin scaffold for articular cartilage tissue engineering. *Acta Biomater* **5**, 670-679 (2009).
110. Murphy, C.M., Haugh, M.G.,O'Brien, F.J. The effect of mean pore size on cell attachment, proliferation and migration in collagen-glycosaminoglycan scaffolds for bone tissue engineering. *Biomaterials* **31**, 461-466 (2010).
111. O'Brien, F.J., Harley, B.A., Yannas, I.V.,Gibson, L.J. The effect of pore size on cell adhesion in collagen-GAG scaffolds. *Biomaterials* **26**, 433-441 (2005).
112. Stenhamre, H., Nannmark, U., Lindahl, A., Gatenholm, P.,Brittberg, M. Influence of pore size on the redifferentiation potential of human articular chondrocytes in poly(urethane urea) scaffolds. *J Tissue Eng Regen M* **5**, 578-588 (2011).
113. Oh, S.H., Park, I.K., Kim, J.M.,Lee, J.H. In vitro and in vivo characteristics of PCL scaffolds with pore size gradient fabricated by a centrifugation method. *Biomaterials* **28**, 1664-1671 (2007).
114. Ishaug-Riley, S.L., Crane-Kruger, G.M., Yaszemski, M.J.,Mikos, A.G. Three-dimensional culture of rat calvarial osteoblasts in porous biodegradable polymers. *Biomaterials* **19**, 1405-1412 (1998).
115. Sobral, J.M., Caridade, S.G., Sousa, R.A., Mano, J.F.,Reis, R.L. Three-dimensional plotted scaffolds with controlled pore size gradients: Effect of scaffold geometry on mechanical performance and cell seeding efficiency. *Acta Biomater* **7**, 1009-1018 (2011).
116. Lee, S.B., Kim, Y.H., Chong, M.S., Hong, S.H.,Lee, Y.M. Study of gelatin-containing artificial skin V: fabrication of gelatin scaffolds using a salt-leaching method. *Biomaterials* **26**, 1961-1968 (2005).
117. Hou, Q.P., Grijpma, D.W.,Feijen, J. Porous polymeric structures for tissue engineering prepared by a coagulation, compression moulding and salt leaching technique. *Biomaterials* **24**, 1937-1947 (2003).
118. Zhou, Q.L., Gong, Y.H.,Gao, C.Y. Microstructure and mechanical properties of poly(L-lactide) scaffolds fabricated by gelatin particle leaching method. *J Appl Polym Sci* **98**, 1373-1379 (2005).

119. Ma, Z.W., Gao, C.Y., Gong, Y.H.,Shen, J.C. Paraffin spheres as porogen to fabricate poly(L-lactic acid) scaffolds with improved cytocompatibility for cartilage tissue engineering. *J Biomed Mater Res B* **67B**, 610-617 (2003).
120. Zhang, R.Y.,Ma, P.X. Synthetic nano-fibrillar extracellular matrices with predesigned macroporous architectures. *J Biomed Mater Res* **52**, 430-438 (2000).
121. O'Brien, F.J., Harley, B.A., Yannas, I.V.,Gibson, L. Influence of freezing rate on pore structure in freeze-dried collagen-GAG scaffolds. *Biomaterials* **25**, 1077-1086 (2004).
122. Zhang, H.,Cooper, A.I. Aligned porous structures by directional freezing. *Adv Mater* **19**, 1529-1533 (2007).
123. Zhang, H.F., Hussain, I., Brust, M., Butler, M.F., Rannard, S.P.,Cooper, A.I. Aligned two- and three-dimensional structures by directional freezing of polymers and nanoparticles. *Nature Materials* **4**, 787-793 (2005).
124. Haugh, M.G., Murphy, C.M.,O'Brien, F.J. Novel freeze-drying methods to produce a range of collagen-glycosaminoglycan scaffolds with tailored mean pore sizes. *Tissue Eng Part C Methods* **16**, 887-894 (2010).
125. Harris, L.D., Kim, B.S.,Mooney, D.J. Open pore biodegradable matrices formed with gas foaming. *J Biomed Mater Res* **42**, 396-402 (1998).
126. Kim, T.K., Yoon, J.J., Lee, D.S.,Park, T.G. Gas foamed open porous biodegradable polymeric microspheres. *Biomaterials* **27**, 152-159 (2006).
127. Yoon, J.J., Kim, J.H.,Park, T.G. Dexamethasone-releasing biodegradable polymer scaffolds fabricated by a gas-foaming/salt-leaching method. *Biomaterials* **24**, 2323-2329 (2003).
128. Yang, S.F., Leong, K.F., Du, Z.H.,Chua, C.K. The design of scaffolds for use in tissue engineering. Part II. Rapid prototyping techniques. *Tissue Eng* **8**, 1-11 (2002).
129. Taboas, J.M., Maddox, R.D., Krebsbach, P.H.,Hollister, S.J. Indirect solid free form fabrication of local and global porous, biomimetic and composite 3D polymer-ceramic scaffolds. *Biomaterials* **24**, 181-194 (2003).
130. Sun, W., Starly, B., Darling, A.,Gomez, C. Computer-aided tissue engineering: application to biomimetic modelling and design of tissue scaffolds. *Biotechnol Appl Bioc* **39**, 49-58 (2004).
131. Fan, H.Y., Lu, Y.F., Stump, A., Reed, S.T., Baer, T., Schunk, R., Perez-Luna, V., Lopez, G.P.,Brinker, C.J. Rapid prototyping of patterned functional nanostructures. *Nature* **405**, 56-60 (2000).

Chapter 2

Preparation of collagen scaffolds with precisely controlled pore structures by using ice particulates as a porogen material

2.1 Summary

Appropriate pore structures and mechanical properties are required for the scaffolds that are used for tissue engineering and regenerative medicine. In this chapter, precisely controlled pore structures were created for the scaffolds to control cell distribution and functions for functional tissue regeneration. The method using pre-prepared ice particulates as a porogen material was developed to precisely control the pore structures of collagen porous scaffolds. The detailed preparation conditions, such as mixing temperature, ice particulates/collagen solution ratio and collagen aqueous solution concentration, were investigated. Bovine articular chondrocytes were cultured in collagen scaffolds to compare their effects on regeneration of cartilage tissue. The porogen ice particulates initiated formation of interconnected large spherical pores surrounded by small pores. The large spherical pores were well compacted and increased the elastic modulus of the scaffolds. The unique pore structures facilitated cell penetration, resulting in a homogeneous cell distribution throughout the scaffolds. The excellent mechanical properties protected the deformation of the scaffolds during cell culturing and implantation. The collagen porous scaffolds facilitated cartilage regeneration when bovine articular chondrocytes were cultured in the scaffolds. The use of pre-prepared ice particulates as a porogen material proved to be a useful method to control the pore structure and improve the mechanical properties of collagen-based porous scaffolds.

2.2 Introduction

Porous scaffolds have been widely used in tissue engineering and regenerative medicine to provide a temporary microenvironment for cell adhesion, proliferation, differentiation and secretion of the newly formed extracellular matrix to guide the formation of new tissues and organs.[1-5] The scaffolds should have an adequate porous structure for enabling cellular penetration into the construct to obtain a desirable cell distribution.[6-10] Although a number of three-dimensional porous scaffolds have been developed from various types of biodegradable polymers[11-15], not all the scaffolds can ensure homogenous tissue formation in the

scaffolds. In general, cells are easily allocated and distributed in the peripheral areas, resulting in partial tissue regeneration in the outermost peripheral layers of the scaffolds. The regeneration of homogenous tissues requires smooth cell delivery and distribution throughout the scaffolds.

To improve spatial cell distribution and promote homogeneous regeneration, a few preparation methods have been developed for controlling various aspects of the pore structures, such as pore size, porosity and interconnectivity of the scaffolds.[16-19] Among these methods, the porogen-leaching method offers many advantages for the easy manipulation and control of pore size and porosity. Although the porogen materials can leave replica pores after leaching, they cannot initiate the formation of surrounding pores. As a result, isolated pores are formed in the scaffold, a situation which is not desirable for tissue engineering scaffolds. To improve pore interconnectivity, the porogen materials are bonded before mixing them with polymer matrix.[20-23] However, the bonded porogen materials require organic solvents for leaching of the porogen materials, and the residual solvents are toxic to cells. Penetration of the polymer solution into the bonded porogen material becomes difficult if the polymer solution has a high viscosity. We have developed a method by using pre-prepared ice particulates as a porogen material for the preparation of porous scaffolds composed of biodegradable synthetic polymers.[24] Embossed ice particulates have also been used to control the surface pore structure and to increase the interconnectivity between the surface pores and inner bulk pores.[25,26] However, it has been difficult to use the method to control the inner bulk pore structure of naturally derived polymers because controlling the mixing temperature has been difficult. Furthermore, porous scaffolds prepared from naturally derived polymers usually have poor mechanical properties, meaning they may not be able to withstand cell-mediated contraction and suppression from surrounding tissues and may deform after implantation. Improved mechanical properties are anticipated for porous scaffolds composed of naturally derived polymers.

In this chapter, we used pre-prepared ice particulates as a porogen material to prepare collagen porous scaffolds with precisely controlled pore structures and improved mechanical properties. Pre-prepared ice particulates not only work as porogens to control the pore size and porosity but also work as nuclei to initiate the formation of new ice crystals in the surrounding aqueous solution, therefore increasing the interconnectivity of the scaffolds. Furthermore, collagen porous scaffolds prepared by this method showed a 15.7-fold improvement in the mechanical properties compared with the control collagen porous scaffolds prepared by the normal freeze-drying method. The collagen porous scaffolds were used for culturing bovine chondrocytes for cartilage tissue engineering.

2.3 Materials and methods

2.3.1 Scaffold preparation

Ice particulates were prepared by spaying Milli Q water into liquid nitrogen using a sprayer. The ice particulates were sieved by sieves with 335 and 425 μm mesh pores to obtain ice particulates having a diameter from 335 to 425 μm. The sieving process was conducted in a -15 °C, low-temperature chamber (Espec, Osaka, Japan). The sieved ice particulates were stored in a closed glass bottle in a -80 °C freezer until use. The ice particulates were observed under a phase-contrast microscope by immersing them in liquid nitrogen to prevent thawing during the observation.

Two groups of collagen porous scaffolds were prepared. Group A: the collagen scaffolds were prepared using a 2% (w/v) collagen aqueous solution with a ratio of ice particulates/collagen solution of 25%,

50% and 75% (w/v) at a freezing temperature of -80 °C. Group B: the collagen porous scaffolds were prepared using 1%, 2% and 3% (w/v) collagen aqueous solution with a ratio of ice particulates/collagen solution of 50% (w/v) at a freezing temperature of -80 °C. The preparation scheme is shown in Figure 2.1. First, the collagen solution was prepared by dissolving freeze-dried porcine type I collagen (Nitta Gelatin, Osaka, Japan) in a solution (20:80 (v/v)) of ethanol and 0.1 M acetic acid (pH 3.0) at 4 °C. The solution of acetic acid and ethanol was used to dissolve collagen to decrease the freezing temperature of the collagen solution below -4 °C. Before mixing, the ice particulates and collagen solution were moved and kept in a -4 °C, low-temperature chamber for 6 h for temperature balance. Subsequently, the ice particulates were added to the collagen solution and mixed thoroughly with a steel spoon to ensure that the ice particulates and collagen solution were homogeneously mixed. The mixture was poured onto a perfluoroalkoxy (PFA)-film wrapped copper plate with a 10 mm thick silicone frame, and then the mixture surface was flattened with a steel spatula and covered with a glass plate wrapped with polyvinylidene chloride film. The manipulation was conducted in the -4 °C, low-temperature chamber. After mixing, the whole set was moved to a deep freezer (-80 °C) and kept there for 6 h of freezing. The frozen mixture was freeze-dried for 3 days in a freeze-dryer under a vacuum of 20 Pa (VirTis AdVantage Benchtop Freeze Dryer, SP Industries Inc.) to form collagen porous scaffolds. Finally, the freeze-dried collagen porous scaffolds were cross-linked for 6 h with glutaraldehyde vapor, which was saturated with a 25% aqueous glutaraldehyde solution at 37 °C in a closed box. Using of glutaraldehyde vapor can avoid the dissolution of collagen or structure collapse that may happen at the beginning of cross-linking methods using aqueous glutaraldehyde solution. After cross-linking, the scaffolds were immersed in a 0.1 M glycine aqueous solution to block any unreacted aldehyde groups. The scaffolds were washed 6 times with pure water. The washed scaffolds were frozen in a deep freezer (-80 °C) for 6 h and freeze-dried again as described above to obtain the dried collagen scaffolds. The control collagen scaffold was prepared by the same procedure with a 2% (w/v) concentration of collagen solution without the use of ice particulates.

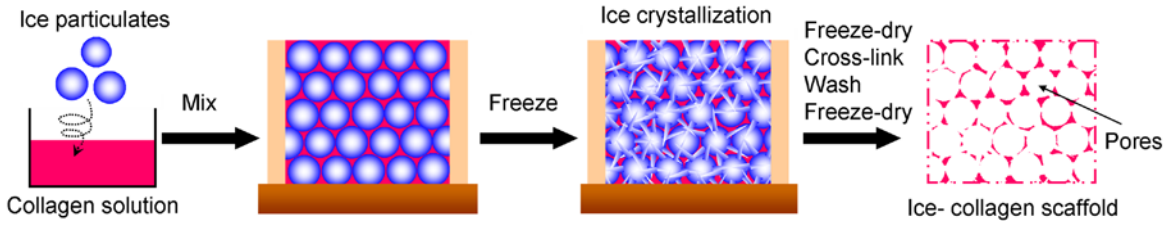

Figure 2.1 Preparation schne of collagen porous scaffolds by using ice particulates as porogen material.

2.3.2 Scaffold characterization

The microstructures of the collagen scaffolds were observed using a JSM-5610 scanning electron microscope (SEM, JEOL, Tokyo, Japan). The cross-sections of the collagen scaffolds were coated with platinum by an ECS-101 sputter coater (Elionix, Tokyo, Japan) before observation.

The porosity of collagen porous scaffolds was measured according to Archimedes' principle (n=3). The porosity was calculated according to the following formula: porosity = ((W2-W1)/(W2-W3)) ×100%, where W1 is the dry weight of the scaffold, W2 is the wet weight of scaffold (including PBS solution), and W3 is the weight of the scaffold in PBS solution (subtracting buoyancy from W1).

The mechanical property of the collagen scaffolds was measured by a static compression mechanical test machine (TMI UTM-10T; Tokyo Baldwin Co., Ltd., Tokyo, Japan). Before testing, the

samples were cut into cubes (10 mm×10 mm×10 mm) with a blade. The samples were wetted by immersing in PBS before measurement. Each sample was compressed at a rate of 2.0 mm/min at room temperature. Load-deformation curves were obtained from a chart record. Young's modulus was calculated from the curves and sample dimensions. The average values were calculated from four samples.

2.3.3 In vitro cell culture

For cell culture use, the collagen scaffolds were cut into cylinders (Ø8 mm×H4 mm). All the collagen scaffolds, including the control collagen scaffold, were used to evaluate the cell distribution. The scaffold cylinders were sterilized with 70% ethanol, washed 3 times with Milli-Q water and exchanged with culture medium. Bovine articular chondrocytes were isolated from articular cartilage derived from the knees of a 9-week-old female calf obtained from a local slaughter house by digestion with an aqueous solution of 0.2 wt/v% collagenase type II (Worthington Biochemical, Lakewood, NJ). The isolated chondrocytes were cultured in 75 cm_2 tissue culture flasks in Dulbecco's Modified Eagle's Medium (DMEM) under an atmosphere of 5% CO_2 at 37 °C. The DMEM contained 10% fetal bovine serum, 4500 mg/L glucose, 4 mM glutamine, 100 U/mL penicillin, 100 μg/mL streptomycin, 0.1 mM nonessential amino acids, 0.4 mM proline, 1 mM sodium pyruvate and 50 μg/mL ascorbic acid. The cell culture medium was changed every 3 days. The chondrocytes were harvested by treatment with trypsin/EDTA solution when the cells reached 80% confluence. The cell concentration was adjusted to 2.5×10^7 cells/mL for cell seeding. Chondrocytes were seeded in the collagen scaffolds by dropping 200 μL of the cell suspension on one side of each collagen scaffold (200 μL cell suspension, 5×10^6 cells/scaffold). The cell/scaffold constructs were then incubated with shaking at 60 times/min for 1 w. The medium was changed every 3 days. After *in vitro* culturing for 1 w, the constructs were washed 3 times with PBS and fixed with 0.25% glutaraldehyde solution at room temperature for 1 h. In addition, the constructs were embedded in paraffin and sectioned (7 μm thick). The cross sections were stained with Hoechst 33258 (10 μg/ml) and observed under a fluorescence microscope (Olympus, Tokyo, Japan) to evaluate the cell distribution in the scaffolds. The photographs of cell distribution in all collagen scaffolds were equally divided into 30 squares. The cell numbers in each square were counted, respectively. The frequency distribution graphs were drew by recording the frequency of occurrence of cell number in each square of collagen scaffolds.

2.3.4 In vivo implantation

For *in vivo* implantation, the collagen porous scaffolds prepared with 2% (w/v) collagen aqueous solution and a ratio of ice particulates/collagen solution of 50% (w/v) and the control collagen scaffold were used. The scaffold cylinders were sterilized and seeded with chondrocytes as described above. For *in vivo* implantation, chondrocytes were seeded twice in the scaffolds, once from the top surface of the scaffold cylinders and once from the bottom. The second seeding was performed after 3 h of culturing after the first cell seeding to allow cell adhesion. In total, 400 μL of cell suspension solution of 2.5×10^7 cells/mL was applied to each scaffold (1.0×10^7 cells/scaffold). The cell/scaffold constructs were then cultured in DMEM under an atmosphere of 5% CO_2 at 37 °C with shaking at 60 times/min for 1 w. The cell culture medium was changed every 3 d. After *in vitro* culture for 1 w, the cell/scaffold constructs were subcutaneously implanted into the dorsa of athymic nude mice (6-week-old). Seven mice were used, and each mouse was implanted with 2 constructs. After implantation for 8 w, the mice were sacrificed, and the implants were harvested for further investigation. The animal experiment was conducted according to the committee guidelines of the

National Institute for Materials Science for Animal Experiments.

2.3.5 Measurement of sulfated glycosaminoglycans (sGAG) and DNA and mechanical testing

The DNA and sGAG contents of the cell/scaffold constructs were measured after 1 w of *in vitro* culture and 8 w of *in vivo* implantation. Before the analysis, the constructs were washed with pure water, freeze-dried and then digested with papain solution (400 μg/mL with 5 mM L-cystein and 5 mM EDTA in 0.1 M phosphate buffer at a pH of 6.0). An aliquot of papain digest was used to measure the DNA amount with Hoechst 33258 dye (Sigma-Aldrich, St. Louis, MO, USA) under a spectrofluorometer (FP-6500, JASCO, Japan). The sGAG content was determined using the above papain digests by a Blyscan sulfated glycosaminoglycan (Benchmark Plus; Bio-Rad Laboratories, Japan) according to the manufacturer's instructions. The ratio of sGAG to DNA was calculated from the sGAG and DNA contents of each sample. Three samples were used to calculate the average and standard deviation.

The mechanical property of the engineered tissue after 8 w of implantation was measured by the same method used for the scaffolds. Three samples were used for each test.

2.3.6 Histological and immunohistochemical evaluation

The engineered tissue after 8 w of implantation was fixed in 10% neutral buffered formalin, embedded in paraffin and sectioned (7 μm thick). The sections were stained with hematoxylin and eosin (HE). The sections were also used for the immunostaining of type II collagen and aggrecan. Briefly, the deparaffinized sections were incubated with proteinase K for 10 min for antigen retrieval, peroxidase blocking solution for 5 min, and 10% goat serum solution for 30 min. The sections were then incubated with the first antibodies for 1 h, followed by incubation with the peroxidase-labeled polymer-conjugated second antibodies (DakoCytomation Envision+) (Dako, Carpinteria, CA, USA) for 30 min. The first antibodies, rabbit polyclonal anti-collagen type II (1:100 working dilution) (Chemicon, Billerica, MA, USA) and rabbit polyclonal anti-aggrecan (1:100 working dilution) (Thermo Scientific, Rockford, IL, USA) were used. The sections were then incubated with 3, 3' diaminobenzidine (DAB) for 5 min to develop the color. The nuclei were counterstained with hematoxylin. All procedures were performed at room temperature.

2.3.7 Statistical analysis

All data were reported as the mean ± standard deviation (SD). One-way analysis of variance was performed to reveal significant differences, followed by Tukey's post hoc test for pairwise comparison. All statistical analyses were executed using KyPlot 2.0 beta 15. The difference was considered significant when the p-value was less than 0.05.

2.4 Results and Discussion

2.4.1 Preparation and characterization of collagen scaffolds

Ice particulates with a diameter range from 355 μm to 425 μm were prepared and used as a porogen material to prepare collagen porous scaffolds. The pre-prepared ice particulates were spherical (Figure 2.2 A).

The spherical ice particulates were mixed with an aqueous solution of collagen that was prepared by dissolving collagen in a solution of ethanol and acetic acid. The mixing process was conducted at -4 °C. At -4 °C, the ice particulates did not melt, and the collagen aqueous solution did not freeze, which facilitated complete mixing of the two components to obtain an even distribution of ice particulates in the collagen aqueous solution. The mixture of ice particulates and collagen aqueous solution was then frozen at -80 °C and freeze-dried. After cross-linking, collagen porous scaffolds were obtained. The collagen porous scaffolds prepared with ice particulates were defined as ice-collagen scaffolds. The ice-collagen scaffolds showed different appearance to that of control collagen scaffolds (Figure 2.2B, C).

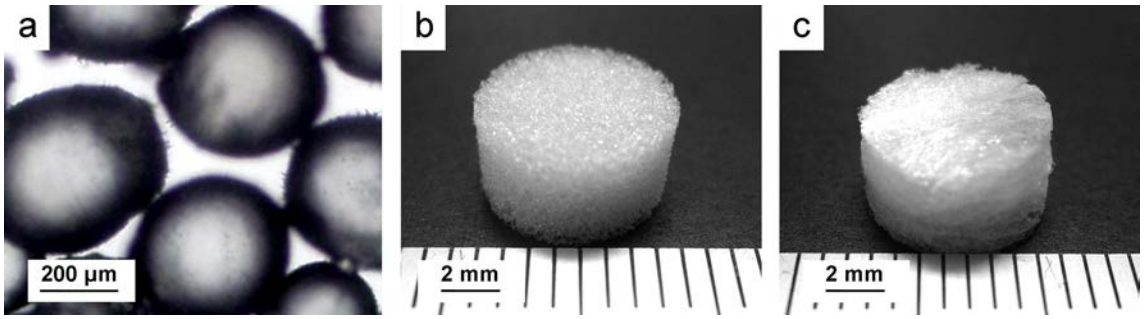

Figure 2.2 A phase-contrast photomicrograph of ice particulates (a) and gross appearance of collagen porous scaffold prepared with ice particulates (b) and control collagen scaffold (c).

Observation by scanning electron microscopy showed that there were interconnected large pores and small pores in the ice-collagen scaffolds (Figure 2.3). The large pores were spherical and were the same size as the ice particulates. The small pores had a random morphology and different sizes. The small pores surrounded the large spherical pores. The large pores were negative replicas of the pre-prepared ice particulates, while the small ice particulates were from the ice crystals formed during freezing. The density of the large spherical pores was low when 25% ice particulates were used to prepare the ice-collagen scaffolds (Figure 2.3 a, b). The large pore density increased when the percentage of ice particulates increased. The ice-collagen scaffolds prepared with 50% ice particulates showed the most homogenous pore structure (Figure 2.3 c, d). When 25% ice particulates were used, the large spherical pores were widely distributed, meaning there was some distance between the large pores. When 75% ice particulates were used, some collapsed large pores were observed (Figure 2.3 e, f). With a high ratio of ice particulates, the collagen aqueous solution filling the spaces between the spherical ice particulates decreased, and the collagen matrix surrounding the large pores decreased. In addition, mixing of the ice particulates and the collagen aqueous solution became difficult when the ice particulate ratio was high. The collapsed large pores could be due to the less dense collagen matrix and incomplete mixing.

The effect of the collagen concentration on the pore structure was investigated by fixing the ice particulate ratio at 50% (w/v) and changing the collagen concentration from 1% to 3% (w/v). Collapsed large pores were observed in ice-collagen scaffolds prepared with 1% and 3% collagen aqueous solutions. The collapsed large pores in collagen scaffolds prepared with the 1% collagen aqueous solution could have occurred because the low concentration resulted in a less dense collagen matrix surrounding the large pores (Figure 2.3 g, h). The case involving the 3% collagen aqueous solution could be due to incomplete mixing because the 3% collagen solution was too viscous (Figure 2.3 i, j). The ice-collagen scaffold prepared with the 2% collagen solution and an ice particulate/collagen solution ratio of 50 % showed the most homogeneous pore structure. The control scaffold prepared without ice particulates showed a heterogeneous

lamellar pore structure (Figure 2.3 k, l), consistent with previous study.[7]

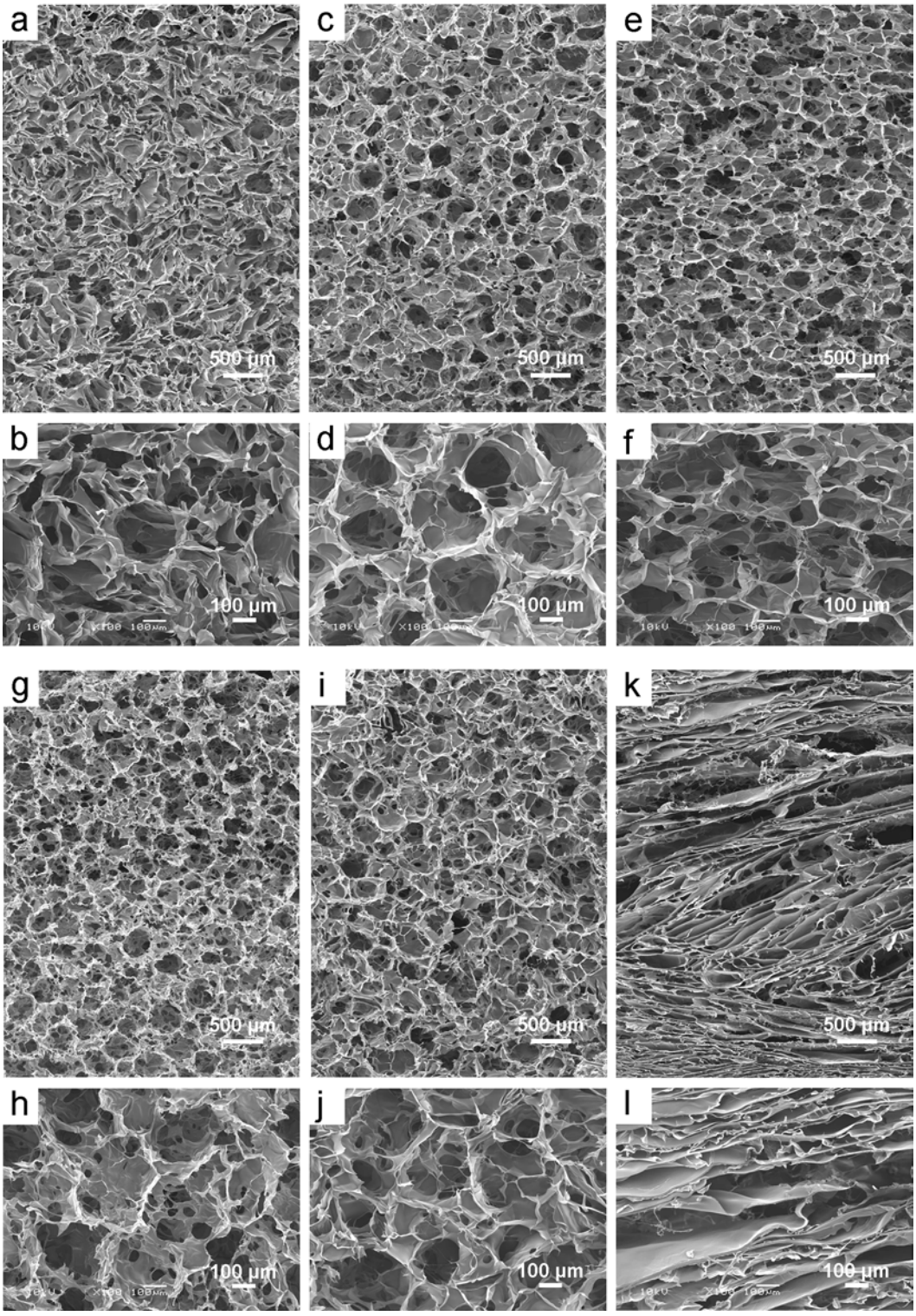

Figure 2.3 SEM images of cross sections of collagen porous scaffolds prepared with 2% collagen aqueous solution and ice particulates at a ratio of ice particulates/collagen solution of 25% (a, b), 50% (c, d) and 75% (e, f); collagen porous scaffolds prepared with a ratio of ice particulates/collagen solution of 50% and a collagen solution concentration of 1% (g, h) and 3% (i, j) and control collagen porous scaffolds prepared with 2% collagen aqueous solution without the use of ice particulates (k, l). The freezing temperature was

-80 °C. The images are shown in low (a, c, e, g, i, k) and high (b, d, f, h, j, l) magnification.

The porosity of collagen porous scaffolds was higher than 96% (Table 2.1). Such high porosity could satisfy the fabrication requirement of an ideal scaffold for tissue regeneration.

Table 2.1 Porosity of collagen porous scaffolds prepared with different amount of ice particulates and collagen solution concentrations. The data represent the mean ± SD, n=3.

Scaffold type	Porosity
No ice	96.3 ± 0.3%
25% ice	98.0 ± 0.2%
50% ice	98.5 ± 0.1%
75% ice	98.7 ± 0.4%
1% col	98.3 ± 0.1%
3% col	98.6 ± 0.2%

No significant difference among the collagen porous scaffolds.

The mechanical properties of ice-collagen scaffolds and control collagen scaffolds were measured by a static compression test (Table 2.2). Young's modulus of the ice-collagen scaffolds prepared with 2% collagen and 25% ice particulates, 2% collagen and 50% ice particulates, and 3% collagen and 50% ice particulates was significantly higher than that of the control collagen sponge. When collagen concentration was fixed at 2% and the ratio of ice particulates was changed, Young's modulus of the ice-collagen scaffolds increased in the following order: 75%<25%<50%. The ice-collagen scaffolds prepared with 50% ice particulates showed the highest Young's modulus. It was 15.7-fold higher than that of the control collagen scaffold. The differences in the mechanical properties were mainly ascribed to the different pore structures. The spherical pores formed by ice particulates were thought to resist mechanical loading, therefore reinforcing the collagen scaffolds. It has been reported that regular polygons can resist anisotropic mechanical loads to ensure stability.[27] The high mechanical strength of the collagen scaffold prepared with 50% ice particulates is due to the most appropriate packing of the large spherical pores and appropriate filling of the collagen matrix between the large spherical pores. The low mechanical strength of the collagen scaffold prepared with 75% ice particulates is due to the partially collapsed large pore structure. The mechanical properties of ice-collagen scaffolds prepared with different collagen concentrations and 50% ice particulates were also compared. Young's modulus increased as the collagen concentration increased, which can be explained by the presence of a dense collagen matrix surrounding the large pores when the collagen concentration increased.

Table 2.2 Compressive modulus of wet collagen porous scaffolds prepared with different amount of ice particulates and collagen solution concentrations. The data represent the mean ± SD, n=4.

Scaffold type	Young's modulus (kPa)
No ice	0.9 ± 0.1
25% ice	12.8 ± 0.9 ***
50% ice	14.1 ± 1.3 ***
75% ice	0.8 ± 0.1
1% col	1.0 ± 0.1
3% col	23.6 ± 2.3 ***

*** significant difference compared with the control the control "no ice" (p<0.001).

The results indicated that the pore structures of collagen porous scaffolds could be controlled by using ice particulates as a porogen material. There were interconnected large pores and small pores surrounding the large pores. The well-packed regular pores reinforced the scaffolds. The use of ice particulates as a porogen material requires good control of the mixing temperature. The temperature should be lower than the melting temperature of the ice particulates and higher than the freezing temperature of the polymer solution. When synthetic polymers are used, the organic solvents that are used to dissolve the biodegradable synthetic polymers have a much lower freezing temperature than the melting temperature of the ice particulates. However, for naturally derived polymers, water is usually used as a solvent. It has been difficult to mix the aqueous solution of naturally derived polymers with ice particulates without melting the ice and freezing the aqueous solution during mixing. In this chapter, a mixture solution of acetic acid and ethanol was used to dissolve collagen to prepare the aqueous solution. The prepared collagen aqueous solution did not freeze at -4 °C, which guaranteed homogeneous mixing of the ice particulates and collagen solution.

2.4.2 Cell distribution in the scaffolds

The ice-collagen scaffolds were used for three-dimensional culturing of bovine articular chondrocytes. Bovine chondrocytes were seeded on one side of the ice-collagen and control collagen scaffolds. After one week of culturing, the cell distribution was examined (Figure 2.4). In a comparison of all collagen scaffolds, the ice-collagen scaffold prepared with 2% collagen and 50% ice particulates showed the most homogeneous cell distribution due to its homogeneous pore structure (Figure 2.4 b). The ice-collagen scaffolds prepared with 25% and 75% ice particulates at a fixed collagen concentration of 2% and different collagen concentrations at a fixed ratio of ice particulates of 50% showed less homogenous cell distributions than did the scaffolds prepared with 50% ice particulates and 2% collagen solution. However, they showed more homogeneous cell distributions than did the control collagen scaffold. The less homogenous distribution of cells in the ice-scaffolds prepared with 25% ice particulates is due to the smaller number of large pores. The less homogenous distribution of cells in the ice-scaffolds prepared with 75% ice particulates and with 1% and 3% collagen solution occurred because of the collapsed pore structures. The lamellar cell distribution in the control collagen scaffold was a result of the lamellar pore structure.

The cell distribution was further quantitatively analyzed by frequency distribution of cell numbers in all collagen scaffolds (Figure 2.5). And the results showed that the ice-collagen scaffold prepared with 2% collagen and 50% ice particulates showed the most homogeneous cell distribution.

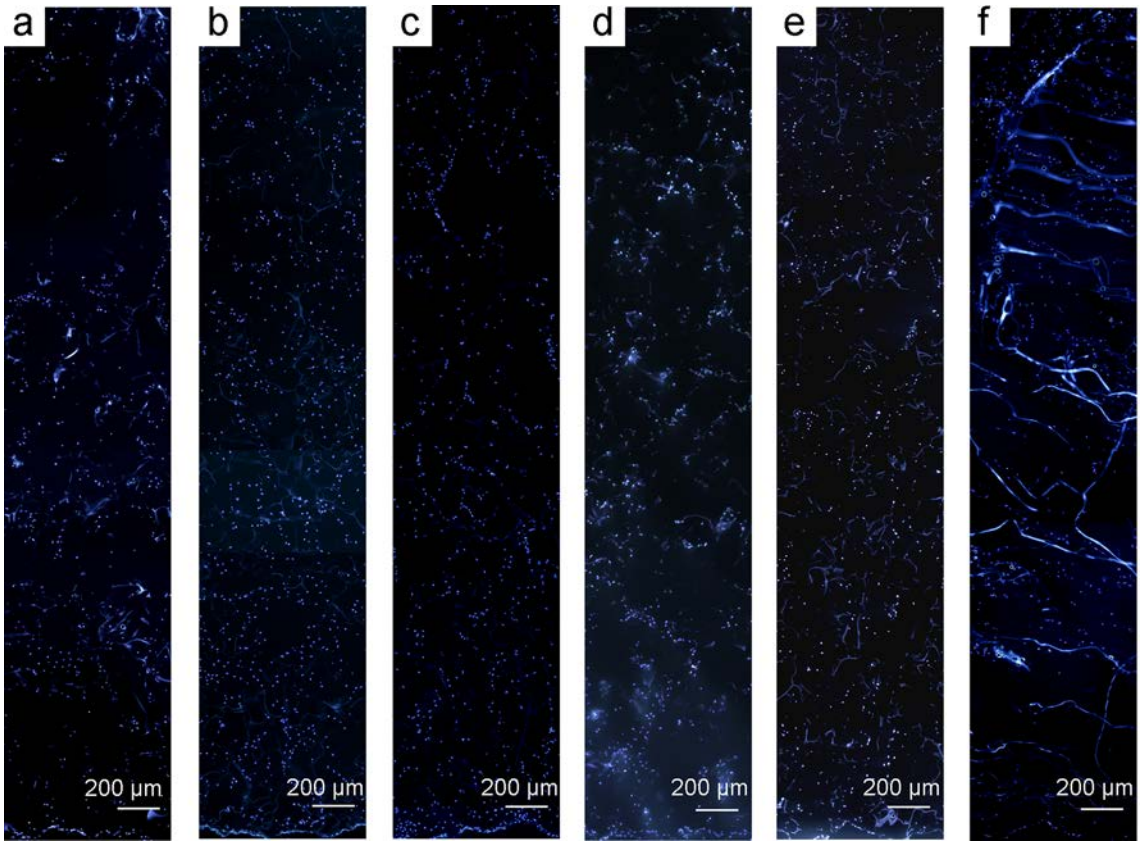

Figure 2.4 Cell distribution in the collagen porous scaffolds prepared with 2% collagen aqueous solution and ice particulates at a ratio of ice particulates/collagen solution of 25% (a), 50% (b) and 75% (c); collagen porous scaffolds prepared with a ratio of ice particulates/collagen solution of 50% and a collagen solution concentration of 1% (d) and 3% (e) and control collagen porous scaffolds prepared with 2% collagen

aqueous solution without the use of ice particulates (f) after 1 week of *in vitro* culture.

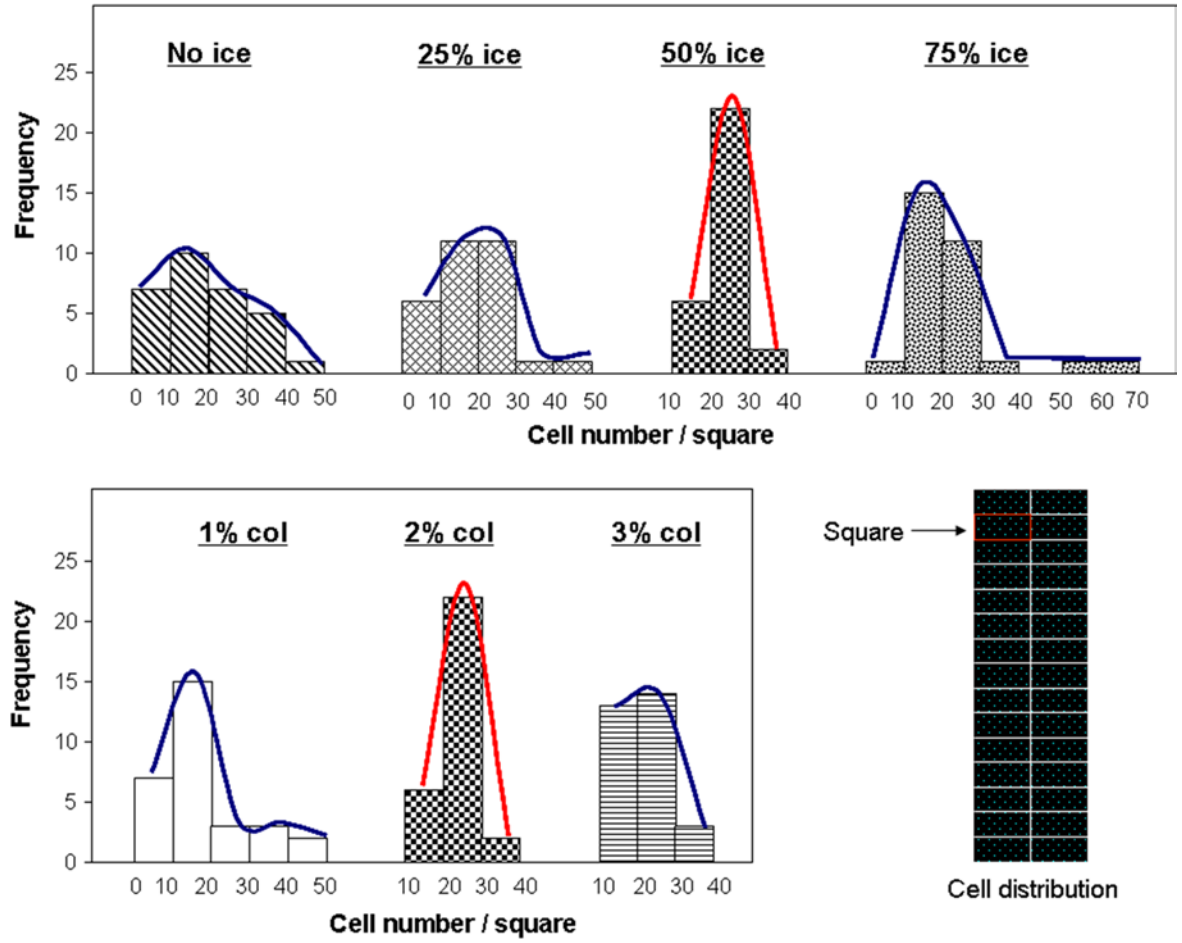

Figure 2.5 Frequency distribution graphs of cell number in each square of collagen scaffolds. The data were calculated using the photographs in figure 2.4.

2.4.3 Cartilage tissue regeneration

The cell distribution throughout the scaffold is a premise for uniform tissue formation. From the above results, the ice-collagen scaffold prepared with 2% collagen and 50% ice particulates showed the most homogeneous cell distribution. Therefore, we chose this scaffold for cartilage regeneration and compared its effect with that of the control collagen scaffold. Chondrocytes were seeded on both sides of the scaffolds and cultured *in vitro* for 1 w before implantation. The cells/scaffold constructs were then subcutaneously implanted in nude mice for 8 w. The gross appearance indicated that the ice-collagen scaffold implant maintained its original shape, while the control collagen scaffold implant deformed (Figure 2.6 a, b). The high mechanical strength of the ice-collagen scaffold protected it from cell-mediated contraction and suppression in the surrounding tissue during implantation.

After 8 w of implantation, the implants were examined by histological staining. HE staining showed a uniform spatial distribution of cells, a uniform extracellular matrx ECM distribution and homogeneous tissue formation in the ice-collagen scaffold (Figure 2.6c, d). However, the control collagen scaffold showed an uneven cell distribution, and some void spaces remained in the scaffold (Figure 2.6e, f).

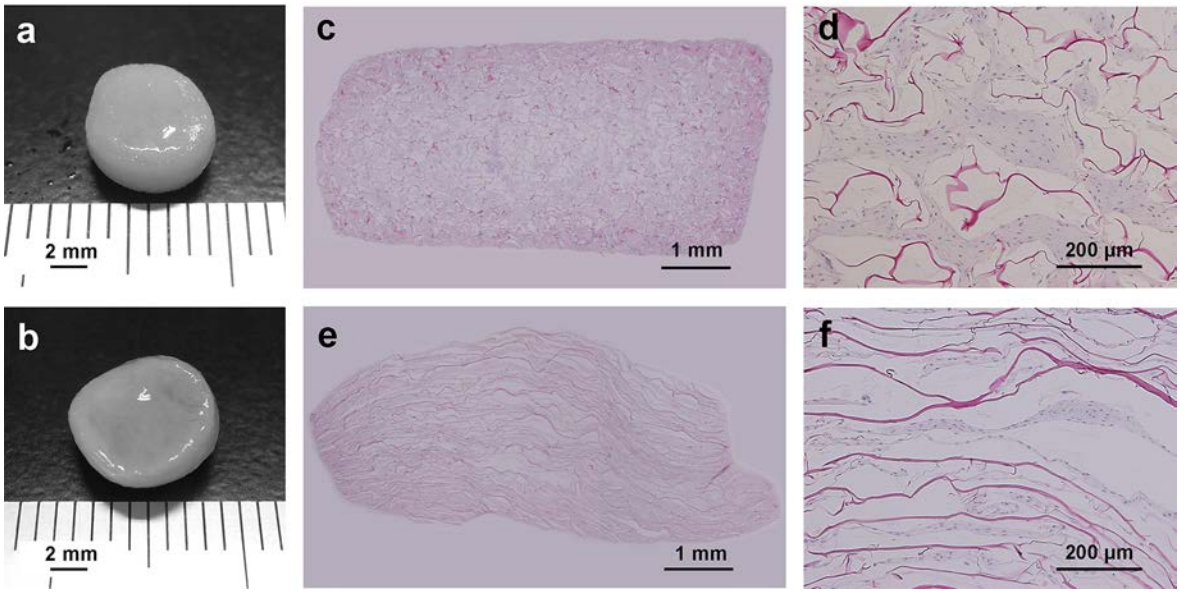

Figure 2.6 Gross appearance (a, b) and photomicrographs of HE staining (c-f) of engineered cartilage after 8 w of *in vivo* implantation of the cells/scaffold of a collagen porous scaffold prepared with 50% ice particulates and 2% collagen aqueous solution (a, c, d) and a control collagen scaffold (b, e, f).

The secretion of extracellular matrices is very important for cartilage regeneration because chondrocytes are surrounded by abundant extracellular matrices in cartilage.[28] The sGAG/DNA ratio in the implants after 1 w of *in vitro* culture and 8 w of *in vivo* implantation was quantified (Table 2.3). The sGAG/DNA ratio increased significantly from 1 w of *in vitro* culture to 8 w of *in vivo* implantation, which indicated that the chondrocytes produced extracellular matrices continually during *in vivo* implantation. The sGAG/DNA ratio in the ice-collagen scaffold was significantly higher than that in the control collagen scaffold. The result indicated that the ice-collagen scaffold was more favorable to the production of cartilaginous ECM and chondrocyte maturation than was the control scaffold.

Table 2.3 Ratio of sGAG/DNA of the cell/scaffold constructs after 1 w of *in vitro* culture and of the engineered cartilage after 8 w of *in vivo* implantation. The data represent the mean ± SD, n=3.

Scaffold type	sGAG/DNA (μg/μg)	
	1 week *in vitro*	8 weeks *in vivo*
50% ice	1.51 ± 0.06 **	6.90 ± 1.59 $^{*, a}$
No ice	1.04 ± 0.15	3.50 ± 0.19 ^{a}

** significant difference compared with the control "no ice" (p<0.01); * significant difference compared with the control "no ice" (p<0.05); ^{a} significant difference compared with the "1 week *in vitro*" (p<0.01).

Immunohistological staining of aggrecan and type II collagen showed that the tissue formed in both collagen scaffolds showed positive staining (Figure 2.7). Aggrecan and type II collagen in the ice-collagen scaffold were much more homogeneously and strongly stained than those in the control scaffold. Furthermore, the chondrocytes retained their typical spherical morphology in the lacunae much better in the ice-collagen scaffold than those in the control scaffold, as shown at a higher magnification.

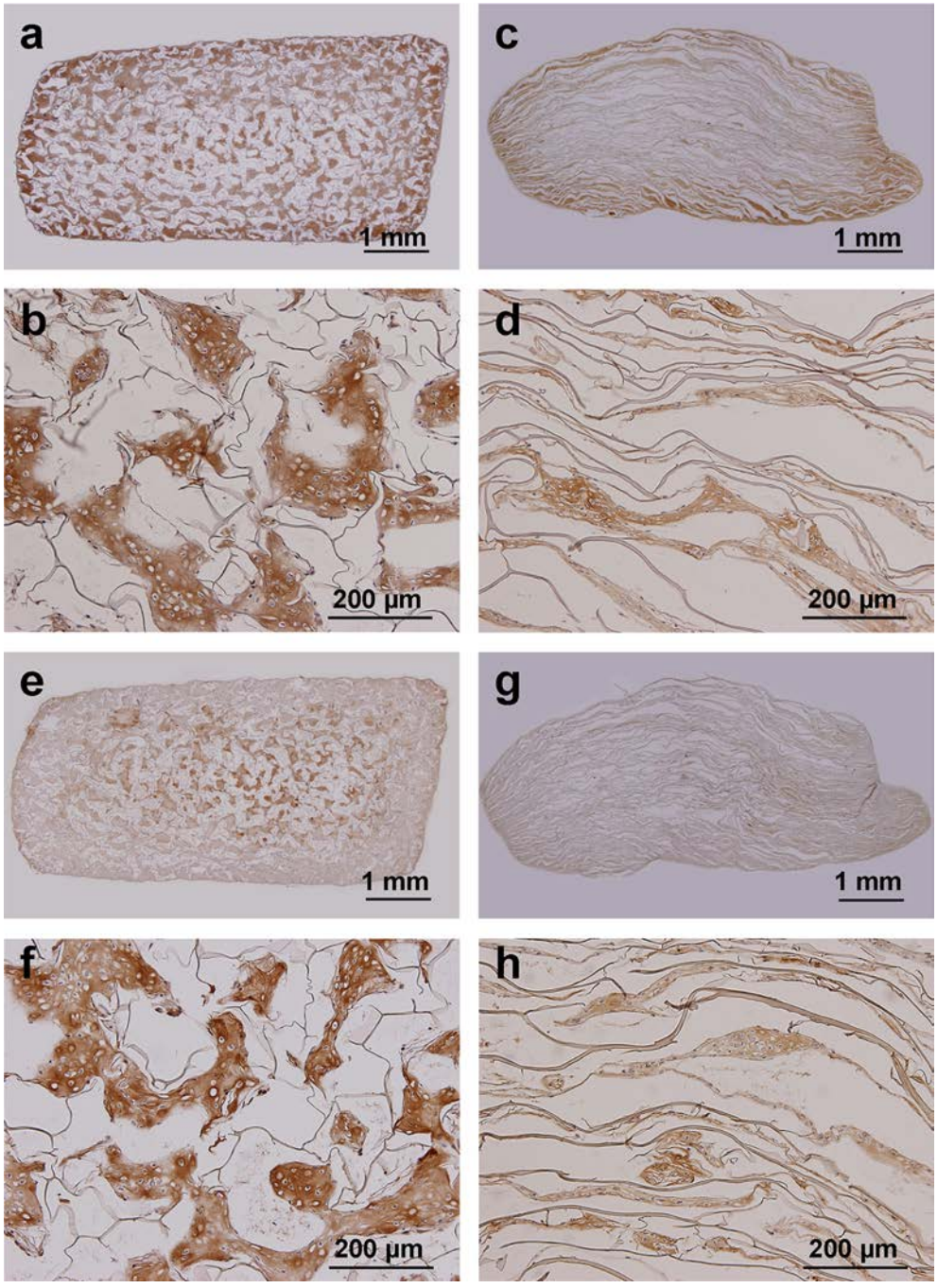

Figure 2.7 Photomicrographs of the immunohistochemical staining of aggrecan (a-d) and collagen II (e-h) of engineered cartilage after 8 w of *in vivo* implantation of the cells/scaffold of a collagen porous scaffold prepared with 50% ice particulates and 2% collagen aqueous solution (a, b, e, f) and a control collagen scaffold (c, d, g, h).

The mechanical properties of regenerated cartilage tissue after 8 w of *in vivo* implantation was measured by a compression test (Table 2.4). The compression Young's moduli of the regenerated cartilage tissue in the collagen porous scaffold prepared with ice particulates and in the control collagen scaffold were 199.0 ± 8.7 and 118.7 ± 7.5 KPa, respectively. Cartilage regenerated in the ice-collagen scaffold showed significantly higher mechanical properties than did that in the control collagen scaffold.

Table 2.4 Compressive modulus of engineered cartilage after 8 w of *in vivo* implantation. The data represent the mean ± SD, n=3.

Scaffold type	Young's modulus (kPa)
50% ice	199.0 ± 8.7 ***
No ice	118.7 ± 7.5

*** significant difference compared with the control the control "no ice" (p<0.001).

These results indicated that the ice-collagen scaffold supported promoted cartilage tissue regeneation more strongly than did the control scaffold. The precisely controlled pore structures involving the interconnected large pores allowed homogeneous distribution of cells throughout the scaffolds, which supported homogenous tissue formation. The improved mechanical properties protected the scaffold from the cell-mediated shrinkage and suppression of the surrounding tissue. These synergistic effects should facilitate the regeneration of cartilage. The collagen porous scaffolds prepared by using ice particulates can also be used for tissue engineering of other tissues and organs. The use of ice particulates as a porogen material had many advantages. The ice particulate template can initiate the formation of a connected ice crystal network inside the aqueous polymer solution during the freezing process, and the ice crystal network can easily be removed by freeze-drying.[29] The spherical nature of the porogen material can produce compact packing of the pores and improve the mechanical properties. The method can also be used to prepare porous scaffolds of other naturally derived polymers for tissue engineering and regenerative medicine.

2.5 Conclusions

Collagen porous scaffolds with precisely controlled pore structures and excellent mechanical properties were prepared by using pre-prepared ice particulates as a porogen material. The scaffolds showed high porosity and had interconnected large spherical pores surrounded by small pores. Young's modulus increased 15.7-fold compared with that of collagen scaffolds prepared by the conventional freeze-drying method. The precisely controlled pore structure and improved mechanical property facilitated an even cell distribution throughout the scaffolds and the regeneration of cartilage tissue. The method will be useful for the preparation of porous scaffolds of naturally derived biodegradable polymers for tissue engineering and regenerative medicine.

2.6 References

1. Indolfi, L., Baker, A.B.,Edelman, E.R. The role of scaffold microarchitecture in engineering endothelial cell immunomodulation. *Biomaterials* **33**, 7019-7027 (2012).
2. Lu, H.X., Kawazoe, N., Kitajima, T., Myoken, Y., Tomita, M., Umezawa, A., Chen, G.P.,Ito, Y. Spatial immobilization of bone morphogenetic protein-4 in a collagen-PLGA hybrid scaffold for enhanced osteoinductivity. *Biomaterials* **33**, 6140-6146 (2012).
3. Bhardwaj, N.,Kundu, S.C. Chondrogenic differentiation of rat MSCs on porous scaffolds of silk fibroin/chitosan blends. *Biomaterials* **33**, 2848-2857 (2012).

4. Moutos, F.T., Freed, L.E.,Guilak, F. A biomimetic three-dimensional woven composite scaffold for functional tissue engineering of cartilage. *Nature Materials* **6**, 162-167 (2007).
5. Hollister, S.J. Porous scaffold design for tissue engineering. *Nature Materials* **4**, 518-524 (2005).
6. Engelmayr, G.C., Cheng, M.Y., Bettinger, C.J., Borenstein, J.T., Langer, R.,Freed, L.E. Accordion-like honeycombs for tissue engineering of cardiac anisotropy. *Nature Materials* **7**, 1003-1010 (2008).
7. Faraj, K.A., Van Kuppevelt, T.H.,Daamen, W.F. Construction of collagen scaffolds that mimic the three- dimensional architecture of specific tissues. *Tissue Eng* **13**, 2387-2394 (2007).
8. Silva, M.M.C.G., Cyster, L.A., Barry, J.J.A., Yang, X.B., Oreffo, R.O.C., Grant, D.M., Scotchford, C.A., Howdle, S.M., Shakesheff, K.M.,Rose, F.R.A.J. The effect of anisotropic architecture on cell and tissue infiltration into tissue engineering scaffolds. *Biomaterials* **27**, 5909-5917 (2006).
9. O'Brien, F.J., Harley, B.A., Yannas, I.V.,Gibson, L.J. The effect of pore size on cell adhesion in collagen-GAG scaffolds. *Biomaterials* **26**, 433-441 (2005).
10. Woodfield, T.B.F., Malda, J., de Wijn, J., Peters, F., Riesle, J.,van Blitterswijk, C.A. Design of porous scaffolds for cartilage tissue engineering using a three-dimensional fiber-deposition technique. *Biomaterials* **25**, 4149-4161 (2004).
11. Gauvin, R., Chen, Y.C., Lee, J.W., Soman, P., Zorlutuna, P., Nichol, J.W., Bae, H., Chen, S.C.,Khademhosseini, A. Microfabrication of complex porous tissue engineering scaffolds using 3D projection stereolithography. *Biomaterials* **33**, 3824-3834 (2012).
12. McClure, M.J., Wolfe, P.S., Simpson, D.G., Sell, S.A.,Bowlin, G.L. The use of air-flow impedance to control fiber deposition patterns during electrospinning. *Biomaterials* **33**, 771-779 (2012).
13. Liu, X.H.,Ma, P.X. Phase separation, pore structure, and properties of nanofibrous gelatin scaffolds. *Biomaterials* **30**, 4094-4103 (2009).
14. Meng, W., Kim, S.Y., Yuan, J., Kim, J.C., Kwon, O.H., Kawazoe, N., Chen, G.P., Ito, Y.,Kang, I.K. Electrospun PHBV/collagen composite nanofibrous scaffolds for tissue engineering. *J Biomat Sci-Polym E* **18**, 81-94 (2007).
15. Sun, W., Starly, B., Darling, A.,Gomez, C. Computer-aided tissue engineering: application to biomimetic modelling and design of tissue scaffolds. *Biotechnol Appl Bioc* **39**, 49-58 (2004).
16. Zhang, H.F., Hussain, I., Brust, M., Butler, M.F., Rannard, S.P.,Cooper, A.I. Aligned two- and three-dimensional structures by directional freezing of polymers and nanoparticles. *Nature Materials* **4**, 787-793 (2005).
17. Yoon, J.J., Kim, J.H.,Park, T.G. Dexamethasone-releasing biodegradable polymer scaffolds fabricated by a gas-foaming/salt-leaching method. *Biomaterials* **24**, 2323-2329 (2003).
18. Hou, Q.P., Grijpma, D.W.,Feijen, J. Porous polymeric structures for tissue engineering prepared by a coagulation, compression moulding and salt leaching technique. *Biomaterials* **24**, 1937-1947 (2003).
19. Harris, L.D., Kim, B.S.,Mooney, D.J. Open pore biodegradable matrices formed with gas foaming. *J Biomed Mater Res* **42**, 396-402 (1998).
20. Choi, S.W., Xie, J.W.,Xia, Y.N. Chitosan-Based Inverse Opals: Three-Dimensional Scaffolds with Uniform Pore Structures for Cell Culture. *Adv Mater* **21**, 2997-+ (2009).
21. Vaquette, C., Frochot, C., Rahouadj, R.,Wang, X. An innovative method to obtain porous PLLA scaffolds with highly spherical and interconnected pores. *J Biomed Mater Res B* **86B**, 9-17 (2008).
22. Chen, V.J.,Ma, P.X. Nano-fibrous poly(L-lactic acid) scaffolds with interconnected spherical macropores. *Biomaterials* **25**, 2065-2073 (2004).

23. Ma, P.X.,Choi, J.W. Biodegradable polymer scaffolds with well-defined interconnected spherical pore network. *Tissue Eng* **7**, 23-33 (2001).
24. Chen, G.P., Ushida, T.,Tateishi, T. Preparation of poly(L-lactic acid) and poly(DL-lactic-co-glycolic acid) foams by use of ice microparticulates. *Biomaterials* **22**, 2563-2567 (2001).
25. Ko, Y.G., Kawazoe, N., Tateishi, T.,Chen, G.P. Preparation of Novel Collagen Sponges Using an Ice Particulate Template. *J Bioact Compat Pol* **25**, 360-373 (2010).
26. Ko, Y.G., Grice, S., Kawazoe, N., Tateishi, T.,Chen, G.P. Preparation of Collagen-Glycosaminoglycan Sponges with Open Surface Porous Structures Using Ice Particulate Template Method. *Macromol Biosci* **10**, 860-871 (2010).
27. Meyers, M.A., Chen, P.Y., Lin, A.Y.M.,Seki, Y. Biological materials: Structure and mechanical properties. *Prog Mater Sci* **53**, 1-206 (2008).
28. Magne, D., Julien, M., Vinatier, C., Merhi-Soussi, F., Weiss, P.,Guicheux, J. Cartilage formation in growth plate and arteries: from physiology to pathology. *Bioessays* **27**, 708-716 (2005).
29. Zhang, H.,Cooper, A.I. Aligned porous structures by directional freezing. *Adv Mater* **19**, 1529-1533 (2007).

Chapter 3

Preparation of collagen porous scaffolds with a gradient pore size structure

3.1 Summary

Some cell functions as well as new tissue regeneration deeply rely on the size of the pores. The use of a gradient pore structure may provide a useful and practical tool to compare the effect of different pore sizes under the same culture conditions. Therefore, in this chapter, collagen porous scaffolds with a gradient pore size were prepared by using pre-prepared ice particulates as a porogen material. The ice particulates had diameters of 150-250, 250-355, 355-425 and 425-500 μm. The gradient collagen scaffolds had well-interconnected pore structures with compactly packed spherical pores. The gradient pore scaffolds were used for culture of bovine articular chondrocytes, directly examining the effect of pore size on cartilage regeneration. Chondrocytes adhered and showed a homogenous distribution throughout the scaffolds. *In vivo* implantation results indicated that the micropores in the scaffolds prepared with ice particulates in the range of 150-250 μm showed the most beneficial effect on cartilage regeneration. Gradient scaffolds prepared with ice particulates were a useful tool to directly compare the effects of scaffold pore size on tissue regeneration.

3.2 Introduction

Porous scaffolds have been widely used in tissue engineering to control cell functions and to guide new tissue formation.[1-3] Scaffolds serve as a temporary template to provide biological and physical cues to support cell adhesion, to promote proliferation and to induce differentiation of stem cells or progenitor cells into specific lineage.[4] The pore structure of scaffolds is an important factor affecting tissue regeneration efficiency. Although a number of porous scaffolds have been developed from various types of biomaterials, controlling the pore structure remains a key factor to create ideal porous scaffolds for tissue engineering.[5-11] Many reports show the effects of the pore size of a porous scaffold on tissue regeneration.[12-24] Some of the reported results do not agree with each other. Thus far, studies on the effects of pore size on tissue regeneration have primarily compared individual scaffolds with different pore sizes after they are separately cultured. Variations in the separate cultures may cause some unpredicted factor to influence the results. The

use of a gradient pore structure may provide a useful and practical tool to compare the effect of different pore sizes under the same culture conditions. In this chapter, collagen porous scaffolds with a gradient pore size structure were prepared by using pre-prepared ice particulates as a porogen material. The scaffolds were used to culture articular chondrocytes, directly comparing the effect of the pore size on cartilaginous matrix production and cartilage regeneration.

3.3 Materials and methods

3.3.1 Scaffold preparation and characterization

Collagen porous scaffolds with a gradient pore size structure were made by using prepared ice particulates as a porogen material. At first, an aqueous collagen solution (2% (w/v)) of porcine type I collagen (Nitta Gelatin, Osaka, Japan) in a mixture of ethanol and acetic acid (20:80 v/v, pH 3.0) was prepared. The ice particulates were prepared by spraying Milli Q water into liquid nitrogen using a sprayer. The ice particulates were sieved by sieves with mesh pores of 150, 250, 355, 425 and 500 μm to obtain ice particulates having diameters of 150-250, 250-355, 355-425, and 425-500 μm. Then, the aqueous collagen solution was mixed with the sieved ice particulates in a 50:50 (v/w) ratio at a -4 °C low-temperature chamber. Each of the four mixtures of collagen solution and ice particulates of different diameters was poured into a silicone frame that was then placed on a PFA film-wrapped copper plate, and the mixture surface was flattened with a steel spatula. The four mixtures in their frames were stacked together with ice particulate sizes increasing from bottom to top (Figure 3.1). Finally, the entire set was frozen at -80 °C for 6 hours, and the frozen constructs were freeze-dried for 3 days in a Wizard 2.0 freeze dryer (VirTis, Gardiner, NY). The freeze-dried constructs were cross-linked with glutaraldehyde vapor that was saturated with a 25% aqueous glutaraldehyde solution at 37 °C for 4 hours. The final scaffolds were freeze-dried again for following analyses. The microstructures were observed using a JSM-5610 scanning electron microscope (JEOL, Tokyo, Japan). The mean pore size of the collagen porous scaffolds was measured from their SEM images by a MetaVue Image System (Universal Imaging Corp., Buckinghamshire, UK). Six images were taken of each scaffold and used for the mean pore size calculation.

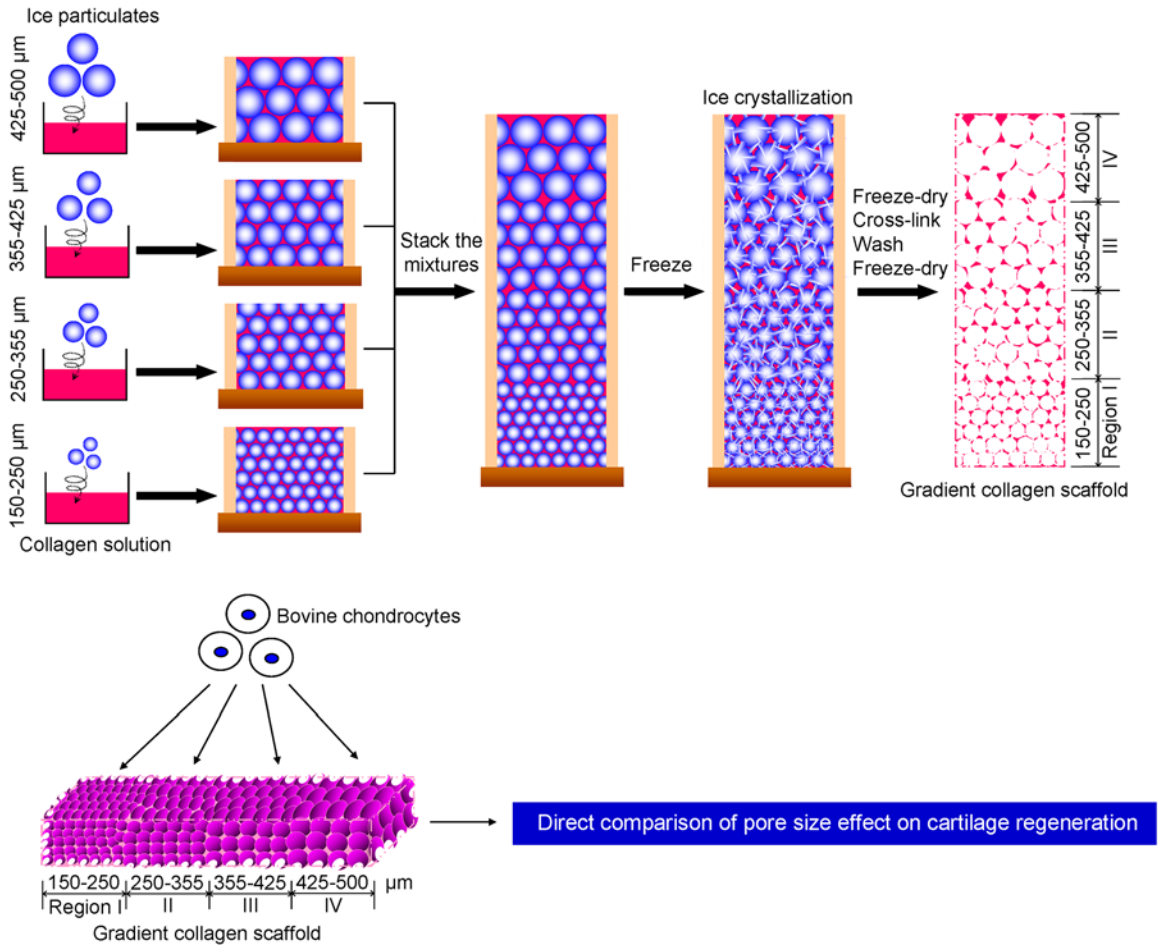

Figure 3.1 Preparation schme of a gradient pore size collagen scaffold.

3.3.2 In vitro cell culture

The gradient collagen porous scaffolds were cut into cuboids (6 mm × 16 mm × 3 mm, W × L × H, where L represents the direction of the pore gradient) which covered the entire pore range. The samples were sterilized with 70% ethanol, washed 3 times with Milli Q water. Bovine articular chondrocytes were statically seeded into the scaffolds twice by adding 200 μL of the cell suspension solution (1.0×10^7 cells/scaffold) to each of the 6 mm × 16 mm (W × L) sides of the scaffolds to guarantee homogeneous cell seeding. The second seeding was performed 3 hours after the first to allow for cell adhesion. The cell/scaffold constructs were then cultured in DMEM containing 10% fetal bovine serum under an atmosphere of 5% CO_2 at 37 °C with shaking (60/min, for diffusion of nutrients and metabolic substances) for 1 week. The medium was changed every 3 days. The cell distribution in the gradient collagen scaffolds was evaluated after 6 hours of culture by examining a cross-section of 0.25% glutaraldehyde solution-fixed samples. The cross-sections (L × H) were stained with Hoechst 33258 (10 μg/mL) and observed under a fluorescence microscope (Olympus, Tokyo, Japan).

3.3.3 In vivo implantation and evaluation of engineered cartilage

After 1 week of *in vitro* culture, the cell/scaffold constructs were subcutaneously implanted into the dorsa of 6-week-old athymic nude mice. The animal experiment was conducted according to the committee

guidelines of the National Institute for Materials Science for Animal Experiments. After the constructs were implanted for 8 weeks, the mice were scarified and the implants were fixed in 10% formalin, embedded in paraffin and sectioned (7 μm thick sections). The cross-sections (L × H) were stained with hematoxylin and eosin (HE), Safranin O and light green staining. The cross-sections (L × H) were also immunostained for type II collagen and aggrecan. Briefly, the deparaffinized sections were incubated with proteinase K for 10 min for antigen retrieval, and then incubated with peroxidase blocking solution for 5 min and 10% goat serum solution for 30 min. The sections were next incubated with the first antibodies for 1 h, followed by incubation with the peroxidase-labeled polymer-conjugated second antibodies (DakoCytomation Envision+) (Dako, Carpinteria, CA, USA) for 30 min. The first antibody was rabbit polyclonal anti-collagen type II (in a 1:100 working dilution) (Thermo Scientific, Rockford, IL, USA). The sections were then incubated with 3, 3' diaminobenzidine (DAB) for 5 min to develop color. The nuclei were counterstained with hematoxylin. All procedures were performed at room temperature.

3.4 Results and Discussion

3.4.1 Collagen porous scaffolds with a gradient pore size structure

The gross appearance of the gradient collagen scaffolds and their illustrated pore structure are shown in Figures 3.2 a and b. The porous structure of the right segment was comprised of large pores, as can be seen in the photo, while the porous structure of the left segment and its small pore size is not obvious in the photo.

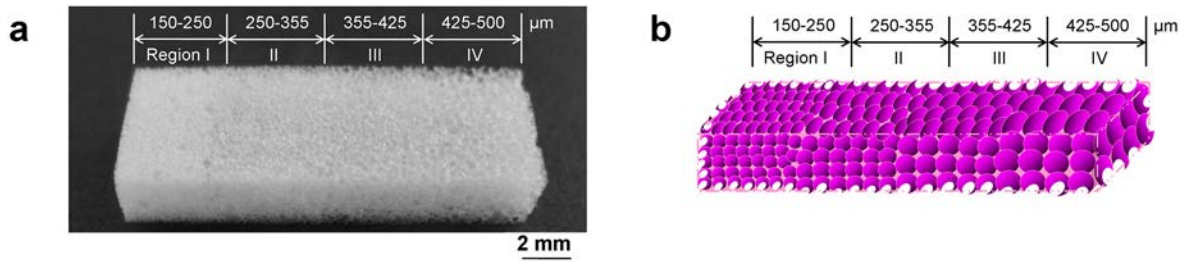

Figure 3.2 A photograph (a) and an illustration (b) of pore structure of the gradient collagen scaffold with four different regions, prepared with ice particulates having a diameter range of 150-250, 250-355, 355-425 and 425-500 μm.

The microstructure observed by SEM indicated that spherical pores were formed (Figure 3.3). Four regions of different pore sizes were also confirmed. The pore size increased from the left to the right. Images at a high magnification showed that the spherical large pores were compactly stacked and well interconnected. The sizes of the large pores in the four regions, which were prepared with ice particulates having diameters of (I) 150-250, (II) 250-355, (III) 355-425 and (IV) 425-500 μm, were 165 ± 33, 259 ± 41, 357 ± 35 and 431 ± 36 μm, respectively. The sizes of the large pores were in a good agreement with the sizes of the prepared ice particulates.

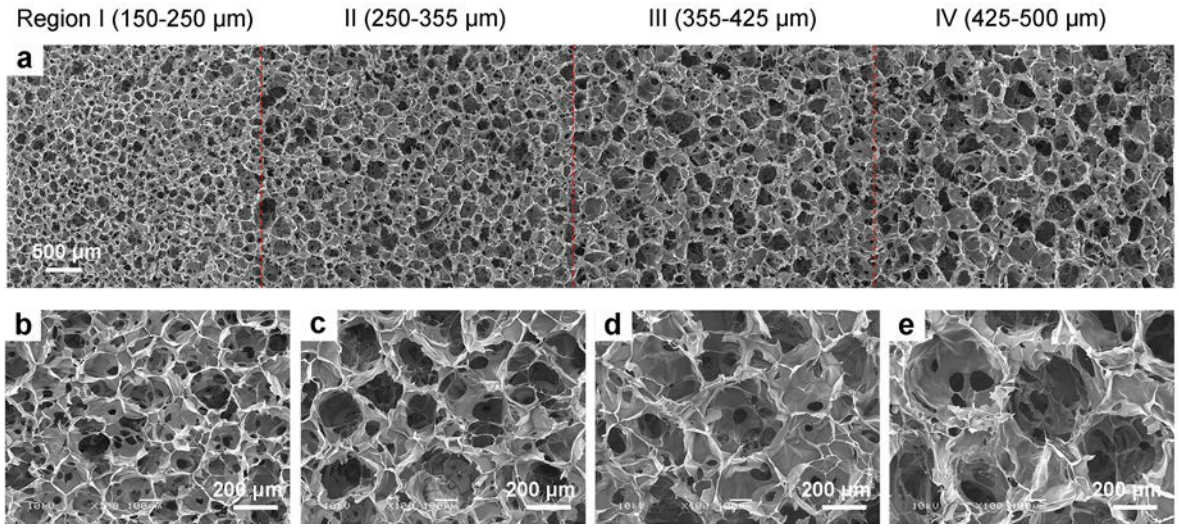

Figure 3.3 SEM photomicrographs of the gradient collagen scaffold cross-section (a) and highly magnified photomicrographs of the four different regions, prepared with ice particulates having a diameter range of 150-250 (b), 250-355 (c), 355-425 (d) and 425-500 μm (e).

3.4.2 Cell distribution in the gradient collagen porous scaffolds

The scaffolds were seeded with bovine articular chondrocytes and cultured *in vitro*. Nucleus staining showed that the chondrocytes were homogeneously distributed throughout the scaffolds (Figure 3.4).

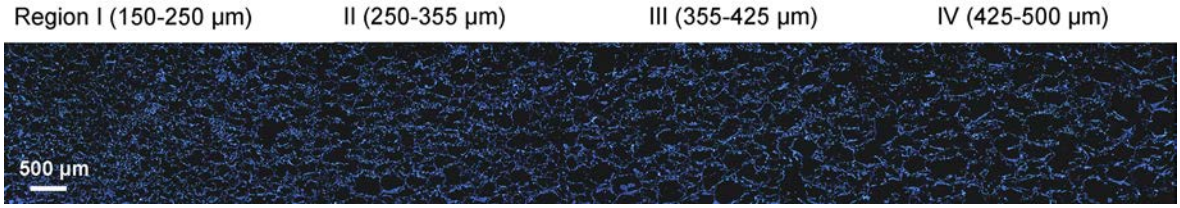

Figure 3.4 Cell distribution in a gradient collagen scaffold. Cell nuclei were stained by Hoechst 33258 and observed under a fluorescence microscope.

3.4.3 Histological and immunohistological stainings of regenerated cartilage

The cell/scaffold constructs were subcutaneously implanted into nude mice for 8 weeks. The implants appeared glisteningly white (Figure 3.5 a). HE staining showed that the spatial cell and extracellular matrix (ECM) distribution was uniform and that tissue formation was homogeneous in the gradient collagen scaffold (Figure 3.5 b-d). Safranin O staining showed that glycosaminoglycan (GAG) was abundant and mainly distributed around the central parts in the scaffolds (Figure 3.5 c). The collagen scaffold with the smallest pore size, 150-250 μm, showed the most compact and abundant glycosaminoglycan (GAG) production by the chondrocytes. Based on the HE and Safranin O staining results, the degree of cartilage regeneration in the 4 regions was determined to increase in the following order: region III ≈ region II < region IV < region I. The smallest pore size, prepared with the 150-250 μm ice particulates, best promoted cartilaginous matrix formation.

Immunostaining of type II collagen was positive for the tissues formed in all 4 regions (Figure 3.5 d). Type II collagen was more strongly stained in the central area of each region than the periphery. The

central area in region I showed the strongest staining. The intensity of the stained type II collagen increased in the following order: region III ≈ region II < region IV < region I. The histological and immunohistological stainings together indicated that the potential for cartilage regeneration in the four regions was the following: region III ≈ region II < region IV < region I. The micropores in the scaffolds prepared with ice particulates in the range of 150-250 μm showed the most beneficial three-dimensional microenvironment for cartilaginous matrix expression and chondrogenic differentiation. Gradient scaffolds prepared with ice particulates were a useful tool to directly compare the effects of scaffold pore size on tissue regeneration.

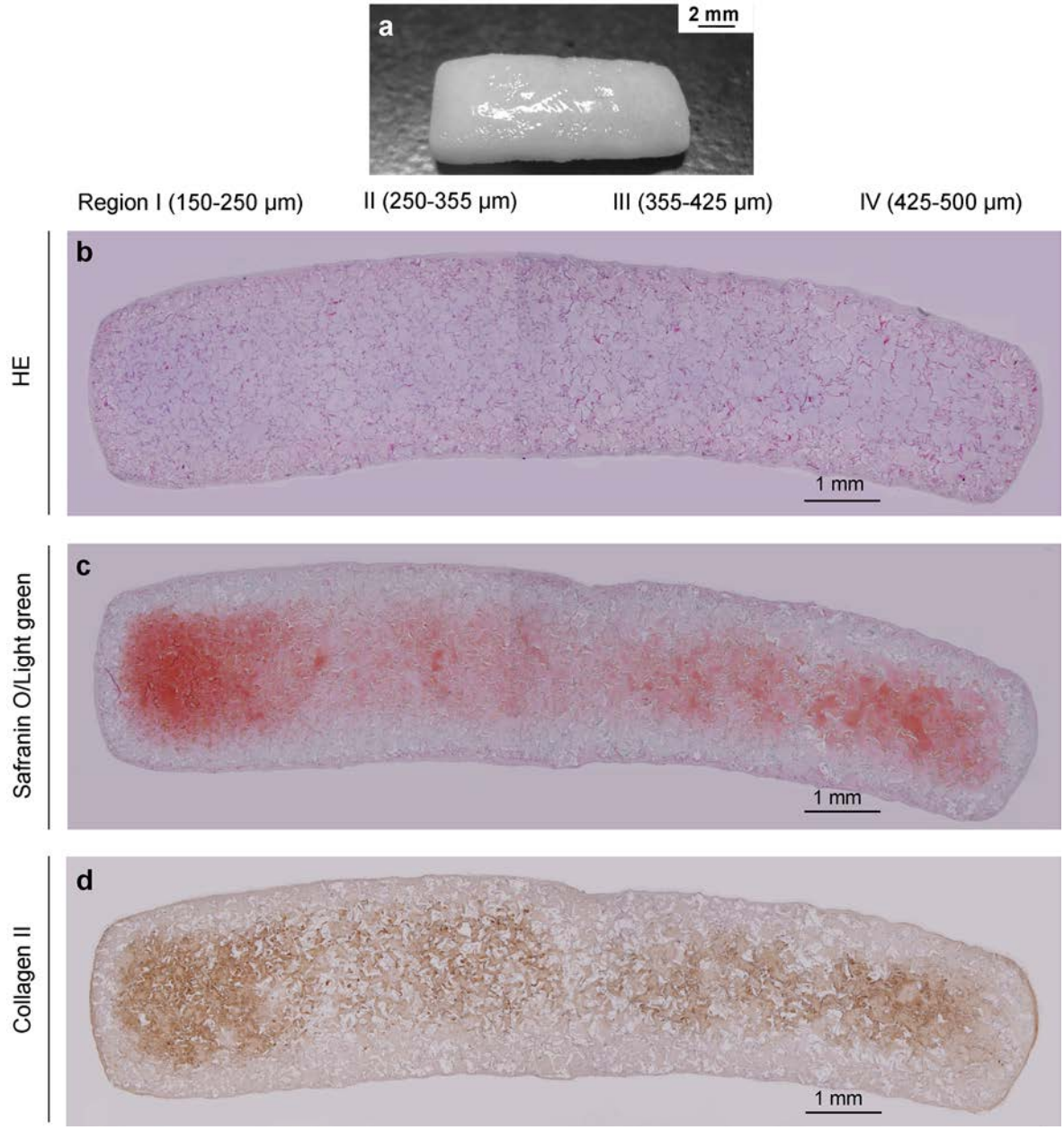

Figure 3.5 Gross appearances (a) and photomicrographs of HE staining (b), Safranin O/light green staining (c) and immunohistochemical staining of type II collagen (d) of the cells in the gradient collagen scaffold constructs after 8 weeks of *in vivo* implantation.

3.5 Conclusions

Collagen porous scaffolds with pore size gradients could be prepared using ice particulates as a porogen material. The gradient collagen scaffolds had spherical pore structures with good interconnectivity. The effect of pore size on cartilage tissue formation was directly compared by culturing bovine articular chondrocytes in the gradient collagen scaffolds. The micropores in the scaffolds prepared with ice particulates in the range of 150-250 μm showed the most beneficial effect on cartilage regeneration. Gradient scaffolds prepared with ice particulates were a useful tool to study the effects of scaffold pore size on tissue regeneration.

3.6 References

1. Lu, H.X., Kawazoe, N., Kitajima, T., Myoken, Y., Tomita, M., Umezawa, A., Chen, G.P.,Ito, Y. Spatial immobilization of bone morphogenetic protein-4 in a collagen-PLGA hybrid scaffold for enhanced osteoinductivity. *Biomaterials* **33**, 6140-6146 (2012).
2. Wang, C.,Wang, M. Dual-source dual-power electrospinning and characteristics of multifunctional scaffolds for bone tissue engineering. *J Mater Sci-Mater M* **23**, 2381-2397 (2012).
3. Lin, K.L., Chang, J., Zeng, Y.,Qian, W.J. Preparation of macroporous calcium silicate ceramics. *Mater Lett* **58**, 2109-2113 (2004).
4. Higuchi, A., Ling, Q.D., Chang, Y., Hsu, S.T.,Umezawa, A. Physical Cues of Biomaterials Guide Stem Cell Differentiation Fate. *Chemical Reviews* (2013).
5. Duan, B.,Wang, M. Customized Ca-P/PHBV nanocomposite scaffolds for bone tissue engineering: design, fabrication, surface modification and sustained release of growth factor. *J R Soc Interface* **7**, S615-S629 (2010).
6. Tong, H.W.,Wang, M. A novel technique for the fabrication of 3D nanofibrous scaffolds using simultaneous positive voltage electrospinning and negative voltage electrospinning. *Mater Lett* **94**, 116-120 (2013).
7. Tong, H.W., Zhang, X.,Wang, M. A new nanofiber fabrication technique based on coaxial electrospinning. *Mater Lett* **66**, 257-260 (2012).
8. Engelmayr, G.C., Cheng, M.Y., Bettinger, C.J., Borenstein, J.T., Langer, R.,Freed, L.E. Accordion-like honeycombs for tissue engineering of cardiac anisotropy. *Nature Materials* **7**, 1003-1010 (2008).
9. Haugh, M.G., Murphy, C.M.,O'Brien, F.J. Novel freeze-drying methods to produce a range of collagen-glycosaminoglycan scaffolds with tailored mean pore sizes. *Tissue Eng Part C Methods* **16**, 887-894 (2010).
10. Lee, J.W., Nguyen, T.A., Kang, K.S., Seol, Y.J.,Cho, D.W. Development of a growth factor-embedded scaffold with controllable pore size and distribution using micro-stereolithography. *Tissue Eng Pt A* **14**, 835-835 (2008).
11. Nuernberger, S., Cyran, N., Albrecht, C., Redl, H., Vecsei, V.,Marlovits, S. The influence of scaffold architecture on chondrocyte distribution and behavior in matrix-associated chondrocyte transplantation grafts. *Biomaterials* **32**, 1032-1040 (2011).

12. Murphy, C.M., Haugh, M.G.,O'Brien, F.J. The effect of mean pore size on cell attachment, proliferation and migration in collagen-glycosaminoglycan scaffolds for bone tissue engineering. *Biomaterials* **31**, 461-466 (2010).
13. O'Brien, F.J., Harley, B.A., Yannas, I.V.,Gibson, L.J. The effect of pore size on cell adhesion in collagen-GAG scaffolds. *Biomaterials* **26**, 433-441 (2005).
14. Stenhamre, H., Nannmark, U., Lindahl, A., Gatenholm, P.,Brittberg, M. Influence of pore size on the redifferentiation potential of human articular chondrocytes in poly(urethane urea) scaffolds. *J Tissue Eng Regen M* **5**, 578-588 (2011).
15. Lien, S.M., Ko, L.Y.,Huang, T.J. Effect of pore size on ECM secretion and cell growth in gelatin scaffold for articular cartilage tissue engineering. *Acta Biomater* **5**, 670-679 (2009).
16. Nehrer, S., Breinan, H.A., Ramappa, A., Young, G., Shortkroff, S., Louie, L.K., Sledge, C.B., Yannas, I.V.,Spector, M. Matrix collagen type and pore size influence behaviour of seeded canine chondrocytes. *Biomaterials* **18**, 769-776 (1997).
17. Oh, S.H., Park, I.K., Kim, J.M.,Lee, J.H. In vitro and in vivo characteristics of PCL scaffolds with pore size gradient fabricated by a centrifugation method. *Biomaterials* **28**, 1664-1671 (2007).
18. Sobral, J.M., Caridade, S.G., Sousa, R.A., Mano, J.F.,Reis, R.L. Three-dimensional plotted scaffolds with controlled pore size gradients: Effect of scaffold geometry on mechanical performance and cell seeding efficiency. *Acta Biomater* **7**, 1009-1018 (2011).
19. Stoppato, M., Carletti, E., Sidarovich, V., Quattrone, A., Unger, R.E., Kirkpatrick, C.J., Migliaresi, C.,Motta, A. Influence of scaffold pore size on collagen I development: A new in vitro evaluation perspective. *J Bioact Compat Pol* **28**, 16-32 (2013).
20. Lee, M., Wu, B.M.,Dunn, J.C.Y. Effect of scaffold architecture and pore size on smooth muscle cell growth. *J Biomed Mater Res A* **87A**, 1010-1016 (2008).
21. Kasten, P., Beyen, I., Niemeyer, P., Luginbuhl, R., Bohner, M.,Richter, W. Porosity and pore size of beta-tricalcium phosphate scaffold can influence protein production and osteogenic differentiation of human mesenchymal stem cells: An in vitro and in vivo study. *Acta Biomater* **4**, 1904-1915 (2008).
22. Im, G.I., Ko, J.Y.,Lee, J.H. Chondrogenesis of Adipose Stem Cells in a Porous Polymer Scaffold: Influence of the Pore Size. *Cell Transplant* **21**, 2397-2405 (2012).
23. Oh, S.H., Kim, T.H., Im, G.I.,Lee, J.H. Investigation of Pore Size Effect on Chondrogenic Differentiation of Adipose Stem Cells Using a Pore Size Gradient Scaffold. *Biomacromolecules* **11**, 1948-1955 (2010).
24. Tanaka, Y., Yamaoka, H., Nishizawa, S., Nagata, S., Ogasawara, T., Asawa, Y., Fujihara, Y., Takato, T.,Hoshi, K. The optimization of porous polymeric scaffolds for chondrocyte/atelocollagen based tissue-engineered cartilage. *Biomaterials* **31**, 4506-4516 (2010).

Chapter 4

Preparation of collagen porous scaffolds with different pore sizes

4.1 Summary

Scaffold pore size was shown in chapter 3 to be an important factor affecting tissue regeneration efficiency. To further quantitatively compare the effect of pore size on the proliferation and gene expression of chondrocytes, four individual ice-collagen porous scaffolds with different pore sizes were prepared by using pre-prepared ice particulates that had diameters of 150-250, 250-355, 355-425 and 425-500 μm. The scaffolds had spherical large pores with good interconnectivity and high porosity that facilitated cell seeding and spatial cell distribution. Chondrocytes adhered to the walls of the spherical pores and showed a homogenous distribution throughout the scaffolds. The *In vivo* implantation results indicated that the pore size did not show evident effect on cell proliferation but showed different effect on cartilage regeneration. The collagen porous scaffolds prepared with ice particulates in the range of 150-250 μm best promoted the expression and production of type II collagen and aggrecan, increasing the formation and the mechanical properties of the cartilage.

4.2 Introduction

Porous materials and scaffolds are important for many biomedical and biological applications.[1-4] In tissue engineering, porous materials can provide a temporary microenvironment to promote cell adhesion, proliferation, differentiation and secretion of a newly formed extracellular matrix to guide the formation of new tissues and organs.[5,6] Biodegradable polymers, ceramics and their composites have been formed into such porous structures for use in tissue engineering.[7-9] Controlling the pore structure, including pore size and interconnectivity, is key to create ideal porous biomaterials and scaffolds.[10-13] Some cell functions as well as new tissue regeneration deeply rely on the size of the pores.[14-19] Many reports show the effects of the pore size of a porous scaffold on tissue regeneration. However, some of the reported results do not agree with each other. The contradictory results may be due to the complexity of factors in three-dimensional culture, which may affect cell penetration and distribution and nutrient diffusion. Except pore size, pore interconnectivity can also affect smooth delivery of cells into the pores and nutrient diffusion during cell culture. Therefore, to compare the effects of the pore size, interconnectivity should also be considered to

ensure homogeneity of cell distribution throughout the scaffolds.[20,21] Many methods have been developed to control the pore structure characteristics of scaffolds made of various materials, including the pore size, porosity and interconnectivity.[22-26] Although some methods control pore size by using porogen materials, this leads to pores that are isolated, not interconnected with other pores. As a result, cells cannot enter the isolated pores and the void space cannot be filled with new tissue, so those pores remain in the newly regenerated tissues as defects. Such problems should be avoided when engineering tissues. In addition to cell penetration and distribution throughout the porous structure, pore interconnectivity is also very important for the exchange and removal of metabolic molecules. Therefore, precisely sized pores with good interconnectivity are required to compare the effect pore size has on tissue regeneration. In this chapter, collagen porous scaffolds with four different ranges of pore sizes were created by using prepared ice particulates as a porogen material. The scaffolds included spherical pores of different sizes that were well-interconnected. The scaffolds were used to culture articular chondrocytes, comparing the effect of the pore size on cartilaginous matrix production and cartilage regeneration (Figure 4.1).

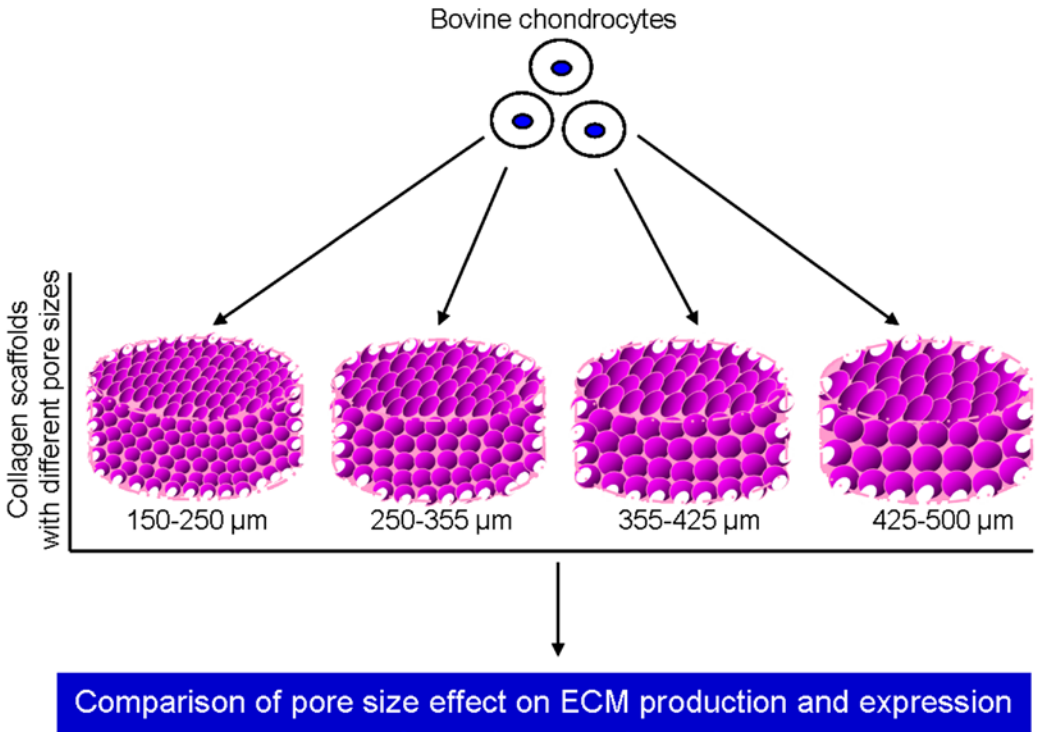

Figure 4.1 Individual collagen scaffolds with different pore sizes.

4.3 Materials and methods

4.3.1 Scaffold preparation

Collagen porous scaffolds were made by using prepared ice particulates as a porogen material. Initially, an aqueous collagen solution as well as ice particulates were made. The 2% (w/v) aqueous collagen solution was prepared by dissolving freeze-dried porcine type I collagen (Nitta Gelatin, Osaka, Japan) in a mixture of ethanol and acetic acid (20:80 v/v, pH 3.0) at 4 °C. The ethanol and acetic acid mixture was used to decrease the freezing temperature of the aqueous collagen solution. The prepared collagen solution did not

freeze at -4 °C, guaranteeing homogeneous mixing with the ice particulates. The prepared collagen solution was stored in a refrigerator (at 4 °C) until use. The ice particulates were prepared by spraying Milli Q water into liquid nitrogen using a sprayer. The ice particulates were sieved by sieves with mesh pores of 150, 250, 355, 425 and 500 μm to obtain ice particulates having diameters of 150-250, 250-355, 355-425 and 425-500 μm. The sieving process occurred at -15 °C in a low-temperature chamber (Espec, Osaka, Japan). The sieved ice particulates were stored in closed glass bottles in a -80 °C freezer until their use. Then, the 2% (w/v) aqueous collagen solution was mixed with the sieved ice particulates. Before mixing, the collagen solution and the ice particulates were moved to a -4 °C low-temperature chamber for 6 h to balance their temperatures. The four sets of ice particulates, each with different diameters, were separately added to four batches of pre-cooled collagen aqueous solution in a 50:50 (v/w) ratio. The components were mixed thoroughly with a steel spoon. Each of the four mixtures of collagen solution and ice particulates was poured into a silicone frame that was then placed on a PFA film-wrapped copper plate, and the mixture surface was flattened with a steel spatula. Finally, the constructs were frozen at -80 °C for 6 h, and freeze-dried for 3 days in a Wizard 2.0 freeze dryer (VirTis, Gardiner, NY). The freeze-dried constructs were cross-linked with glutaraldehyde vapor by placing the constructs in a closed box with 20 mL of a 25% aqueous glutaraldehyde solution at 37 °C. After cross-linking, the constructs were washed with Milli Q water three times and immersed in 0.1 M aqueous glycine solution for 24 hours to block the unreacted aldehyde groups. After the glycine treatment, the constructs were washed with Milli Q water six more times. The final scaffolds were obtained by second freeze-drying.

4.3.2 Scaffold characterization

The microstructures of the collagen porous scaffolds were observed using a JSM-5610 scanning electron microscope (JEOL, Tokyo, Japan). The cross-sections of the collagen porous scaffolds were coated with platinum by an ECS-101 sputter coater (Elionix, Tokyo, Japan) before observation. The mean pore size of the collagen porous scaffolds was measured from their SEM images by a MetaVue Image System (Universal Imaging Corp., Buckinghamshire, UK). Six images were taken of each scaffold and used for the mean pore size calculation.

The mechanical properties of the collagen porous scaffolds were measured by a static compression mechanical test machine (TMI UTM-10T; Tykyo Baldwin Co., Ltd., Tokyo, Japan). Before testing, the samples were punched into cylindrical samples (Ø8 mm × H4 mm) with a biopsy punch, and wetted in PBS for 1h. Each test sample was compressed at a rate of 2.0 mm/min at room temperature. Load-deformation curves were obtained from a chart record. The Young's modulus was calculated from the curves and the sample dimensions. The average values were calculated from four samples (n=4).

The porosity of collagen porous scaffolds was measured according to Archimedes' principle (n=3).[27] The porosity was calculated according to the following formula: porosity = ((W2-W1)/(W2-W3)) ×100%, where W1 is the dry weight of the scaffold, W2 is the wet weight of scaffold (including PBS solution), and W3 is the weight of the scaffold in PBS solution (subtracting buoyancy from W1).

4.3.3 In vitro cell culture

For cell culture use, the collagen porous scaffolds were punched into cylindrical samples (8 mm × 4 mm, Ø × H). The samples were sterilized with 70% ethanol, washed 3 times with Milli Q water and conditioned with Dulbecco's Modified Eagle Medium (DMEM) at 37 °C for 30 min. Bovine articular

chondrocytes were cultured in the scaffolds. The chondrocytes were isolated from articular cartilage in the knees of a 9-week-old female calf, which were obtained from a local slaughter house and digested with an aqueous solution of 0.2% w/v collagenase type II (Worthington Biochemical, Lakewood, NJ). The isolated chondrocytes were cultured in 75 cm^2 tissue culture flasks in DMEM with an atmosphere of 5% CO_2 at 37 °C. The DMEM was supplemented with 10% fetal bovine serum, 4500 mg/L glucose, 4 mM glutamine, 100 U/mL penicillin, 100 μg/mL streptomycin, 0.1 mM nonessential amino acids, 0.4 mM proline, 1 mM sodium pyruvate and 50 μg/mL ascorbic acid. The cell culture medium was refreshed every 3 days. The chondrocytes were harvested by treatment with a trypsin/EDTA solution when the cells reached a confluence of 80%. The harvested chondrocytes were re-suspended in DMEM to prepare a cell suspension solution of 2.5×10^7 cells/mL for cell seeding. The chondrocytes were seeded into the scaffolds twice by adding 200 μL of the cell suspension solution (1.0×10^7 cells/scaffold) to each of the cylindrical sides of the scaffolds. The second seeding was performed 3 hours after the first to allow for cell adhesion. Cell seeding efficiency was analyzed at 6 h after cell seeding on both sides (before adding the medium). The cells on the surface of culture plates were collected and counted as inadhesive cells to scaffolds. The number of adhered cells to scaffolds was obtained by subtracting inadhesive cell number from initial cell seeding number. The cell seeding efficiency of each scaffold was calculated by dividing the number of adhered cells by the number of seeded cells (n=6). The cell/scaffold constructs were then cultured in DMEM under an atmosphere of 5% CO_2 at 37 °C with shaking (60/min) for 1 week. The medium was changed every 3 days.

The cell distribution in the collagen scaffolds was evaluated after 6 hours of culture by examining a cross-section. After *in vitro* culturing for 6 hours, the cell/scaffold constructs were harvested, washed 3 times with PBS and fixed using a 0.25% glutaraldehyde solution at room temperature for 1 h. The constructs were embedded in paraffin and sectioned (7 μm thick sections). The vertical cross-sections were stained with Hoechst 33258 (10 μg/mL) and observed under a fluorescence microscope (Olympus, Tokyo, Japan).

4.3.4 In vivo implantation

After 1 week of *in vitro* culture, the cell/scaffold constructs were subcutaneously implanted into the dorsa of 6-week-old athymic nude mice. Fourteen mice were used, and each mouse was implanted with 2 constructs. After the constructs were implanted for 8 weeks, the mice were scarified and the implants were harvested for further investigation. The animal experiment was conducted according to the committee guidelines of the National Institute for Materials Science for Animal Experiments.

4.3.5 Histological and immunohistochemical evaluations

The implants, harvested after 8 weeks of *in vivo* implantation, were fixed in 10% formalin, embedded in paraffin and sectioned (7 μm thick sections). The cross-sections were stained with hematoxylin and eosin (HE), Safranin O and light green staining. The cross-sections were also immunostained for type II collagen and aggrecan. Briefly, the deparaffinized sections were incubated with proteinase K for 10 min for antigen retrieval, and then incubated with peroxidase blocking solution for 5 min and 10% goat serum solution for 30 min. The sections were next incubated with the first antibodies for 1 h, followed by incubation with the peroxidase-labeled polymer-conjugated second antibodies (DakoCytomation Envision+) (Dako, Carpinteria, CA, USA) for 30 min. The first antibodies were rabbit polyclonal anti-collagen type II (in a 1:100 working dilution) (Thermo Scientific, Rockford, IL, USA) and rabbit polyclonal anti-aggrecan

(1:100 working dilution) (Thermo Scientific, Rockford, IL, USA). The sections were then incubated with 3, 3' diaminobenzidine (DAB) for 5 min to develop color. The nuclei were counterstained with hematoxylin. All procedures were performed at room temperature.

4.3.6 Measurements of cell proliferation and sulfated glycosaminoglycans (sGAG) levels as well as mechanical testing

The scaffold/cells implants were harvested after 8 weeks of *in vivo* implantation. The cell proliferation into the scaffold was investigated by measuring the DNA contents of the cell/scaffold constructs after 6 h and 1 week of *in vitro* culture and after 8 weeks of *in vivo* implantation. Before this analysis, the constructs were washed with pure water, freeze-dried and digested with papain solution (400 μg/mL, with 5 mM L-cysteine and 5 mM EDTA in 0.1 M phosphate buffer at a pH of 6.0). An aliquot of the papain-digested material was dyed with Hoechst 33258 dye (Sigma-Aldrich, St. Louis, MO, USA) and the DNA amount was measured under a spectrofluorometer (FP-6500, JASCO, Japan). The sGAG content was determined using a Blyscan sulfated glycosaminoglycan assay (Benchmark Plus; Bio-Rad Laboratories, Japan) on the above papain digests according to the manufacturer's instructions. The ratio of sGAG to DNA was calculated from the sGAG and DNA contents of each sample. Three samples were used to calculate the average and standard deviation.

The mechanical properties of the engineered tissues after 8 weeks of *in vivo* implantation were measured by the same method as that used for scaffolds described above. The average values were calculated from three samples (n=3).

4.3.7 Gene expressions of the cartilaginous matrix proteins

The expression of cartilaginous genes in the cell/scaffold constructs of individual collagen scaffolds was analyzed by real-time PCR (RT-PCR). After *in vivo* implantation for 8 weeks, the harvested individual collagen scaffold constructs were washed with PBS and frozen in liquid nitrogen. The frozen constructs were crushed into powder by an electric crusher and dissolved in Sepasol solution (Nacalai Tesque, Kyoto, Japan) to isolate the contained RNA. The RNA was converted to cDNA by MuLV Reverse Transcriptase (Applied Biosystems, USA). RT-PCR was used to amplify hypoxanthine guanine phosphoribosyl transferase 1 (HPRT 1), glyceraldehyde-3-phosphate dehydrogenase (GAPDH), type II collagen (Col2a1), and aggrecan (Acan). The reaction were performed with 2 μL cDNA, 18 mM forward and reverse primers, and 5 mM PCR problem and qPCR Master Mix (Eurogentec, Seraing, Belgium). The reactions were run for 40 cycles using a 7500 Real-Time PCR System (Applied Belgium). The expression levels of Gapdh were used as endogenous controls, and the gene expression levels relative to Hprt 1 were calculated using the comparative Ct method. The primer and probe sequences were also calculated using the comparative Ct method. The primer and probe sequences are listed in table 4.1.

Table 4.1. Primers and probes for real-time PCR analysis.

Gene	Primer 5'→3'	Probe 5'→3'
HPRT1	F: TGGCGTCCCAGTGAAATCA R: AGCAGCTGGCCACAGAACA	HRPTCAGTGACATGATCCAATG
GAPDH	F: GCATCGTGGAGGGACTTATGA R: GGGCCATCCACAGT CTTCTG	CACTGTCCACGCCATCACTGCCA
Col2a1	F: AAGAAACACATCTGGTTTGGAGAAA R: TGGGAGCCAGGTTGTCATC	CAACGGTGGCTTCCACTTCAGCTATGG
Acan	F: CCAACGAAACCTATGACGTGTACT R: GCACTCGTTGGCTGCCTC	ATGTTGCATAGAAGACCTCGCCCTCCAT

4.3.8 Statistical analysis

Statistical analysis was carried out by the same method described in 2.3.7.

4.4 Results and Discussion

4.4.1 Collagen porous scaffolds with different pore sizes

The gross appearance of the collagen porous scaffolds after being punched into cylindrical shapes is shown in Figure 4.2 A. The microstructure observed by SEM indicated that large pores were formed in the collagen scaffolds (Figure 4.2 B-I). The large pores were spherical and well stacked. Many small holes could be seen on the walls of the spherical large pores. The small holes connected the spherical large pores, making the scaffold well interconnected. The sizes of the large pores in the collagen scaffolds prepared with ice particulates having diameters of 150-250, 250-355, 355-425 and 425-500 μm were 169 ± 27, 263 ± 34, 354 ± 32 and 435 ± 37 μm, respectively. The sizes of small holes in the four collagen scaffolds were 52 ± 21, 60 ± 29, 65 ± 28 and 70 ± 30 μm, respectively. The sizes of the large pores were in a good agreement with the sizes of the prepared ice particulates; the large pores should be negative replicas of the ice particulates. The sizes of the small holes in all four scaffolds were similar. The small pores should be negative replicas of ice crystals that formed during freezing, whose sizes were dependent upon the freezing temperature. The porosity was higher than 98.8%. The four collagen scaffolds showed the same high porosity (Table 4.2). This is because the same ration of ice particulates was used to prepare the four collagen scaffolds. Under the same porosity, the results of pore size effect should be more reasonable and comparable. The collagen scaffolds had high mechanical property (Figure 4.3). The mechanical property decreased with the increase of pore size. The collagen scaffold prepared with ice particulates having diameters of 150-250 μm showed the highest young's modulus.

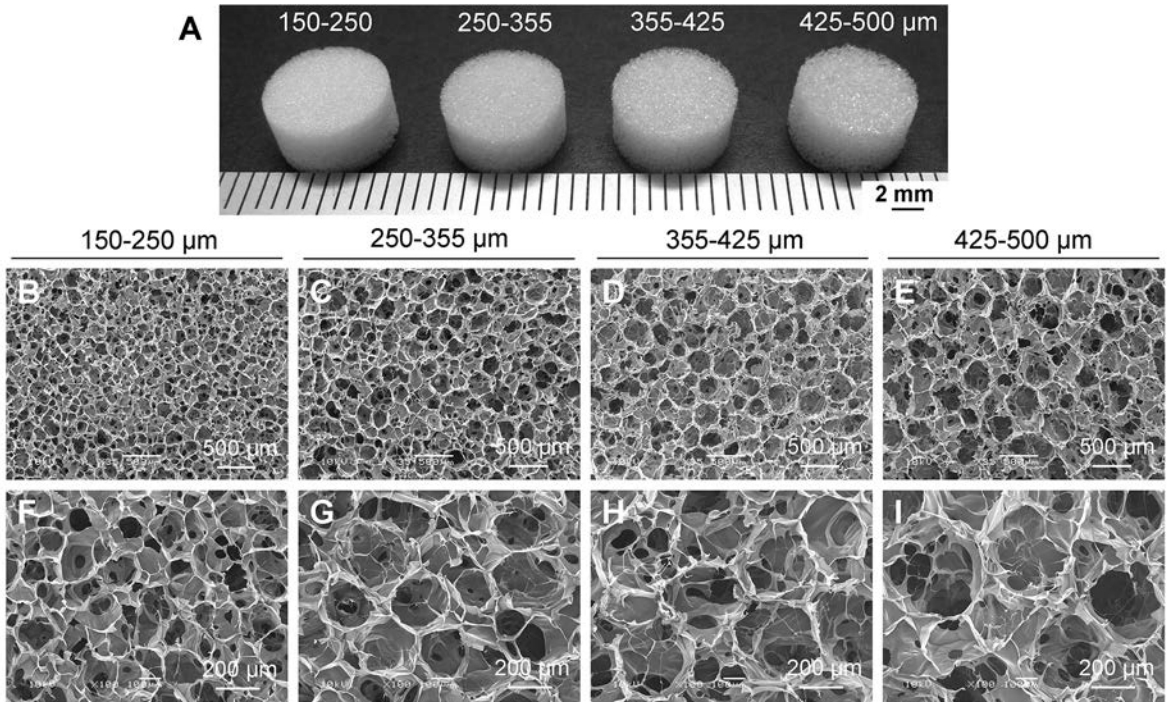

Figure 4.2 Gross appearances (A) and SEM photomicrographs (B-I) of the cross-sections of the four collagen porous scaffolds prepared with ice particulates having a diameter range of 150-250 (B, F), 250-355 (C, G), 355-425 (D, H) and 425-500 μm (E, I) at low (B, C, D, E) and high (F, G, H, I) magnifications.

Table 4.2 Porosity of collagen scaffolds with different pore sizes.

Scaffold type	Porosity
150-250 μm	98.8 ± 0.1%
250-355 μm	98.8 ± 0.2%
355-425 μm	98.8 ± 0.1%
425-500 μm	98.8 ± 0.2%

No significant difference among the collagen scaffolds with different pore sizes.

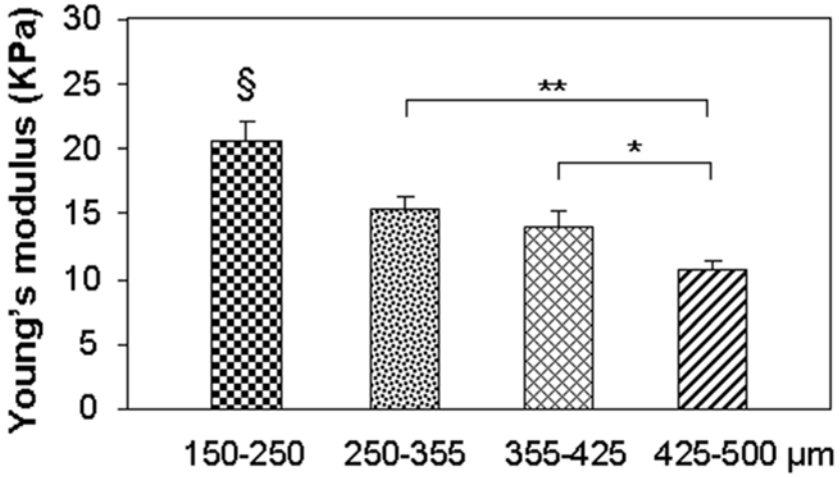

Figure 4.3 Young's modulus of wet collagen porous scaffolds with different pore sizes. Data represent mean ± SD, n=3. §, significant difference compared to all other groups, $p<0.001$. **, significant difference, $p<0.01$. *, significant difference, $p<0.05$.

4.4.2 Cell distribution in the collagen scaffolds

The collagen scaffolds were seeded with bovine articular chondrocytes and cultured *in vitro*. The scaffolds showed high cell seeding efficiency (Table 4.3). Most of the seeded cells were trapped in the collagen scaffolds. The cell distribution was investigated by a nucleus staining of the cross-section after 6 hours in culture. Nucleus staining showed that the chondrocytes were distributed homogeneously throughout all the four scaffolds (Figure 4.4). The cell distribution showed the same pattern as that of microporous structure as shown in Figure 4.2. The result indicated that cells surrounded the spherical large pores. The homogenous cell distribution in all the scaffolds should be due to the good interconnectivity of the scaffolds. The interconnectivity among the spherical large pores facilitated the smooth delivery of cells throughout the scaffolds to all the pores in the scaffolds.

Table 4.3 Cell seeding efficiency in the collagen scaffolds with different pore sizes.

Scaffold type	Cell seeding efficiency
150-250 μm	93.8 ± 2.0%
250-355 μm	93.2 ± 1.6%
355-425 μm	94.9 ± 1.4%
425-500 μm	94.1 ± 1.2%

No significant difference among the collagen scaffolds with different pore sizes.

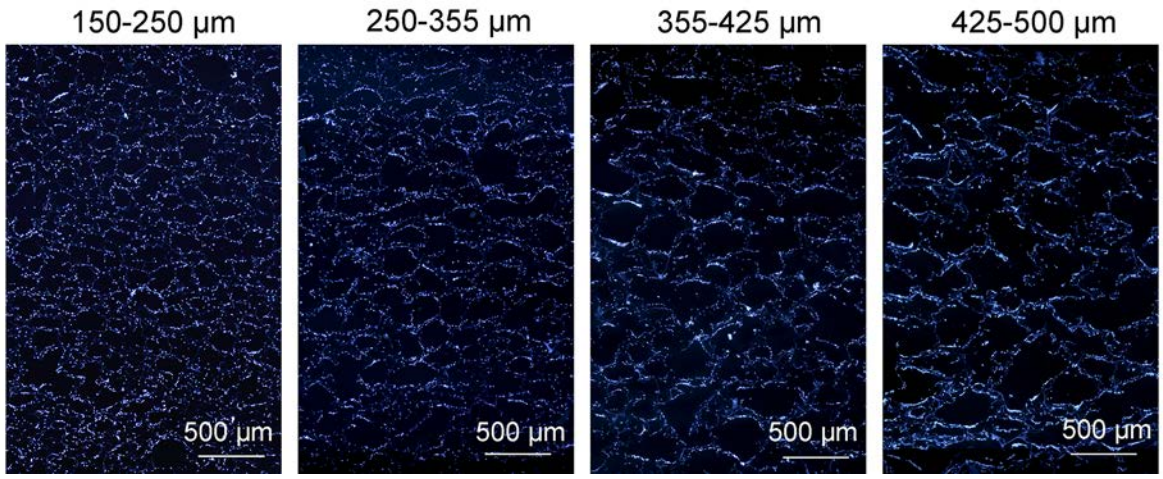

Figure 4.4 Cell distribution in the individual collagen porous scaffolds. Cell nuclei were stained by Hoechst 33258 and observed under a fluorescence microscope.

4.4.3 Histological and immunohistological stainings of regenerated cartilage

The cell/scaffold constructs were subcutaneously implanted into nude mice for 8 weeks. All the four implants appeared glisteningly white (Figure 4.5 A). Cell morphology and extracellular matrices were examined by Histological and immunohistological stainings. The stainings showed that the spatial cell and ECM distribution was uniform and that tissue formation was homogeneous in the scaffolds (Figure 4.5 B-E). HE staining indicated that the chondrocytes showed their typical round morphology in all four scaffolds. The collagen scaffold was not degraded and some collagen debris was still observed (the red shown in Figure 4.5 B). Safranin O staining showed that GAG was abundant in the implants (Figure 4.5 C). Immunostainings of type II collagen and aggrecan were positive for the tissues formed in all four scaffolds (Figure 4.5 D and E). These results indicated that chondrocytes maintained their round morphology and produced cartilaginous matrices in all the four collagen scaffolds, suggesting cartilage-like tissue formation in all the scaffolds. The cells cultured in the scaffolds prepared with ice particulates having diameters of 150-250 μm showed the strongest staining for Safranin O staining and immunostaining of type II collagen and aggrecan.

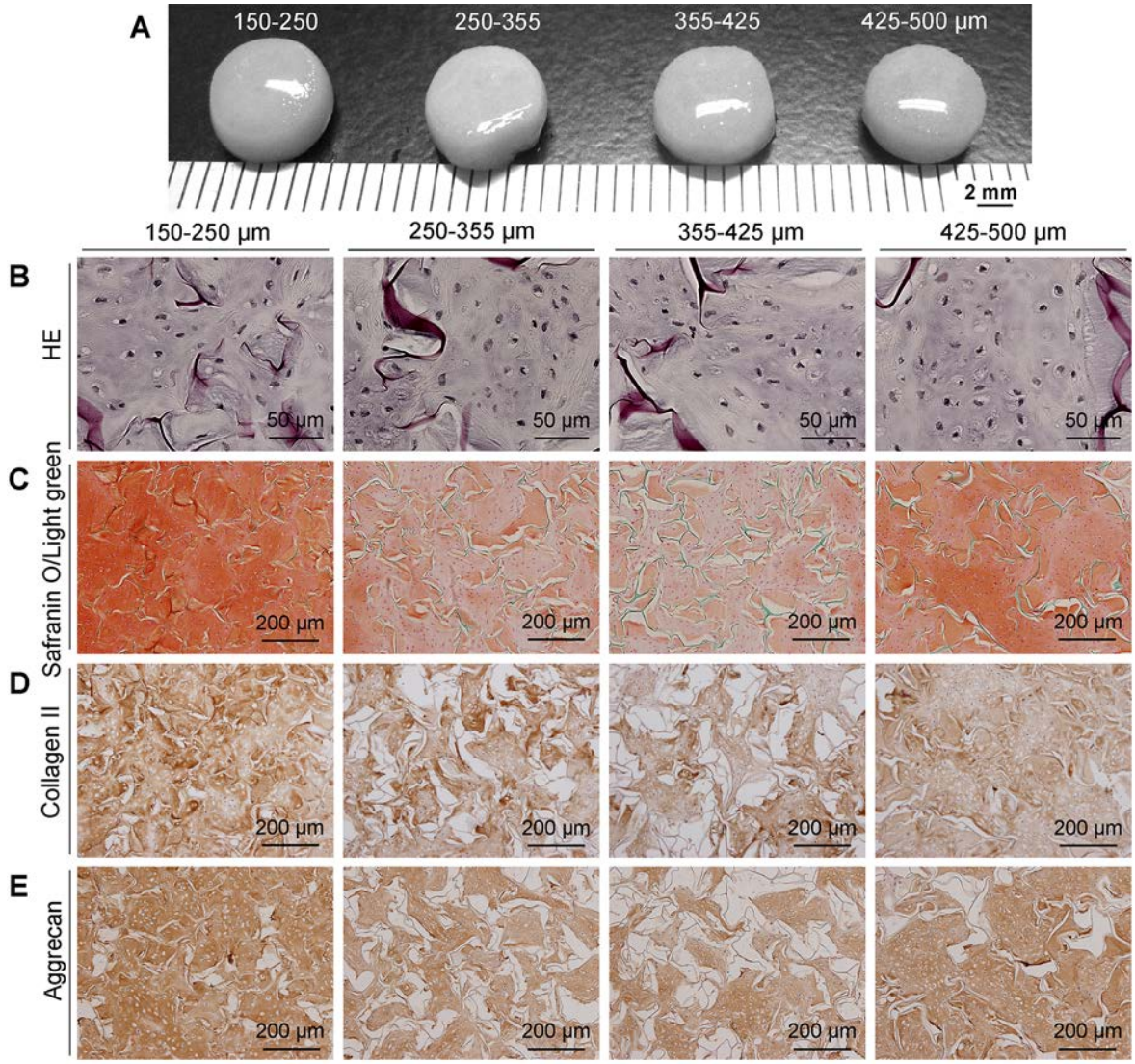

Figure 4.5 Gross appearances (A) and photomicrographs of HE staining (B), Safranin O/light green staining (C) and immunohistochemical staining of type II collagen (D) and aggrecan (E) of the cells in the four collagen porous scaffolds after 8 weeks of *in vivo* implantation.

4.4.4 Quantification of the cartilaginous matrices and their gene expression

The cell proliferation was investigated by measuring the DNA contents of the cell/scaffold constructs after 6 hours and 1 week of *in vitro* culture and after 8 weeks of *in vivo* implantation (Figure 4.6). The DNA amount increased almost 4-fold after 1 week of *in vitro* culture and almost 6-fold after 8 weeks of *in vivo* implantation. These results indicated that the cells proliferated continually during both *in vitro* culture and *in vivo* implantation. The cells showed high proliferation during the *in vitro* culture and slow proliferation during the *in vivo* implantation, which suggests that proliferation dominated during culture while differentiation might have dominated during implantation.

The secretion of extracellular matrix proteins is very important for cartilage regeneration because chondrocytes in cartilage are surrounded by abundant extracellular matrices. The sGAG amount was at almost the same level in all four collagen scaffolds, which were prepared with different sizes of ice particulates, after 1 week of *in vitro* culture. The amount of sGAG increased significantly after 8 weeks of *in*

vivo implantation (Figure 4.6 B), when the chondrocytes cultured in the collagen scaffold prepared with 150-250 µm ice particulates produced the highest amount of sGAG. To show the sGAG amount produced per cell, the sGAG/DNA ratio was calculated from the sGAG and DNA amounts (Figure 4.6 C). The sGAG/DNA ratio increased significantly from 1 week of *in vitro* culture to 8 weeks of *in vivo* implantation. The chondrocytes produced more extracellular matrix proteins during their *in vivo* implantation than they did during their *in vitro* culture, which suggests the prevalence of differentiation during implantation. The sGAG/DNA ratio in the collagen scaffold with the smallest pores was significantly higher than that in the collagen scaffolds prepared with the 250-355, 355-425 and 425-500 µm ice particulates. These results indicate that the collagen scaffold prepared with ice particulates of 150-250 µm was most favorable towards the production of cartilaginous ECM and chondrocyte maturation.

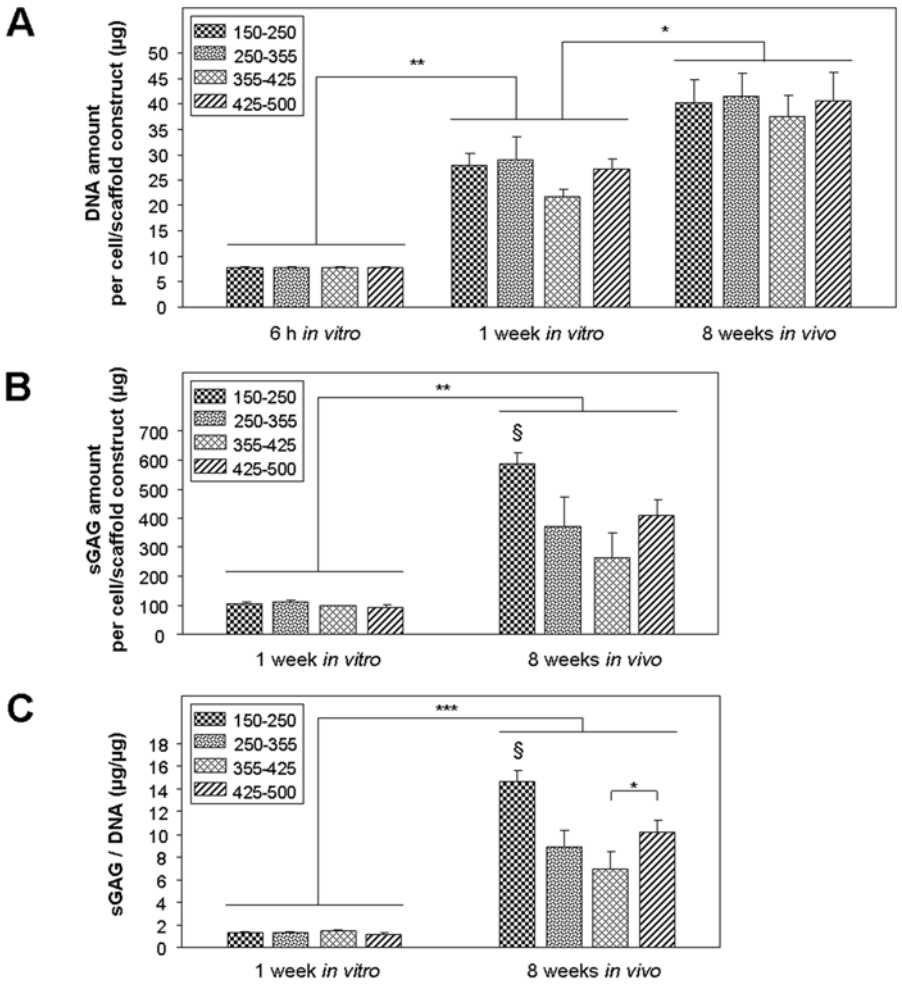

Figure 4.6 DNA amount (A), sGAG amount (B) and sGAG/DNA ratio (C) in the cell/scaffold implants of the four collagen porous scaffolds. Time points were after 6 h and 1 week of *in vitro* culture and after 8 weeks of *in vivo* implantation. The data are represented as the mean ± SD, n=3. §, significant difference compared to all other groups after 8 weeks, P<0.001. ***, significant difference, P<0.001. **, significant difference, P<0.01. *, significant difference, P<0.05.

The expressions of genes encoding type II collagen and aggrecan were analyzed by real-time RT PCR (Figure 4.7). Compared to P1 chondrocytes, the chondrocytes in the individual collagen scaffolds showed higher expression levels of the Col2a1 and Acan genes after 8 weeks of implantation. This result

suggests that the three-dimensional culture occurring in the collagen scaffolds promoted the expression of cartilaginous genes. The chondrocytes cultured in the collagen scaffold with the smallest pores expressed the highest levels of Col2a1 and Acan among all the individual collagen scaffolds.

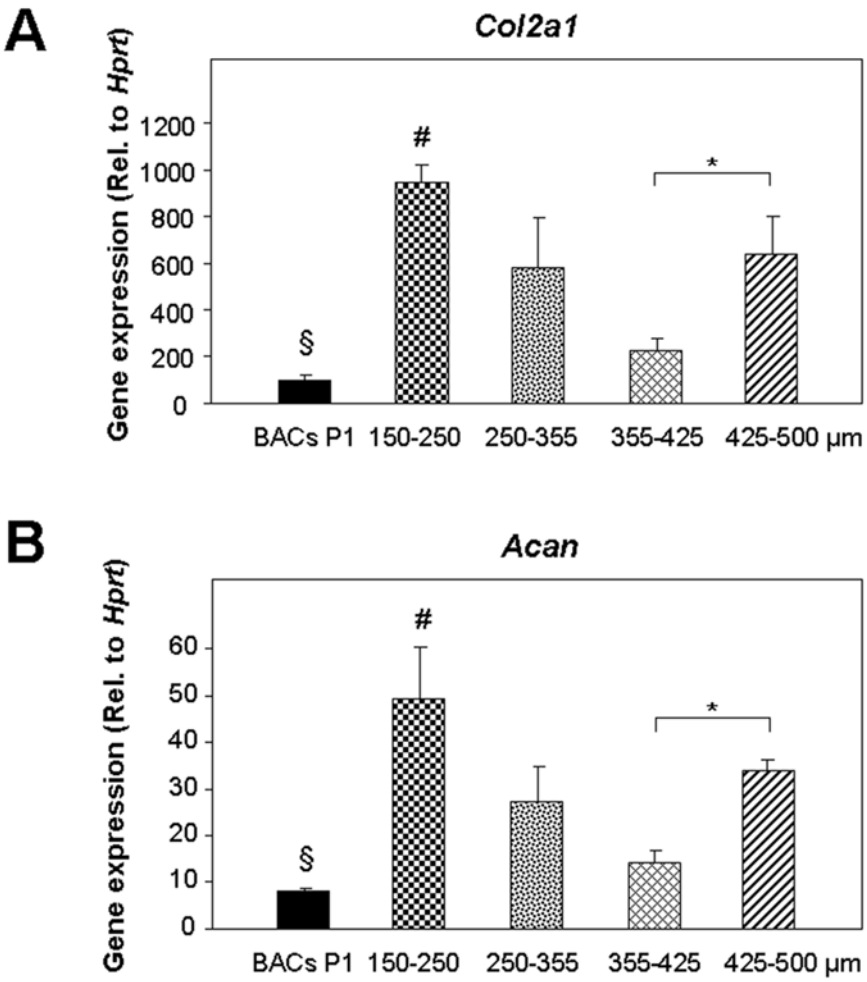

Figure 4.7 Expressions of genes encoding type II collagen (A) and aggrecan (B) in the cell/scaffold implants of the four collagen porous scaffolds after 8 weeks of *in vivo* implantation. The data are represented as the mean ± SD, n=3. §, significant difference compared to all other groups, $p<0.001$. #, significant difference compared to all other groups, $p<0.01$. *, significant difference, $p<0.05$.

The Young's moduli of the implants after 8 weeks of implantation were measured (Figure 4.8). The individual collagen scaffold implant prepared with 150-250 µm ice particulates had the highest Young's modulus.

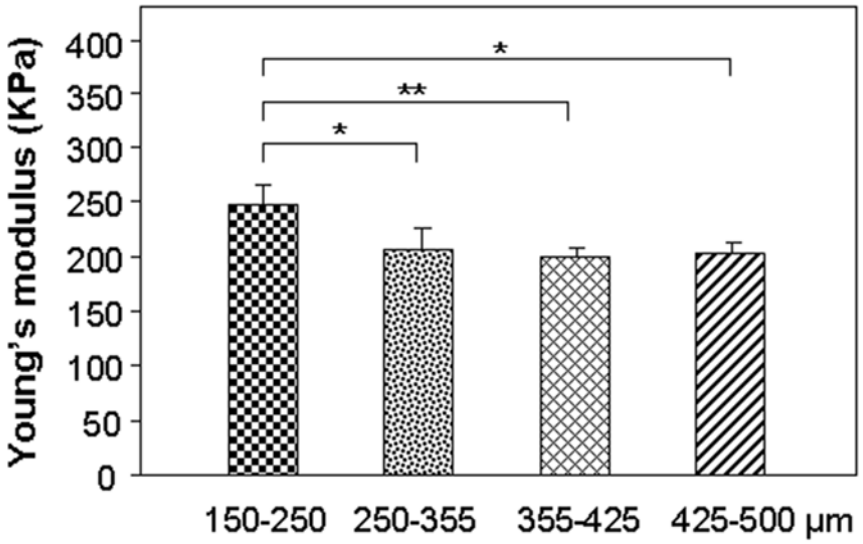

Figure 4.8 Young's modulus of the cell/scaffold implants of the four collagen porous scaffolds after 8 weeks of *in vivo* implantation. The data are represented as the mean ± SD, n=3. **, significant difference, $p<0.01$. *, significant difference, $p<0.05$.

Four collagen porous scaffolds with different pore sizes were prepared using pre-prepared ice particulates that had diameters of 150-250, 250-355, 355-425 and 425-500 μm. Spherical large pores with diameters that were in a good agreement with the sizes of the prepared ice particulates were formed in the collagen scaffolds. Many small holes were found in the walls of the spherical large pores, increasing the interconnectivity of the scaffolds. The sizes of the spherical large pores varied with the sizes of the prepared ice particulates because they were negative replicas of the ice particulates. The sizes of the small holes in the pore walls were dependent on the freezing temperature because they should be negative replicas of the ice crystals that formed during freezing. Typically, a low temperature results in the quick formation of dense, small ice crystals and a high temperature results in the slow formation of sparse, large ice crystals.[28,29] The formation of these small holes on the walls of the spherical large pores suggests that the new ice crystals formed during freezing were connected with the prepared ice particulates. In other words, it can be speculated that during the freezing process, the ice particulates serve as nuclei that initiate ice crystallization at their interface with the liquid phase collagen solution. This leads to ice crystal growth from the surface of the prepared ice particulates into the bulk aqueous solution. The ice particulates, together with the newly formed ice crystal network, determined the pore structures of the collagen porous scaffolds. By choosing the appropriate ice particulate sizes and freezing temperature, collagen porous scaffolds with designed pore structures could be prepared.

The four collage porous scaffolds were used for the three-dimensional culture of chondrocytes to investigate the effect of pore size on cartilage tissue regeneration. The four scaffolds with different pore sizes showed different effects on cartilaginous matrix production and cartilage formation. The collage scaffolds prepared with 150-250 μm ice particulates best promoted cartilage regeneration, based on the performed histological and immunohistological examinations. The promotion effect of cartilage regeneration in the four scaffolds was in the following order: 250-355 μm scaffold ≈ 355-425 μm scaffold < 425-500 μm scaffold < 150-250 μm scaffold. A comparison of the gene expression and production of two cartilaginous matrix proteins (type II collagen and aggrecan) also confirmed that the scaffolds prepared with 150-250 μm ice

particulates promoted the highest expression and production of type II collagen and aggrecan. The Young's modulus of the cartilage tissue formed in the collagen scaffold prepared with 150-250 μm ice particulates was the highest. All of these results indicated that the beneficial effect of pore size on cartilage tissue regeneration was in the following increasing order: 250-355 μm ≈ 355-425 μm < 425-500 μm < 150-250 μm.

The fact that a pore size of 150-250 μm has the most beneficial effect can be explained by cell distribution. Typically, large pores are more easily accessible to cells than are small pores.[18] However, interconnectivity is also a very important factor for cell delivery and spatial distribution.[20,22,23] The good interconnectivity among the spherical large pores in the collagen scaffolds facilitated the smooth delivery of cells throughout the scaffolds. Therefore, the cells could be smoothly delivered and homogenously distributed not only in the larger pore region, but also in the smaller pore region. Although all four scaffolds showed similarly homogenous cell distribution, the larger pores required more cells to fill the entire free space, while the smaller pores were more easily filled with cells. Filling the pores can increase the cell-cell interactions and provide a real three-dimensional microenvironment to promote chondrogenic differentiation and cartilage tissue formation.

There are many reports regarding the effect pore size has on tissue regeneration.[14-19] However, the results of those reports are not in good consensus because the various pore structures have not been precisely controlled. Some of the scaffolds used for such comparisons were prepared by freeze-drying.[14] However, ice crystals formed during the conventional freeze-drying process have flake-like shapes and result in the formation of a flake-like pore structure. Additionally, the pore size and shape can change depending on manipulation conditions and matrix materials. Preparing the same pore structure at different times and in different laboratories is difficult. Therefore, the use of porogen materials is desirable to guarantee the repeatability of a pore structure in a scaffold, which makes the data more comparable. When using the conventional porogen leaching methods, some of the pores are isolated and some are interconnected.[30] To precisely control the pore shape and maintain good interconnectivity, the use of prepared ice particulates as a porogen material is an effective and practical method. The pore size can be precisely controlled by the size of the ice particulates, which can initiate the formation of new ice crystals to increase the interconnectivity. Another advantage is the spherical pore structures that can be created. It has been reported that spherical and ellipsoidal pores support chondrocytes to produce more cartilaginous matrix materials than do cubical pores.[31]

4.5 Conclusions

The effect of pore size on cartilage regeneration was investigated by using four collagen porous scaffolds that were prepared using a porogen material of ice particulates having diameters of 150-250, 250-355, 355-425 and 425-500 μm. The collagen scaffolds had spherical pore structures of different pore sizes with good interconnectivity. The pore structures could be precisely controlled by selecting the ice particulate size and the freezing temperature. The collagen porous scaffolds prepared with ice particulates in the range of 150-250 μm showed the most promotive effect on the gene expression and the production of cartilaginous matrix proteins as well as on cartilage regeneration.

4.6 References

1. Hollister, S.J. Porous scaffold design for tissue engineering. *Nat Mater* **4**, 518-524 (2005).
2. Higuchi, A., Ling, Q.D., Hsu, S.T.,Umezawa, A. Biomimetic Cell Culture Proteins as Extracellular Matrices for Stem Cell Differentiation. *Chemical Reviews* **112**, 4507-4540 (2012).
3. Wu, C.H., Lee, F.K., Kumar, S., Ling, Q.D., Chang, Y., Chang, Y., Wang, H.C., Chen, H., Chen, D.C., Hsu, S.T.,Higuchi, A. The isolation and differentiation of human adipose-derived stem cells using membrane filtration. *Biomaterials* **33**, 8228-8239 (2012).
4. Wang, P.Y., Clements, L.R., Thissen, H., Jane, A., Tsai, W.B.,Voelcker, N.H. Screening Mesenchymal Stem Cell Attachment and Differentiation on Porous Silicon Gradients. *Adv Funct Mater* **22**, 3414-3423 (2012).
5. Lu, H., Kawazoe, N., Kitajima, T., Myoken, Y., Tomita, M., Umezawa, A., Chen, G.,Ito, Y. Spatial immobilization of bone morphogenetic protein-4 in a collagen-PLGA hybrid scaffold for enhanced osteoinductivity. *Biomaterials* **33**, 6140-6146 (2012).
6. Engelmayr, G.C., Jr., Cheng, M., Bettinger, C.J., Borenstein, J.T., Langer, R.,Freed, L.E. Accordion-like honeycombs for tissue engineering of cardiac anisotropy. *Nat Mater* **7**, 1003-1010 (2008).
7. Ko, E.C., Fujihara, Y., Ogasawara, T., Asawa, Y., Nishizawa, S., Nagata, S., Takato, T.,Hoshi, K. BMP-2 Embedded Atelocollagen Scaffold for Tissue-Engineered Cartilage Cultured in the Medium Containing Insulin and Triiodothyronine-A New Protocol for Three-Dimensional In Vitro Culture of Human Chondrocytes. *Tissue Eng Part C-Me* **18**, 374-386 (2012).
8. Tanaka, Y., Yamaoka, H., Nishizawa, S., Nagata, S., Ogasawara, T., Asawa, Y., Fujihara, Y., Takato, T.,Hoshi, K. The optimization of porous polymeric scaffolds for chondrocyte/atelocollagen based tissue-engineered cartilage. *Biomaterials* **31**, 4506-4516 (2010).
9. Chen, C.C., Wang, W.C.,Ding, S.J. In vitro physiochemical properties of a biomimetic gelatin/chitosan oligosaccharide/calcium silicate cement. *J Biomed Mater Res B Appl Biomater* **95**, 456-465 (2010).
10. Faraj, K.A., Van Kuppevelt, T.H.,Daamen, W.F. Construction of collagen scaffolds that mimic the three- dimensional architecture of specific tissues. *Tissue Eng* **13**, 2387-2394 (2007).
11. Silva, M.M.C.G., Cyster, L.A., Barry, J.J.A., Yang, X.B., Oreffo, R.O.C., Grant, D.M., Scotchford, C.A., Howdle, S.M., Shakesheff, K.M.,Rose, F.R.A.J. The effect of anisotropic architecture on cell and tissue infiltration into tissue engineering scaffolds. *Biomaterials* **27**, 5909-5917 (2006).
12. O'Brien, F.J., Harley, B.A., Yannas, I.V.,Gibson, L.J. The effect of pore size on cell adhesion in collagen-GAG scaffolds. *Biomaterials* **26**, 433-441 (2005).
13. Woodfield, T.B.F., Malda, J., de Wijn, J., Peters, F., Riesle, J.,van Blitterswijk, C.A. Design of porous scaffolds for cartilage tissue engineering using a three-dimensional fiber-deposition technique. *Biomaterials* **25**, 4149-4161 (2004).
14. Murphy, C.M., Haugh, M.G.,O'Brien, F.J. The effect of mean pore size on cell attachment, proliferation and migration in collagen-glycosaminoglycan scaffolds for bone tissue engineering. *Biomaterials* **31**, 461-466 (2010).

15. Nuernberger, S., Cyran, N., Albrecht, C., Redl, H., Vecsei, V.,Marlovits, S. The influence of scaffold architecture on chondrocyte distribution and behavior in matrix-associated chondrocyte transplantation grafts. *Biomaterials* **32**, 1032-1040 (2011).
16. Stenhamre, H., Nannmark, U., Lindahl, A., Gatenholm, P.,Brittberg, M. Influence of pore size on the redifferentiation potential of human articular chondrocytes in poly(urethane urea) scaffolds. *J Tissue Eng Regen M* **5**, 578-588 (2011).
17. Lien, S.M., Ko, L.Y.,Huang, T.J. Effect of pore size on ECM secretion and cell growth in gelatin scaffold for articular cartilage tissue engineering. *Acta Biomater* **5**, 670-679 (2009).
18. Oh, S.H., Park, I.K., Kim, J.M.,Lee, J.H. In vitro and in vivo characteristics of PCL scaffolds with pore size gradient fabricated by a centrifugation method. *Biomaterials* **28**, 1664-1671 (2007).
19. Nehrer, S., Breinan, H.A., Ramappa, A., Young, G., Shortkroff, S., Louie, L.K., Sledge, C.B., Yannas, I.V.,Spector, M. Matrix collagen type and pore size influence behaviour of seeded canine chondrocytes. *Biomaterials* **18**, 769-776 (1997).
20. Choi, S.W., Xie, J.W.,Xia, Y.N. Chitosan-Based Inverse Opals: Three-Dimensional Scaffolds with Uniform Pore Structures for Cell Culture. *Adv Mater* **21**, 2997-+ (2009).
21. Chen, V.J.,Ma, P.X. Nano-fibrous poly(L-lactic acid) scaffolds with interconnected spherical macropores. *Biomaterials* **25**, 2065-2073 (2004).
22. Vaquette, C., Frochot, C., Rahouadj, R.,Wang, X. An innovative method to obtain porous PLLA scaffolds with highly spherical and interconnected pores. *J Biomed Mater Res B* **86B**, 9-17 (2008).
23. Zhang, H.F., Hussain, I., Brust, M., Butler, M.F., Rannard, S.P.,Cooper, A.I. Aligned two- and three-dimensional structures by directional freezing of polymers and nanoparticles. *Nature Materials* **4**, 787-793 (2005).
24. Yoon, J.J., Kim, J.H.,Park, T.G. Dexamethasone-releasing biodegradable polymer scaffolds fabricated by a gas-foaming/salt-leaching method. *Biomaterials* **24**, 2323-2329 (2003).
25. Hou, Q.P., Grijpma, D.W.,Feijen, J. Porous polymeric structures for tissue engineering prepared by a coagulation, compression moulding and salt leaching technique. *Biomaterials* **24**, 1937-1947 (2003).
26. Harris, L.D., Kim, B.S.,Mooney, D.J. Open pore biodegradable matrices formed with gas foaming. *J Biomed Mater Res* **42**, 396-402 (1998).
27. Zreiqat, H., Ramaswamy, Y., Wu, C.T., Paschalidis, A., Lu, Z.F., James, B., Birke, O., McDonald, M., Little, D.,Dunstan, C.R. The incorporation of strontium and zinc into a calcium-silicon ceramic for bone tissue engineering. *Biomaterials* **31**, 3175-3184 (2010).
28. Grad, S., Gogolewski, S., Alini, M.,Wimmer, M.A. Effects of simple and complex motion patterns on gene expression of chondrocytes seeded in 3D scaffolds. *Tissue Eng* **12**, 3171-3179 (2006).
29. O'Brien, F.J., Harley, B.A., Yannas, I.V.,Gibson, L. Influence of freezing rate on pore structure in freeze-dried collagen-GAG scaffolds. *Biomaterials* **25**, 1077-1086 (2004).
30. Mikos, A.G., Thorsen, A.J., Czerwonka, L.A., Bao, Y., Langer, R., Winslow, D.N.,Vacanti, J.P. Preparation and Characterization of Poly(L-Lactic Acid) Foams. *Polymer* **35**, 1068-1077 (1994).
31. Jeong, C.G.,Hollister, S.J. Mechanical and biochemical assessments of three-dimensional poly(1,8-octanediol-co-citrate) scaffold pore shape and permeability effects on in vitro chondrogenesis using primary chondrocytes. *Tissue Eng Part A* **16**, 3759-3768 (2010).

Chapter 5

Preparation of hybrid porous scaffolds of collagen and wollastonite nanowires

5.1 Summary

Porous materials and scaffolds have wide applications in biomedical and biological fields. They can provide biological and physical cues to promote cell adhesion, proliferation, differentiation and extracellular matrix secretion to guide new tissue formation. In this chapter, hybrid scaffolds of collagen and wollastonite nanowires with well controlled pore structures were prepared by using ice particulates having a diameter from 335 to 425 μm. The hybrid scaffolds had interconnected large spherical pores with wollastonite nanowires embedded in the walls of the pores. The wollastonite nanowires reinforced the hybrid scaffolds and showed some stimulatory effects on cell functions. Human bone marrow-derived mesenchymal stem cells showed higher proliferation and osteogenic differentiation and expressed higher level of genes encoding angiogenesis-related genes in the hybrid scaffolds than did in the collagen scaffold. The results suggest the hybrid scaffolds could facilitate osteogenic differentiation and induce angiogenesis and will be useful for bone tissue engineering.

5.2 Introduction

Porous materials and scaffolds play an important role for tissue engineering and regenerative medicine.[1-3] Biodegradable porous scaffolds for bone tissue engineering should have biological and physical cues to induce the osteogenic differentiation of stem cells and progenitor cells to guide new bone tissue formation.[4,5] Biological cues such as proteins and ions from the scaffolds will promote cell adhesion, proliferation and differentiation.[6-10] Physical cues such as pore structures will control cell penetration, distribution and cell assembly into newly regenerated tissues.[11] Angiogenesis is another very important effect of scaffolds for bone tissue engineering in order to provide necessary nutrients and remove metabolic substances in the regenerated tissues.[12] Scaffolds used for bone tissue engineering should promote capillary formation to ensure the adequate supply of oxygen and nutrients throughout the scaffolds and regenerated tissues.[13,14] Furthermore, high mechanical property is desirable for bone tissue engineering scaffolds because

high mechanical strength is required to support the porous structure and maintain the shape of engineered bone tissues.[15] And it has been reported that high stiffness is good for bone tissue formation.[16]

Collagen has been used for bone tissue engineering because collagen is one of the main extracellular matrix components of bone.[17,18] It can provide biological cues to support cell adhesion, proliferation and differentiation. Meanwhile, bioceramics such as hydroxyapatite and beta-tricalcium phosphate have also been widely used to prepare bone tissue engineering scaffolds because of their similarity to the inorganic components in bone.[19] Wollastonite, a naturally occurring calcium silicate, has attracted much attention for its excellent bioactivity and biocompatibility in bone tissue engineering.[20-23] The Si and Ca ions released from wollastonite have been reported to stimulate proliferation and osteogenic differentiation of osteoprogenitor cells. Recently angiogenesis effect of calcium silicates has been reported.[24-26]

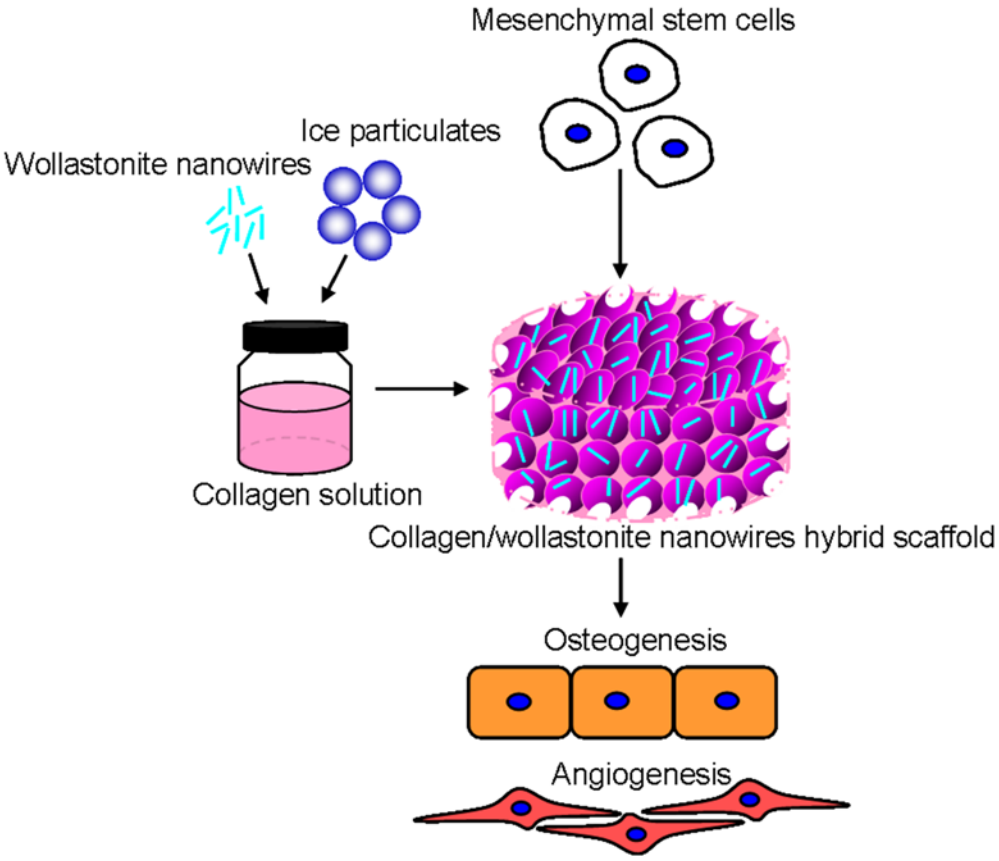

Figure 5.1 Hybrid scaffolds of collagen and wollastonite nanowires by using ice particulates as a porogen material.

Therefore, in this chapter, wollastonite nanowires were incorporated in collagen porous scaffolds to prepare hybrid scaffold of collagen and wollastonite nanowires. The porous structure of the hybrid scaffold was precisely controlled by using the method described in chapter 1. The nanowires were used because nano-structured materials have been reported to increase mechanical strength of porous scaffolds of biodegradable polymers.[27] The hybrid scaffold was used for three-dimensional culture of humen bone marrow-derived mesenchymal stem cells (Figure 5.1). The osteogenic differentiation and angiogenesis effects were investigated and compared with collagen scaffold.

5.3 Materials and methods

5.3.1 Preparation of wollastonite nanowires and collagen solution

The wollastonite nanowires were prepared according to the following method.[28] At first, 0.5 M $Ca(NO_3)_2$ solution and 0.5 M Na_2SiO_3 solution were obtained by dissolving $Ca(NO_3)_2$•$4H_2O$ and Na_2SiO_3•$9H_2O$ in distilled water, respectively. The reactant molar ratio of Ca/Si was kept at 1.0. The $Ca(NO_3)_2$ solution was dropwisely added into the Na_2SiO_3 solution at room temperature under stirring to obtain a white suspension. Subsequently, the suspension solution was transferred into Teflon-lined stainless-steel autoclaves and heated at 200 °C for 24 h. After the hydrothermal reaction, the suspension was washed with distilled water and anhydrous ethanol for three times, respectively. The resultant powders were dried at 60 °C for 24 h, and finally calcined at 800 °C in a furnace for 2 h.

The aqueous collagen solution was prepared by dissolving freeze-dried porcine type I collagen (Nitta Gelatin, Osaka, Japan) in a mixture solvent of ethanol and acetic acid (20:80 v/v, pH 3.0) at 4 °C. The ethanol and acetic acid mixture solvent was used to decrease the freezing temperature of the aqueous collagen solution. The prepared collagen solution did not freeze at -4 °C, guaranteeing homogeneous mixing with ice particulates during the next experiment. The prepared collagen solution was stored in a refrigerator (at 4 °C) until use.

5.3.2 Preparation of hybrid porous scaffolds using ice particulates

Pre-prepared ice particulates were used as a porogen material. The ice particulates were prepared by spraying Milli Q water into liquid nitrogen using a sprayer. The ice particulates were sieved by sieves with mesh pores of 355 and 425 μm to obtain ice particulates having a range of diameter of 355-425 μm. The sieving was done at -15 °C in a low-temperature chamber (Espec, Osaka, Japan). The sieved ice particulates were kept in a closed glass bottle at a -4 °C low-temperature chamber to balance their temperature. The wollastonite nanowires were dispersed in 99.5% ethanol with ultrasonic treatment for 2 h. The collagen/wollastonite nanowires solution was obtained by homogeneously mixing the pre-cooled collagen solution (-4 °C) and wollastonite nanowires solution (-4 °C) at -4 °C for 30 min. The final collagen concentration in collagen/wollastonite nanowires solution was 2% (w/v) and the weight ratio of wollastonite to collagen was 10:90 (w/w). The temperature-balanced ice particulates were added into the collagen/wollastonite nanowires solution in a 50:50 (v/w) ratio at -4 °C. The components were mixed thoroughly with a steel spoon. The mixture suspension solution of collagen/wollastonite nanowires and ice particulates was poured into a silicone frame that was then placed on a PFA film-wrapped copper plate. The top surface was flattened with a steel spatula and then covered with a glass plate wrapped with polyvinylidene chloride film. The entire set was frozen at -80 °C for 6 h. The frozen construct of collagen/wollastonite nanowires/ice particulates was freeze-dried for 3 days in a Wizard 2.0 freeze dryer (VirTis, Gardiner, NY) to obtain the porous scaffolds. The freeze-dried scaffolds were cross-linked with glutaraldehyde vapor by placing them in a closed box with 20 mL of a 25% aqueous glutaraldehyde solution at 37 °C. After cross-linking, the scaffolds were washed with Milli Q water three times and immersed in 0.1 M aqueous glycine solution for 24 hours to block the unreacted aldehyde groups. After the glycine treatment, the scaffolds were washed with Milli Q water for more than six times. The hybrid scaffolds of collagen and wollastonite nanowires were prepared after a second freeze-drying. The control collagen scaffold was

prepared by the same procedure but without wollastonite nanowires. The collagen/wollastonite nanowires hybrid scaffold and control collagen scaffold are defined as Col/nCS hybrid scaffold and Col scaffold, respectively.

5.3.3 Scaffold characterization

The morphology and size of wollastonite nanowires were characterized by transmission electron microscopy (JEM-2100F, JEOL, Japan). The micro- and nano-structures of the Col/nCS hybrid scaffold and Col scaffold were observed using a scanning electron microscope (S-4800, Hitachi, Japan). The cross-sections of the two scaffolds were coated with platinum by a sputter coater (E-1030, Hitachi, Japan) before observation. The mean pore size of the collagen porous scaffolds was measured from their SEM images by a MetaVue Image System (Universal Imaging Corp., Buckinghamshire, UK). Six images were taken of each scaffold and used for the mean pore size calculation.

The mechanical property of the Col/nCS hybrid scaffold and Col scaffold were measured by a static compression mechanical test machine (TA.XTPlus, Texture Technologies Corp.). Before testing, the samples were punched into cylindrical samples (Ø6 mm×H4 mm). The samples were wetted by immersing in PBS before measurement. Each sample was compressed at a rate of 0.1 mm/s to generate stress-strain curves. The Young's modulus was calculated from the initial linear region of the stress-strain curve. A minimum of four samples were tested for each type of scaffold.

5.3.4 In vitro cell culture

For cell culture use, the Col/nCS hybrid scaffold and Col scaffold were punched into cylindrical samples (Ø6 mm×H4 mm). The samples were sterilized with 70% ethanol, washed 3 times with Milli Q water and conditioned with Dulbecco's Modified Eagle Medium (DMEM) at 37 °C for 30 min. Human mesenchymal stem cells (hMSCs) were cultured in the scaffolds. The hMSCs were purchased from Lonza (Walkersville, MD) and subcultured twice in DMEM containing 10% fetal bovine serum, 1000 mg/L glucose, 584 mg/L glutamine, 100 U/mL penicillin, 100 µg/mL streptomycin, 0.1 mM nonessential amino acids, 0.4 mM proline, 1 mM sodium pyruvate and 50 µg/mL ascorbic acid under an atmosphere of 5% CO_2 at 37 °C. The hMSCs (Passage 4) were harvested by treatment with a trypsin/EDTA solution after confluence. The harvested MSCs were re-suspended in DMEM to prepare a cell suspension solution of 7.4×10^5 cells/mL for cell seeding. The hMSCs were seeded into the scaffolds twice by adding 135 µL of the cell suspension solution to each of the Ø6 mm sides of the scaffolds (2.0×10^5 cells/scaffold). The second seeding was performed 3 hours after the first to allow for cell adhesion. The cell/scaffold constructs were then cultured in DMEM (1 mL DMEM/cell scaffold construct) under an atmosphere of 5% CO_2 at 37 °C with shaking (60/min) for 14 days. The medium was changed every 3 days.

5.3.5 Measurements of DNA content

Cell proliferation in the Col/nCS hybrid scaffold and Col scaffold was investigated by measuring the DNA content of the cell/scaffold constructs after 1, 3, 7 and 14 days of *in vitro* culture. The constructs were washed with pure water, freeze-dried and digested with papain solution (400 µg/mL, with 5 mM L-cysteine and 5 mM EDTA in 0.1 M phosphate buffer at a pH of 6.0). An aliquot of the papain-digested material was dyed with Hoechst 33258 dye (Sigma-Aldrich, St. Louis, MO, USA) and the DNA amount (n =

4) was measured under a spectrofluorometer (FP-6500, JASCO, Japan).

5.3.6 Gene expression analysis

The expression of osteogenesis and angiogenesis genes in the cell/scaffold constructs were analyzed by real-time PCR. After 14 days of *in vitro* culture, the cell/scaffold constructs were washed with PBS and frozen in liquid nitrogen. The frozen constructs were crushed into powder by an electric crusher and dissolved in Sepasol solution (Nacalai Tesque, Kyoto, Japan) to isolate the contained RNA from the cells. Total RNA (1.0 μg) was used as a first strand reaction that included random hexamer primers and murine leukemia virus reverse transcriptase (Applied Biosystems, Foster City, CA). Real-time PCR was amplified for 18 S rRNA, glyceraldehyde 3 phosphate dehydrogenase (GAPDH), alkaline phosphatase (ALP), integrin binding sialoprotein (IBSP), osteopontin (SPP1), runt-related transcription factor 2 (RUNX2), vascular endpthelial growth factor (VEGF), epidermal growth factor (EGF) and insulin-like growth factor-1 (IGF-1). The reaction was performed with 10 ng of cDNA, 90 nM PCR primers, 25 nM PCR probe, and TaqMan Universal PCR Master Mix (Applied Biosystems). The expression levels of 18 S rRNA were used as an endogenous control, and gene expression levels relative to GAPDH were calculated using the comparative Ct method. The sequences of primers and probes are listed in Table 5.1. The primers and probes were obtained from Applied Biosystems and Hokkaido System Science (Sapporo, Japan).

Table 5.1. Primers and probes for real-time PCR analysis.

mRNA		Oligonucleotide
18S rRNA		Hs99999901_s1
GAPDH		Hs99999905_m1
ALP	Forward	5’-GACCCTTGACCCCCACAAT-3’
	Reverse	5’-GCTCGTACTGCATGTCCCCT-3’
	Probe	5’-TGGACTACCTATTGGGTCTCTTCGAGCCA-3’
IBSP	Forward	5’-TGCCTTGAGCCTGCTTCC-3’
	Reverse	5’-GCAAAATTAAAGCAGTCTTCATTTTG-3’
	Probe	5’-CTCCAGGACTGCCAGAGGAAGCAATCA-3’
SPP1	Forward	5’-CTCAGGCCAGTTGCAGCC-3’
	Reverse	5’-CAAAAGCAAATCACTGCAATTCTC-3’
	Probe	5’-AAACGCCGACCAAGGAAAACTCACTACC-3’
RUNX2		Hs00231692_m1
VEGF		Hs00900054_m1
EGF		Hs00153181_m1
IGF-1		Hs00153126_m1

5.3.7 Statistical analysis

Statistical analysis was carried out by the same method described in 2.3.7.

5.4 Results and Discussion

5.4.1 Hybrid porous scaffold of collagen and wollastonite nanowires

The wollastonite nanowires had a wire-like structure with a diameter of 20~30 nm and a length of 250~500 nm (Figure 5.2) which should be good for increase of scaffold mechanical strength and release of stimulatory ions.

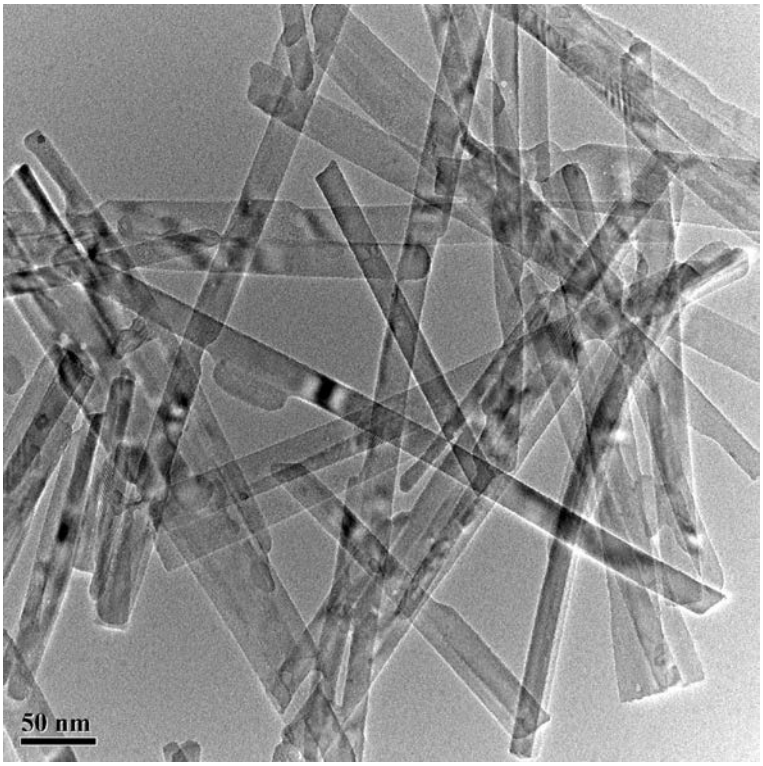

Figure 5.2 TEM image of the wollastonite nanowires.

The nanowires were mixed with collagen aqueous solution to prepare mixture suspension solution. The solution was applied to pre-prepared ice particulates to fill the space among the ice particulates. After freezing and freeze-drying, a hybrid porous scaffold of collagen and wollastonite nanowires (Col/nCS hybrid scaffold) was formed. Collagen porous scaffold without wollastonite nanowires was also prepared as a control by using the pre-prepared ice particulates (Col scaffold). The scaffolds showed white appearance(Figure 5.3 a). Observation by scanning electron microscopy showed that porous structures were formed in Col/nCS hybrid scaffold and Col scaffolds (Figure 5.3 b-e). The Col/nCS hybrid scaffold and Col scaffold showed similar microstructures, indicating that wollastonite nanowires did not change the porous structure of the scaffolds. Spherical large pores were formed in the porous scaffolds. Some small pores could be seen on the walls of the large pores, which connected the spherical large pores. The interconnect pore structure will benefit cell seeding and spatially homogeneous cell distribution. The size of the spherical large pores in Col/nCS hybrid scaffold and Col scaffold was 356 ± 34 and 359 ± 38 μm, respectively. The size of small pores in Col/nCS hybrid scaffold and Col scaffold was 63 ± 25 and 69 ± 33 μm, respectively. The large pores were the replica of the pre-prepared spherical ice particulates and their size was in a good agreement

with the size of the pre-prepared ice particulates. The small pores were the replica of ice crystals formed during freezing, which were decided by freezing temperature. Therefore, pore structure of the porous scaffolds can be controlled by the pre-prepared ice particulates and freezing temperature. Observation at a high magnification of cross-section of the walls of the scaffolds showed the presence of wollastonite nanowires in the hybrid scaffold (Figure 5.3 g). The wollastonite nanowires were embedded in the walls of the pores.

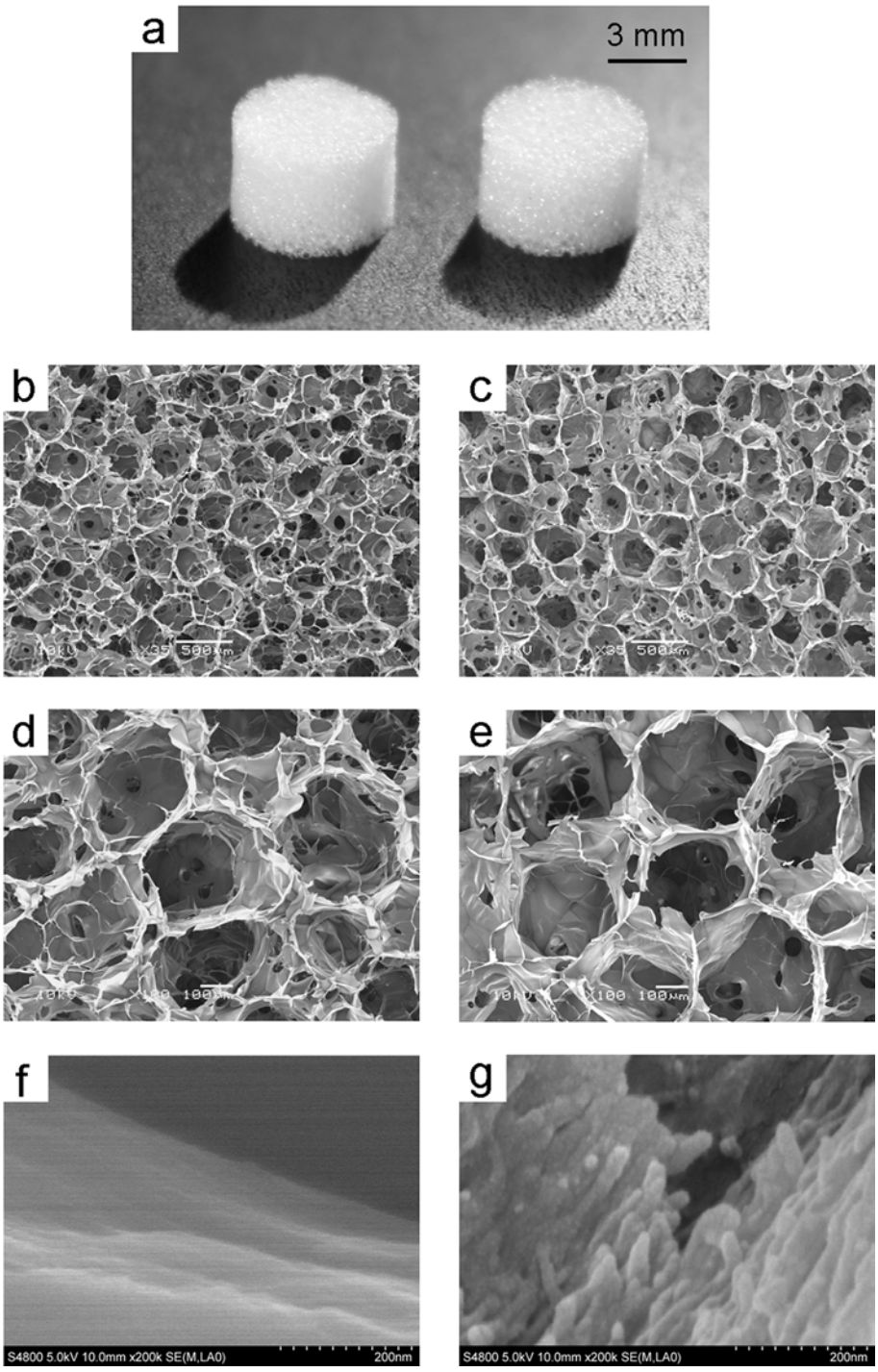

Figure 5.3 Gross appearance (a) and SEM images of cross sections of collagen scaffold (b, d, f) and collagen/wollastonite nanowires hybrid scaffold (c, e, g). The images are shown in low (b,c) and high (d, e, f, g) magnification.

Mechanical property of porous scaffold is important to protect the deformation of scaffold during cell culture and implantation. 15 The Young's modulus of the Col/nCS hybrid scaffold was significantly higher than that of Col porous scaffold (Figure 5.4). It was 2.8-fold higher than that of Col scaffold. The wollastonite nanowires increased the mechanical property of the collagen porous scaffold. This may be due to the reinforcing effect of wollastonite nanowires on collagen fibers and in pore walls as shown in Figure 5.3 g. The role of the wollastonite nanowires as mechanical reinforcement is similar to that of carbon nanotubes, which have been used to increase the mechanical property of porous scaffolds.[27] Collagen is a biocompatible polymer that has been widely used for biomedical applications. However, the weak mechanical property of collagen porous scaffolds restricts some of their applications, especially for load-bearing defect treatment. To increase the mechanical property of collagen-based porous scaffolds, hybridization of collagen with mechanically strong biodegradable synthetic polymers has been reported.[29,30] In this chapter, the wollastonite nanowires reinforced the collagen porous scaffolds and will broaden the applications of collagen-based porous scaffolds.

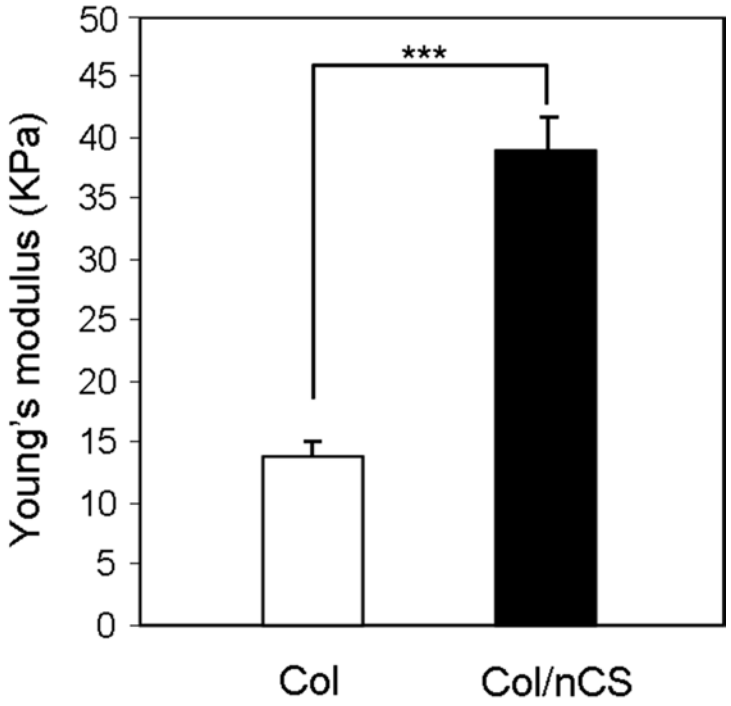

Figure 5.4 Young's modulus of wet collagen scaffold and collagen/wollastonote nanowires hybrid scaffold. The data represent the mean ± SD, n=4. ***, significant difference, $p<0.001$.

5.4.2 Cell adhesion and proliferation in collagen/wollastonite nanowires hybrid scaffold

The Col/nCS hybrid scaffold and Col scaffold were used for three-dimensional culture of hMSCs. The cells adhered and spread on both Col/nCS hybrid scaffold and Col scaffold (Figure 5.5). Cell morphology was similar for the cells cultured in the two types of porous scaffolds. Incorporation of wollastonite nanowires did not affect cell adhesion.

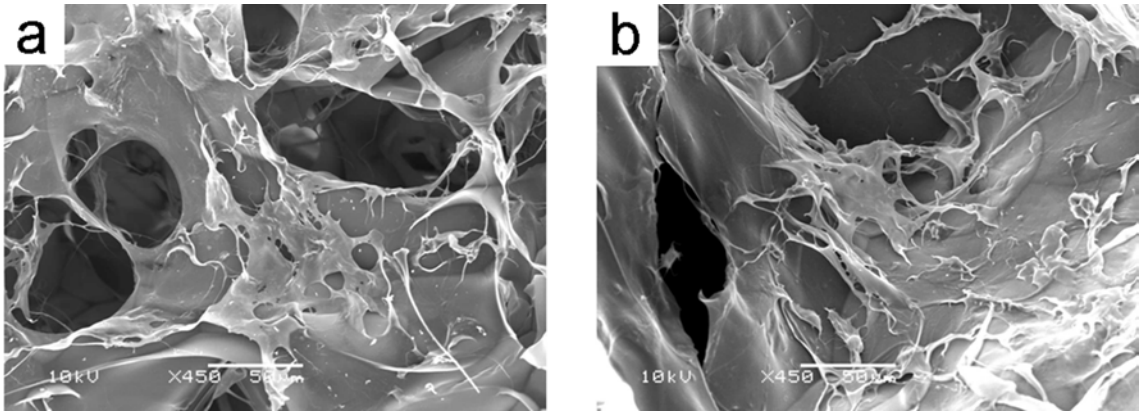

Figure 5.5 Cell attachment in collagen scaffold (a) and collagen/wollastonote nanowires hybrid scaffold (b) after 6 h of *in vitro* culture.

DNA quantification showed DNA amount increased with culture time when the cells were cultured in the scaffolds (Figure 5.6). The result indicates that cells proliferated in the porous scaffolds during cell culture. The DNA amount in the Col/nCS hybrid scaffold was significantly higher than that in the Col scaffold after culture for 7 and 14 days. Cell number in Col/nCS scaffold was nearly 1.4-fold higher than that in Col scaffold after culture for 14 days. The cells proliferated more quickly in Col/nCS hybrid scaffold than did in Col scaffold during long period culture. The wollastonite nanowires in the hybrid scaffold showed a promotive effect on the proliferation of hMSCs. It has been reported that some ions, such as Si ions, released from the wollastonite can stimulate the proliferation of mesenchymal stem cells.[20-23] Ions released from the wollastonite nanowires in the Col/nCS hybrid scaffold should promote cell proliferation in the hybrid scaffold.

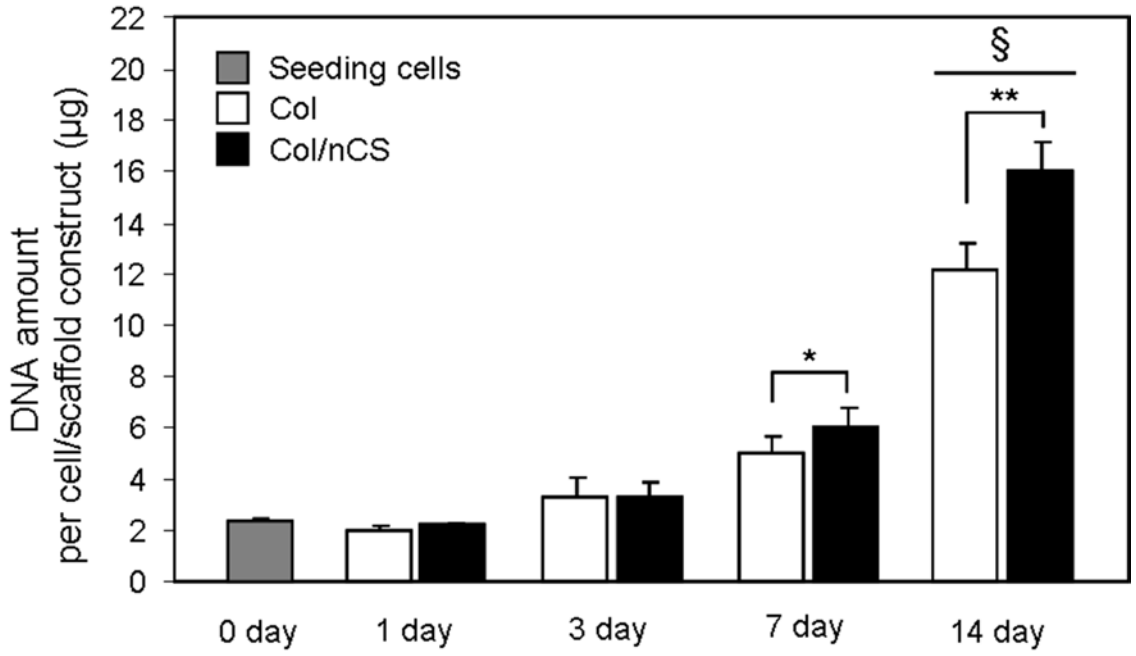

Figure 5.6 DNA amount in the cell/scaffold constructs of collagen scaffold and collagen/wollastonite nanowires hybrid scaffold after 1d, 3d, 7d and 14d of *in vitro* culture. The data represent the mean ± SD, n=4. **, significant difference, $p<0.01$. *, significant difference, $p<0.05$. §, significant difference compared to the ones after 1d, 3d and 7d of *in vitro* culture, $p<0.001$.

5.4.3 Osteogenic differentiation of MSCs in collagen/wollastonite nanowires hybrid scaffold

Induction of osteogenic differentiation of mesenchymal stem cells is important for bone tissue engineering when porous scaffolds are used for three-dimensional culture of stem cells. When hMSCs differentiate into osteoblasts, they should express ALP, SPP1, IBSP and an osteoblast-relating transcription factor, RUNX2. The osteogenic differentiation of hMSCs in the Col/nCS hybrid scaffold and Col scaffold was compared by investigating expression of osteogenic genes, ALP, SPP1, IBSP and RUNX2, by real-time PCR analysis after 2 weeks of culture. The hMSCs cultured in the Col/nCS hybrid scaffold showed higher expression levels of ALP, SPP1, IBSP and RUNX2 than did cells in the Col scaffold (Figure 5.7). The Col/nCS hybrid scaffold promoted expression of these osteogenic genes. The results indicate that the Col/nCS hybrid scaffold should facilitate osteogenic differentiation of mesenchymal stem cells and bone tissue formation.

Because the diffusion of oxygen and nutrients from existing blood vessels is limited to within 150-200 μm of the blood supply, there is insufficient oxygen and nutrients passing through large size scaffolds to maintain a viable activity and metastasis level for cells.[31] Therefore, angiogenesis effect of scaffold is important to induce formation of capillary network to support the regenerated bone tissue. The potential of the Col/nCS hybrid scaffold to induce angiogenesis was analyzed by investigating expression of genes encoding angiogenesis factors when cells were cultured in the scaffolds. Angiogenesis factor genes, VEGF, IGF-1 and EGF, were investigated. The hMSCs cultured in the Col/nCS hybrid scaffold showed significantly higher expression levels of these genes than did the cells cultured in the Col scaffold. Higher expression levels of these genes will promote angiogenesis when hybrid scaffold and mesenchymal stem cells are implanted *in vivo*. Incorporation of wollastonite nanowires in the hybrid scaffold showed promotive effect on expression of angiogenesis factor genes.

The gene expression results indicated that the Col/nCS hybrid scaffold promoted the expression of osteogenesis and angiogenesis genes without induction of osteogenic medium. The effects may be due to the Si and Ca ions released from the wollastonite nanowires in the Col/nCS hybrid scaffold. Si and Ca ions from calcium silicates have been reported to stimulate cell proliferation and induce capillary formation.[24-26] Hybridization of collagen with wollastonite nanowires showed stimulatory effect on proliferation and osteogenic differentiation of mesenchymal stem cells. And the porogen material, pre-prepared ice particulates, created interconnected large pores in the hybrid scaffold to facilitate cell seeding and distribution. Furthermore, the mechanical property of the hybrid scaffold increased by adding wollastonite nanowires as a strength-enhancing additive. The Col/nCS hybrid scaffold will be a good candidate scaffold for bone tissue engineering.

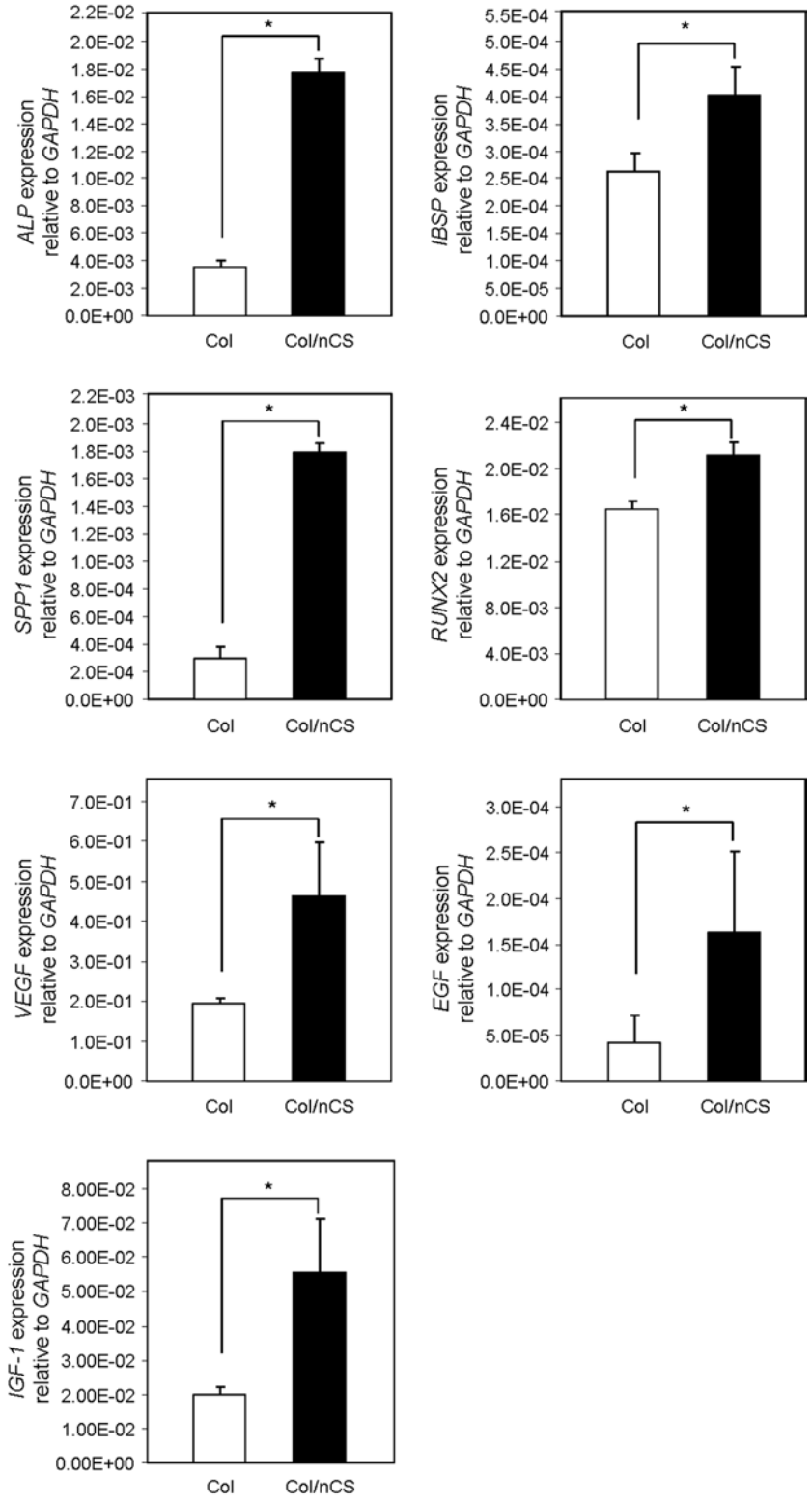

Figure 5.7 Expression of genes encoding ALP, IBSP, SPP1, RUNX2, VEGF, EGF and IGF-1 in the cell/scaffold constructs of collagen scaffold and collagen/wollastonite nanowires hybrid scaffold after 14 days of *in vitro* culture. The data represent the mean ± SD, n=3. *, significant difference, $p<0.05$.

5.5 Conclusions

Hybrid scaffolds of collagen/wollastonite nanowires with precisely controlled pore structure were prepared by using ice particulates as a porogen material. The hybrid scaffolds facilitated cell seeding and cell distribution. Compared to collagen scaffold, the hybrid scaffolds showed higher mechanical property, higher cell proliferation and angiogenesis stimulation effects. Hybridization of collagen with wollastonite nanowires has been proved to be a good strategy for the preparation of bone tissue engineering scaffolds.

5.6 References

1. Marcos-Campos, I., Marolt, D., Petridis, P., Bhumiratana, S., Schmidt, D.,Vunjak-Novakovic, G. Bone scaffold architecture modulates the development of mineralized bone matrix by human embryonic stem cells. *Biomaterials* **33**, 8329-8342 (2012).
2. Hoshiba, T., Lu, H., Kawazoe, N.,Chen, G. Decellularized matrices for tissue engineering. *Expert Opin Biol Ther* **10**, 1717-1728 (2010).
3. Chen, G.P., Ushida, T.,Tateishi, T. Scaffold design for tissue engineering. *Macromol Biosci* **2**, 67-77 (2002).
4. Higuchi, A., Ling, Q.D., Chang, Y., Hsu, S.T.,Umezawa, A. Physical Cues of Biomaterials Guide Stem Cell Differentiation Fate. *Chem Rev* (2013).
5. Higuchi, A., Ling, Q.D., Hsu, S.T.,Umezawa, A. Biomimetic Cell Culture Proteins as Extracellular Matrices for Stem Cell Differentiation. *Chemical Reviews* **112**, 4507-4540 (2012).
6. Lee, S.S., Huang, B.J., Kaltz, S.R., Sur, S., Newcomb, C.J., Stock, S.R., Shah, R.N.,Stupp, S.I. Bone regeneration with low dose BMP-2 amplified by biomimetic supramolecular nanofibers within collagen scaffolds. *Biomaterials* **34**, 452-459 (2013).
7. Lu, H.X., Kawazoe, N., Kitajima, T., Myoken, Y., Tomita, M., Umezawa, A., Chen, G.P.,Ito, Y. Spatial immobilization of bone morphogenetic protein-4 in a collagen-PLGA hybrid scaffold for enhanced osteoinductivity. *Biomaterials* **33**, 6140-6146 (2012).
8. Lu, H.X., Kawazoe, N., Tateishi, T., Chen, G.P., Jin, X.G.,Chang, J.A. In vitro Proliferation and Osteogenic Differentiation of Human Bone Marrow-derived Mesenchymal Stem Cells Cultured with Hardystonite (Ca2ZnSi2O7) and beta-TCP Ceramics. *J Biomater Appl* **25**, 39-56 (2010).
9. Huang, Y., Jin, X.G., Zhang, X.L., Sun, H.L., Tu, J.W., Tang, T.T., Chang, J.,Dai, K.R. In vitro and in vivo evaluation of akermanite bioceramics for bone regeneration. *Biomaterials* **30**, 5041-5048 (2009).
10. Liu, Q.H., Cen, L., Yin, S., Chen, L., Liu, G.P., Chang, J.,Cui, L. A comparative study of proliferation and osteogenic differentiation of adipose-derived stem cells on akermanite and beta-TCP ceramics. *Biomaterials* **29**, 4792-4799 (2008).
11. Murphy, C.M., Haugh, M.G.,O'Brien, F.J. The effect of mean pore size on cell attachment, proliferation and migration in collagen-glycosaminoglycan scaffolds for bone tissue engineering. *Biomaterials* **31**, 461-466 (2010).
12. Bramfeldt, H., Sabra, G., Centis, V.,Vermette, P. Scaffold vascularization: a challenge for

three-dimensional tissue engineering. *Curr Med Chem* **17**, 3944-3967 (2010).
13. Yao, R., Zhang, R.J., Yan, Y.N.,Wang, X.H. In Vitro Angiogenesis of 3D Tissue Engineered Adipose Tissue. *J Bioact Compat Pol* **24**, 5-24 (2009).
14. Lee, H., Chung, H.J.,Park, T.G. Perspectives on: Local and sustained delivery of angiogenic growth factors. *J Bioact Compat Pol* **22**, 89-114 (2007).
15. Alge, D.L., Bennett, J., Treasure, T., Voytik-Harbin, S., Goebel, W.S.,Chu, T.M.G. Poly(propylene fumarate) reinforced dicalcium phosphate dihydrate cement composites for bone tissue engineering. *J Biomed Mater Res A* **100A**, 1792-1802 (2012).
16. Engler, A.J., Sen, S., Sweeney, H.L.,Discher, D.E. Matrix elasticity directs stem cell lineage specification. *Cell* **126**, 677-689 (2006).
17. Ferreira, A.M., Gentile, P., Chiono, V.,Ciardelli, G. Collagen for bone tissue regeneration. *Acta Biomater* **8**, 3191-3200 (2012).
18. Holzwarth, J.M.,Ma, P.X. Biomimetic nanofibrous scaffolds for bone tissue engineering. *Biomaterials* **32**, 9622-9629 (2011).
19. Yoshikawa, H., Tamai, N., Murase, T.,Myoui, A. Interconnected porous hydroxyapatite ceramics for bone tissue engineering. *J R Soc Interface* **6**, S341-S348 (2009).
20. Li, H.Y., Zhai, W.Y.,Chang, J. Effects of Wollastonite on Proliferation and Differentiation of Human Bone Marrow-derived Stromal Cells in PHBV/Wollastonite Composite Scaffolds. *J Biomater Appl* **24**, 231-246 (2009).
21. Zhao, L.,Chang, J. Preparation and characterization of macroporous chitosan/wollastonite composite scaffolds for tissue engineering. *J Mater Sci-Mater M* **15**, 625-629 (2004).
22. Zhang, N.L., Molenda, J.A., Fournelle, J.H., Murphy, W.L.,Sahai, N. Effects of pseudowollastonite (CaSiO3) bioceramic on in vitro activity of human mesenchymal stem cells. *Biomaterials* **31**, 7653-7665 (2010).
23. Zhu, H.L., Shen, J.Y., Feng, X.X., Zhang, H.P., Guo, Y.H.,Chen, J.Y. Fabrication and characterization of bioactive silk fibroin/wollastonite composite scaffolds. *Mat Sci Eng C-Mater* **30**, 132-140 (2010).
24. Li, H.Y.,Chang, J. Stimulation of proangiogenesis by calcium silicate bioactive ceramic. *Acta Biomater* **9**, 5379-5389 (2013).
25. Li, H.,Chang, J. Bioactive silicate materials stimulate angiogenesis in fibroblast and endothelial cell co-culture system through paracrine effect. *Acta Biomater* (2013).
26. Zhai, W., Lu, H., Chen, L., Lin, X., Huang, Y., Dai, K., Naoki, K., Chen, G.,Chang, J. Silicate bioceramics induce angiogenesis during bone regeneration. *Acta Biomater* **8**, 341-349 (2012).
27. Shi, X., Sitharaman, B., Pham, Q.P., Liang, F., Wu, K., Edward Billups, W., Wilson, L.J.,Mikos, A.G. Fabrication of porous ultra-short single-walled carbon nanotube nanocomposite scaffolds for bone tissue engineering. *Biomaterials* **28**, 4078-4090 (2007).
28. Lin, K.L., Chang, J., Chen, G.F., Ruan, M.L.,Ning, C.Q. A simple method to synthesize single-crystalline beta-wollastonite nanowires. *J Cryst Growth* **300**, 267-271 (2007).
29. He, X.M., Lu, H.X., Kawazoe, N., Tateishi, T.,Chen, G.P. A Novel Cylinder-Type Poly(L-Lactic Acid)-Collagen Hybrid Sponge for Cartilage Tissue Engineering. *Tissue Eng Part C-Me* **16**, 329-338 (2010).
30. Dai, W.D., Kawazoe, N., Lin, X.T., Dong, J.,Chen, G.P. The influence of structural design of PLGA/collagen hybrid scaffolds in cartilage tissue engineering. *Biomaterials* **31**, 2141-2152 (2010).
31. Colton, C.K. Implantable biohybrid artificial organs. *Cell Transplant* **4**, 415-436 (1995).

Chapter 6

Concluding remarks and future prospects

6.1 Concluding remarks

This research demonstrated a method by using ice particulates as a porogen material to precisely control the pore structures of collagen-based porous scaffolds. At first, the method was established by mixing the pre-prepared ice particulates with collagen aqueous solution at different mixture ratios and concentrations and the detailed preparation conditions were investigated. Subsequently, the method was used to prepare a collagen scaffold with a gradiently changed pore size to direcetly investigate the effect of pore size on cartilage tissue regeneration. Furthermore, individual collagen porous scaffolds with different pore sizes were prepared to quantitatively compare the pore size effect on proliferation and cartilaginous gene expression of chondrocytes. Finally, the method was used to prepared hybrid scaffolds of collagen and wollastonite nanowires with precisely controlled pore structures for bone tissue engineering.

Chapter 1 introduces the principles of tissue engineering and its key factors of cells, scaffolds and growth factors. Subsequently, the development of scaffolds in tissue engineering was reviewed. Furthermore, the role of scaffold pore structure in tissue regeneration was emphasized, and the current challenges in fabrication of porous scaffolds with controlled pore structure were discussed. Finally, the objective of this study was defined.

Chapter 2 describes the preparation of collagen porous scaffold with controlled pore structure by using ice particulates as a porogen material. The detailed preparation conditions were investigated by mixing pre-prepared ice paticulates into collagen aqueous solution at different mixture ratios of ice particulates to collagen solution and different concentrations of collagen solutions. The collagen scaffold prepared with 2% collagen and 50% ice particulates showed precisely controlled pore structure, such as uniformity, interconnectivity and porosity and high mechanical property. What’s more, such collagen scaffold supported chondrogenesis more strongly than did the control scaffold prepared using normal freeze-drying. These results suggest that the method will be useful for the preparation of collagen-based porous scaffolds for tissue engineering and regenerative medicine.

Chapter 3 describes the use of a gradient pore structure for comparing the effect of different pore

sizes on cartilage regeneration under the same culture conditions. Firstly, the gradient collagen scaffold with four different regions was prepared with ice particulates having a diameter range of 150-250, 250-355, 355-425 and 425-500 μm. Then, bovine chondrocytes were cultured in this gradient collagen scaffold. Cell distribution, HE staining, Safranin O/light green staining and immunohistochemical staining of type II collagen were performed to investigate cellular activity and cartilage regeneration. The micropores in the gradient collagen scaffold prepared with ice particulates in the range of 150-250 μm showed the most beneficial effect on cartilage regeneration. Gradient scaffolds prepared with ice particulates were a useful tool to directly compare the effects of scaffold pore size on tissue regeneration.

Chapter 4 describes the further comparison of pore size effect on chondrocytes proliferation and gene expression by using individual collagen scaffolds with different pore sizes. Firstly, individual collagen scaffolds with different pore sizes were prepared with ice particulates having a diameter range of 150-250, 250-355, 355-425 and 425-500 μm. Then, bovince chondrocytes were cultured in these individual collagen scaffolds and the cell/scaffold constructs were implanted *in vivo* for 8 weeks. The quantitative analyses, such as physical property of collagen scaffolds, DNA and sGAG contents of cell/scaffold constructs, expressions of genes encoding type II collagen and aggrecan and young's modulus were calculated. The results showed that the collagen porous scaffolds prepared with ice particulates in the range of 150-250 μm showed the most promotive effect on the gene expression and the production of cartilaginous matrix proteins as well as on cartilage regeneration.

Chapter 5 describes the preparation of hybrid scaffolds of collagen and wollastonite nanowires with precisely controlled pore structure by using the method in chapter 1 for bone tissue engineering. The scaffolds were used for three-dimensional culture of human bone marrow-derived mesenchymal stem cells (hMSCs). Cell proliferation, osteogenic differentiation and angiogenesis factor gene expression were investigated. The hybrid scaffolds facilitated cell seeding and cell distribution. Compared to collagen scaffold, the hybrid scaffolds showed higher mechanical property, higher cell proliferation and osteogenic differentiation and expressed higher level of genes encoding angiogenesis-related genes. Hybridization of collagen with wollastonite nanowires was proved to be a good strategy for the preparation of bone tissue engineering scaffolds.

In conclusion, a method using pre-preapred ice particulates as a porogen material was developed for preparation of collagen-based scaffolds with precisely controlled pore structures such as pore size and interconnectivity. The method was used to prepare collagen porous scaffolds with a pore size gradient and different pore sizes to compare the effect of pore size on cell functions and cartilage tissue regeneration. The effect of pore size on cartilage tissue formation was directly compared by culturing bovine articular chondrocytes in the gradient collagen scaffolds. The effect of pore size on production and expression of cartilaginous extracellular matrices was compared by using individual scaffolds having different pore sizes. The collagen porous scaffolds prepared with ice particulates in the range of 150-250 μm showed the most promotive effect on the gene expression and the production of cartilaginous matrix proteins as well as on cartilage regeneration. The method was also used to prepare hybrid scaffolds of collagen/wollastonite nanowires for bone tissue engineering. The hybrid scaffolds could facilitate osteogenic differentiation and induce angiogenesis when hMSCs were cultured in the scaffolds. The ice particulates method was demonstrated to be a useful method to prepare collagen-based porous scaffolds and its hybrid scaffolds for tissue engineering.

6.2 Future prospects

This research demonstrated a method by using ice particulates as a porogen material to precisely control the pore structures of collagen-based porous scaffolds, such as pore size and interconnectivity. This method is very simple and low in cost, without the worry of residual solvents. The collagen scaffolds produced by this method showed highly interconnected pore structure, which is essential for homogeneous cell distribution and tissue formation. Besides collagen, the application of this method can be extended in other nature polymers, such as gelatin, chitosan, silk fibroin, etc.

As we know, the optimal pore size may vary with different cell type and biomaterials. In this study, the effect of pore size on cartilage tissue formation was directly compared by culturing bovine articular chondrocytes in the gradient collagen scaffolds prepared by this method. Furthermore, the quantitative reasearch of pore size effect was further inversigated by individual collagen scaffolds. This method provides a good choice for determining optimal pore size for different cell type and biomaterials on the premise of well interconnectivity of scaffolds.

The hybrid scaffolds of collagen and wollastonite nanowires with precisely controlled pore structures could facilitate osteogenic differentiation and induce angiogenesis for bone repair.Base on this research, combination of multi-biomaterials prepared by this method could be applied in more complicate tissue regeneration.

The scaffold prepared by this method could support as a basic scaffold for drug delivery. This process could be performed by modifying the scaffolds with proper bioactive molecules and growth factors, enzymes, ECM proteins and DNA to facilitate the tissue regeneration process by mimicking the ECM environment. The advantage of this method is that it could retain the biological activity of the bioactive molecule within the scaffolds by utilizing less harmful processes, such as the use of organic solvents and high temperature.

Above all, the scaffolds prepared by using ice particulates as a porogen material would have a promising future in tissue engineering.

List of publications

1. Qin Zhang, Tomoko Nakamoto, Shangwu Chen, Naoki Kawazoe, Kaili Lin, Jiang Chang and Guoping Chen. Collagen/wollastonite nanowire hybrid scaffolds promoting osteogenic differentiation and angiogenic factor expression of mesenchymal stem cells. Journal of Nanoscience and Nanotechnology, accepted.

2. Qin Zhang, Hongxu Lu, Naoki Kawazoe and Guoping Chen. Preparation of collagen scaffolds with controlled pore structures and improved mechanical property for cartilage tissue engineering. Journal of Bioactive and Compatible Polymers, accepted.

3. Qin Zhang, Hongxu Lu, Naoki Kawazoe and Guoping Chen. Preparation of collagen porous scaffolds with a gradient pore size structure using ice particulates. Materials Letters, accepted.

4. Qin Zhang, Hongxu Lu, Naoki Kawazoe and Guoping Chen. Pore size effect of collagen scaffolds on cartilage regeneration. Tissue Engineering, submitted.

5. Shangwu Chen, Qin Zhang, Tomoko Nakamoto, Naoki Kawazoe, Guoping Chen. Preparation of collagen-hyaluronic acid porous scaffolds with improved properties through the suppression of polyion complex formation. Biomaterials, submitted.

Acknowledgements

First and foremost, I would like to express my sincere gratitude to my supervisor Professor Guoping Chen for the continuous support of my Ph.D study and research, for your patience, motivation, enthusiasm and immense knowledge. I feel privileged to have been your student. Your guidance helped me in all the time of research and preparing papers. I could not have imagined having a better advisor and mentor for my Ph.D study and life in Japan. The experience of learning from you is a great treasure in my whole life.

Besides my advisor, I would like to acknowledge thesis committee members: Prof. Takao Aoyagi, Prof. Seiya Tsujimura and Prof. Tetsushi Taguchi. Thank you for taking time out of your busy schedule.

My sincere thanks also go to Dr. Naoki Kawazoe for your warm support and encouragement on my doctoral study over the years. Your professional skill and modest character have deeply impressed me. It is my great pleasure to work and learn from you.

I really appreciate the selfless assistance from Dr. Hongxu Lu. Thank you so much for teaching me so much experiment skills and supporting me just like elder brother.

I really appreciate Professor Kaili Lin for your valuable suggestion and assistance in my experiments and paper work.

I am thankful to Mrs. Harue Nagata for your countless help since I came to Japan. And I would like to give my thanks to current and former members in Tissue Regeneration Unit. They are Ms. Nobue Kobayashi, Dr. Takashi Hoshiba, Dr. Wei Song, Dr. Hwan Hee Oh, Dr. Tomoko Nakamoto, Dr. Ida Dulinska Molak, Dr. Jasmine Li, Dr. Lingfeng Guo, Mr. Koki Hagiwara, Mr. Himansu Nandasekhar, Mr. Hongli Mao, Ms. Rong Cai, Mr. Shangwu Chen, Mr. Xinlong Wang, Ms. Jia Hui NG. Mr.Yuichi Hirayama, Mr. Radyum Ikono, Ms. Megumi Nozato. Thank you for your cooperation and bring me so much colorful memory in our lab.

Also I thank my friends in Tsukuba, Dr. Zhi Rao, Dr. Yuling Zhou, Mr. Jianchen Hu, Mr. Peng Chen, Mr. Zhao Huang, Ms. Xiangfen Jiang, Mr. Xuebin Wang. Thanks for your kind support and help to me in Japan.

I would like to acknowledge the financial support of the Doctoral Program in Materials Science and Engineering of Graduate School of Pure and Applied Science, the University of Tsukuba and the National Institute for Materials Science, Japan.

Last but not the least, I would like to thank my family and my love who are always standing by me and supporting me spiritually throughout my life.